AD-A063 704 NAVAL ACADEMY ANNAPOLIS MD DIV OF ENGINEERING AND WEAPONS F/G 19/5
A COMPARATIVE STUDY OF FIRE CONTROL TARGET STATE ESTIMATORS.(U)
NOV 78 R DEMOYER
UNCLASSIFIED USNA-EW-18-78 NL

1 OF 2
AD A063704

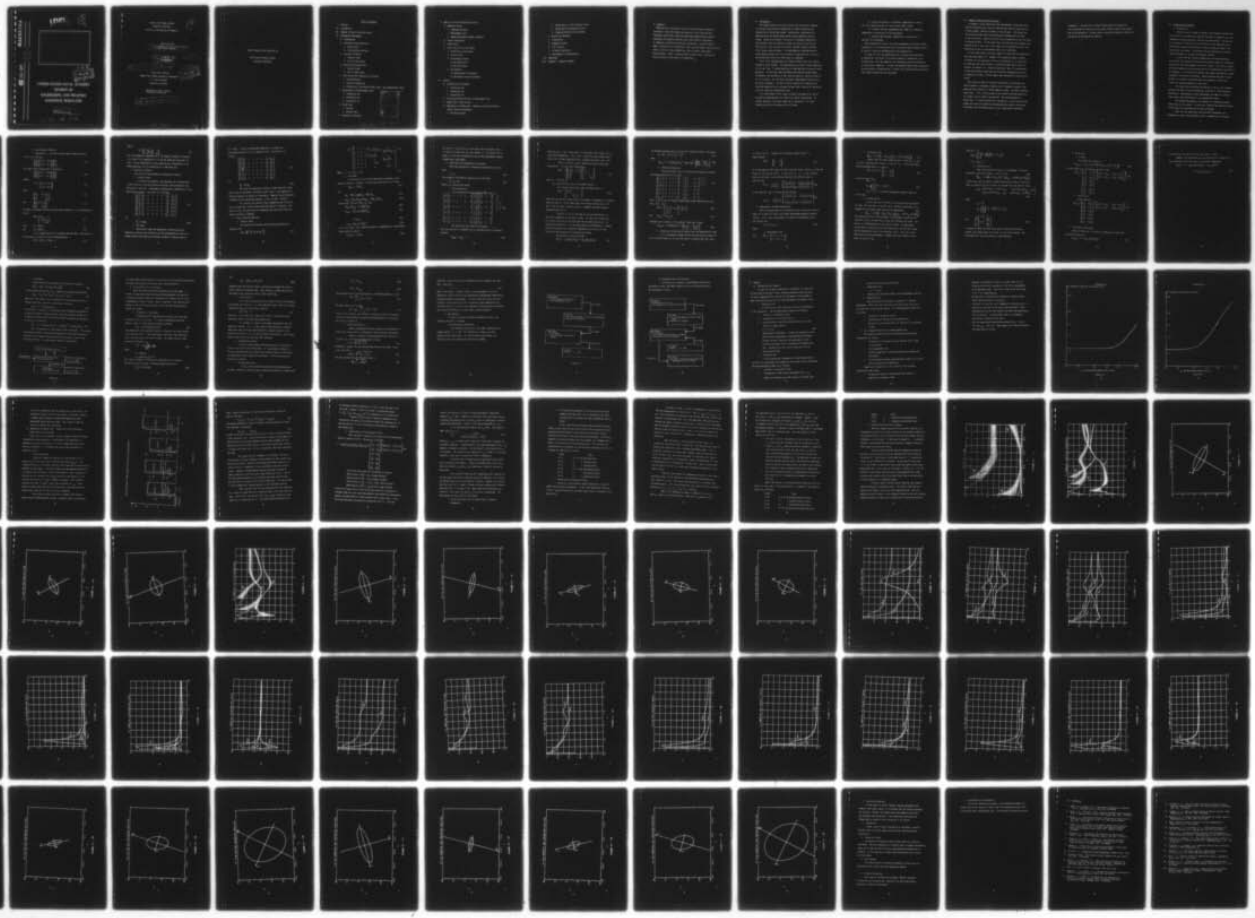

LEVEL II

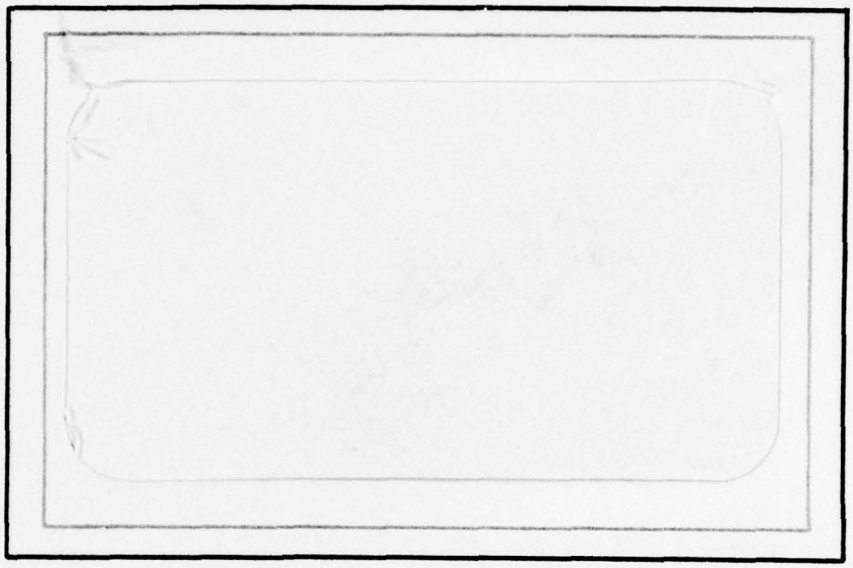

UNITED STATES NAVAL ACADEMY

DIVISION OF

ENGINEERING AND WEAPONS

ANNAPOLIS, MARYLAND

(2)

UNITED STATES NAVAL ACADEMY

Annapolis, Maryland

Division of Engineering and Weapons

Report EW-18-78

(6) A Comparative Study of Fire Control Target State Estimators.

(12) 134 p.

(10) R. DeMoyer, Jr. *

(11) November 1978

(9) Final rept. Jul - Aug 78,

* Assistant Professor

Weapons and Systems Engineering Department

U. S. Naval Academy

Annapolis, Maryland

Approved for public release;
distribution unlimited

(14) USNA-EW-18-78

406 923

JOB

Report funded by and submitted to:

Naval Surface Weapons Center

Dahlgren Laboratory

Table of Contents

V. Means of Filter Performance Evolution

A. Numerical Values

1. Reference Accuracy

2. Measurement Error

3. Markov Acceleration Model Parameters

B. Target Trajectories

C. Truth Model

D. Error Statistics at the Target

1. Projection of Covariance

2. Error Ellipse

3. Performance Criteria

a) Sum Square Error

b) RSS Error Ratio

4. Run Sequence

a) Establishment of Reference

b) Sub-Optimal Run and Evaluation

VI. Results

A. Sub-Optimization Sequence

1. Formulation (A)

2. Formulation (B)

3. Formulation (C)

B. Fully Coupled Sensitivities to Measurement Error

C. Added Error in Real Filters

D. Computation of Kalman Gain: Comparison of LOS Coordinates Versus Inertial Coordinates

1. Position Variance

I. Abstract

Application of the Kalman Filter to the fire control problem is considered. While the theory and practice in this field are well developed, conflicting claims have been made regarding the relative advantages of statistical decoupling in fixed inertial coordinates as compared to rotating non-inertial coordinates. An error analysis model, consisting of a sub-optimal filter and truth model, shows the error added, in each of three formulations, due to several sub-optimal approximations. Plots, including error ellipses, help to provide an intuitive feel for the results of decoupling.

II. Introduction

The primary purpose of an anti-aircraft gun fire control computer is to compute gun direction information in order to maximize the probability of hitting the target. Specifically, lead angles are computed which anticipate target motion during projectile time of flight. During an encounter, time series of redundant measurements are available from such devices as radar and inertial position and rate sensors. Most current fire control computers contain a Kalman Filter target state estimator. This mathematical algorithm makes an approximately optimal real time estimate of target position, velocity, and acceleration from which lead angles are computed.

A full scale implementation of a Kalman Filter to the fire control problem is quite complex. The problem must be solved in three dimensions and in real time. A target model must in some way help to predict future maneuvers. To this end, some algorithms have adaptive target models. Furthermore, the optimality of the solution require a careful accounting of error sources. All of these, and other, requirements cannot be met by present computers. The most effective reduction of computational load with moderate loss in accuracy follows from a statistical decoupling of errors among the computational axes.

It is the purpose of this study to compare the added error due to sub-optimal approximations for three fire control formulations. Of primary interest is the error added due to decoupling. The three formulations which are compared are as follows:

A. Using rate gyros as a reference, computation is carried out in a rotating tracker, or line of sight (LOS), frame.

B. Using an inertial measurement unit (IMU) as a reference, computation is carried out in LOS coordinates.

C. Using an IMU reference, computation is carried out in inertial (I) coordinates.

While formulations A and C have been implemented in existing systems, formulation B is considered here as an alternative where software similar to that of A could be implemented with the hardware of C.

In order to limit the computation and to clearly show the effects of decoupling, the overall fire control problem is simplified in the following way. Only two dimension are considered, with the elimination of the vertical dimension. A simple, non-adaptive Markov model represents the uncertainty in target motion. Finally, only non-accelerating straight line target trajectories are considered.

III. Summary of Results and Conclusions

In general, it was found that radar measurements, being made along the LOS coordinate axes, tend to align position error ellipses, and to a lesser extent, velocity ellipses, to the LOS axes. This causes the LOS covariance terms which are eliminated by decoupling to be small in the first place. Hence, the effect due to decoupling on LOS covariance is relatively minor. On the other hand, since LOS axes are rotating with respect to the I axes, the I cross terms are not necessarily small, and decoupling can have a considerable effect on I covariance.

For the above reason, the error added to A and B due to decoupling is less than that added to C. However, for reasons discussed in detail in Chapter VI, the reduction in error in B relative to C is not great, so based upon the cases studied, it would not appear that a shift in software to convert C to B would be justified. But, if a system were in the design stages, based upon the relatively inexpensive rate gyro as compared to an IMU, it would appear that formulation A would be preferred.

Care should be taken to interpret the results for what they are: Having prepared a reasonably extensive set of computer programs, time permitted the running of a limited number of cases. Two major questions remain open. First, to what extent do the results obtained generalize to a wider class of target trajectories? The second question is tantalizing. In marked contrast to I decoupling, it was found that the Kalman gain terms not zeroed by LOS decoupling are nearly undisturbed. Furthermore, the LOS Kalman gains are to a large extent trajectory

independent. The question is whether simple empirical expressions can be developed to replace the lost terms, further reducing the penalty due to LOS decoupling. Further study is required to develop a definitive conclusion to the decoupling question.

IV. Formulation Development

A. Introduction

There are quite a number of target state estimator formulations, all of which are designed to accomplish the goal of producing real time estimates of target position, velocity, and acceleration. The purpose is, of course, to form the initial conditions of the equations which will project target position ahead in time to projectile impact, thus forming gun lead angles. Differences from one formulation to another cause differences in accuracy and computer loading.

A few of the more obscure formulations are worth mentioning. In one case, the equations of motion are written in spherical coordinates so that the radar measurements are strictly linear. This leads to badly non-linear equations of motion which can be ill-conditioned, and difficult to integrate. To alleviate this problem, one author resorted to a highly unorthodox linearization technique. Another approach has been to work entirely in cartesian coordinate where the equations of motion are linear, but the measurements are non-linear.

As target state estimation has evolved, a more or less standard approach has been to write the equations of motion in fixed cartesian coordinates. Approximately linear measurements are made in a tracker fixed frame, then transformed to the computational frame.

An alternative approach is to compute in a rotating cartesian frame fixed to the tracker. In this case, linearity has been maintained, and the need for transformation has been eliminated.

These last two approaches have been both implemented, and proponents of each claim advantages of one in comparison to the other.

It is the purpose of this study to simulate both of the latter formulations in the error analysis mode in an attempt to resolve some of the conflicting claims.

The formulation using a fixed inertial (I) reference frame is established by an inertial measurement unit (IMU) and will be termed pure inertial. The formulation using rotating cartesian coordinates, aligned to the tracker line of sight (LOS) will be termed pure LOS. While pure LOS uses rate gyros to establish rotation rates, a third formulation will be considered which derives rates from an IMU, and will be termed a hybrid formulation. The three formulations under consideration are summarized below.

Formulation	Pure LOS (A)	Hybrid (B)	Pure Inertial (C)
Propagation of State	LOS	I	I
Propagation of Variance	LOS	LOS	I
Residual Formation	LOS	LOS	LOS
Reference	Rate Gyros	IMU	IMU

TABLE IV-1

An ultimate goal of the study is to compare decoupling in LOS to I. It is for this reason that propagation of variance in (B) is in LOS. However, given the presence of an IMU in (B), it is more accurate to propagate state in I. In all cases the residual is formed in the LOS frame. Cross range error consists of the error due to radar servo mistracking. Because these angular errors are quite small the measurements are very nearly linear.

The remaining sections of chapter IV consist of a detailed development of formulations A, B, and C.

B. Coordinate Frame Definition

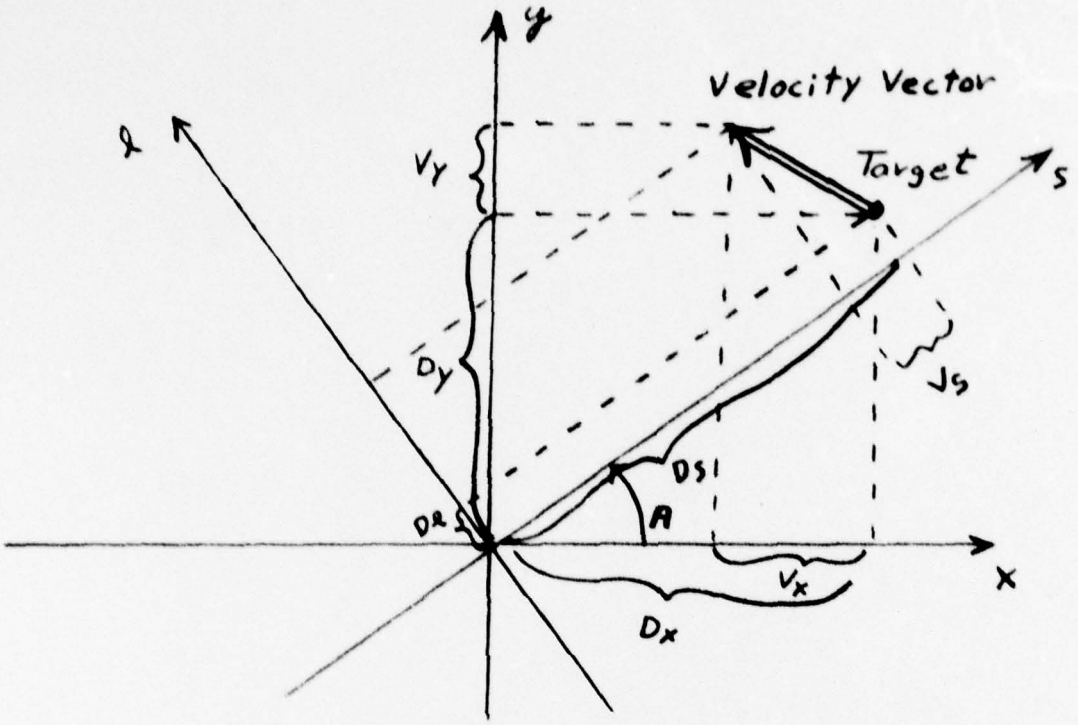

Figure IV-1

The (x,y) frame is fixed (I), where the target position and velocity are (D_x, D_y) and V_x, V_y) respectively.

The (s, ℓ) frame (LOS) is rotated through an angle, A, relative to (I), and is rotating at a rate $\dot{A}$. Target position and velocity are (D_s, D_ℓ) and V_s, V_ℓ) and are inertial quantities resolved onto these axes.

1. State Vectors

(I) $\underline{XI} = [D_x \; D_y \; V_x \; V_y \; a_x \; a_y]^T$ (1)

(LOS) $\underline{XL} = [D_s \; D_\ell \; V_s \; V_\ell \; a_s \; d_\ell]^T$ (2)

The study is carried out in two dimensions for the sake of simplicity. The extension to the third dimension is straightforward.

2. Transformation Matrices

From Figure 1, the Euler rotation which transforms (LOS) to (I) is as follows:

$$\begin{bmatrix} D_x \\ D_y \end{bmatrix} = \begin{bmatrix} \cos A & -\sin A \\ \sin A & \cos A \end{bmatrix} \begin{bmatrix} D_s \\ D_\ell \end{bmatrix} \tag{3}$$

Or, due to the orthogonality of the matrix,

$$\begin{bmatrix} D_s \\ D_\ell \end{bmatrix} = \begin{bmatrix} \cos A & \sin A \\ -\sin A & \cos A \end{bmatrix} \begin{bmatrix} D_x \\ D_y \end{bmatrix} \tag{4}$$

Define

$$[T] = \begin{bmatrix} \cos A & \sin A \\ -\sin A & \cos A \end{bmatrix} \tag{5}$$

Then

$$\begin{bmatrix} D_s \\ D_\ell \end{bmatrix} = [T] \begin{bmatrix} D_x \\ D_y \end{bmatrix} \tag{6}$$

and

$$\begin{bmatrix} D_x \\ D_y \end{bmatrix} = [T]^T \begin{bmatrix} D_s \\ D_\ell \end{bmatrix} \tag{7}$$

In order to transform the entire state vector, define a 6 x 6 transformation matrix:

$$[\Phi] = \begin{bmatrix} [T] & | & \\ \hline & [T] & | \\ \hline & | & [T] \end{bmatrix} \tag{8}$$

Then $\underline{XL} = [\Phi]\,\underline{XI}$ (9)

and $\underline{XI} = [\Phi]^T \underline{XL}$. (10)

It is assumed that [T] is available from the IMU. Alternatively, if rate gyros are used, [T] can be integrated from

$$\dot{[T]} = [\Omega][T] \; ; \; [T(0)] = I \tag{11}$$

where

$$[\Omega] = \begin{bmatrix} 0 & \dot{A} \\ \dot{A} & 0 \end{bmatrix} \equiv \begin{bmatrix} 0 & \Omega \\ -\Omega & \mathbf{0} \end{bmatrix} \tag{12}$$

This last method of computing [T] is included as a matter of interest. It is used if all computation is in the LOS frame and rate gyros are used. In our formulation A, these equations are incorporated in the state equations, and in formulation B, an IMU forms [T].

C. Equations of Motion

Look first at the deterministic equations of motion.

1. Inertial Frame

In inertial coordinates, the equations are straightforward in that velocity is the derivative of position, and acceleration the derivative of velocity. Furthermore, acceleration is modeled as a first order Markov process. The result is as follows:

$$\begin{bmatrix} \dot{D}_x \\ \dot{D}_y \\ \dot{V}_x \\ \dot{V}_y \\ \dot{a}_x \\ \dot{a}_y \end{bmatrix} = \begin{bmatrix} 0 & 0 & 1 & 0 & 0 & 0 \\ 0 & 0 & 0 & 1 & 0 & 0 \\ 0 & 0 & 0 & 0 & 1 & 0 \\ 0 & 0 & 0 & 0 & 0 & 1 \\ 0 & 0 & 0 & 0 & -b & 0 \\ 0 & 0 & 0 & 0 & 0 & -b \end{bmatrix} \begin{bmatrix} D_x \\ D_y \\ V_x \\ V_y \\ a_x \\ a_y \end{bmatrix} \tag{13}$$

or,

$$\dot{\underline{XI}} = [FI]\underline{XI} \tag{13a}$$

2. LOS Frame

There are at least two approaches to deriving the LOS equations of motion, one of which is by the consideration of the cross product which arises when one coordinate system is rotating relative

to another. A more straightforward approach is to apply the transformation matrix, [T], to equation (13a). The result is as follows:

$$\begin{bmatrix} \dot{D}_s \\ \dot{D}_\ell \\ \dot{V}_s \\ \dot{V}_\ell \\ \dot{a}_s \\ \dot{a}_\ell \end{bmatrix} = \begin{bmatrix} 0 & \Omega & 1 & 0 & 0 & 0 \\ -\Omega & 0 & 0 & 1 & 0 & 0 \\ 0 & 0 & 0 & \Omega & 1 & 0 \\ 0 & 0 & -\Omega & 0 & 0 & 1 \\ 0 & 0 & 0 & 0 & -b & \Omega \\ 0 & 0 & 0 & 0 & -\Omega & -b \end{bmatrix} \begin{bmatrix} D_s \\ D_\ell \\ V_s \\ V_\ell \\ a_s \\ a_\ell \end{bmatrix} \tag{14}$$

or,

$$\dot{\underline{XL}} = [FL]\underline{XL} \tag{14a}$$

Note that the equations of motion in both cases are linear, and so long as the Markov correlation time, (1/b), is not adapted, the inertial equations of motion are stationary. However, the LOS equations of motion are not stationary because $\Omega = \Omega(t)$, so $[FL] = [FL(t)]$.

As a result, the inertial state propagation may be carried out in closed form, and the state transition matrix is constant. However, for LOS, the state must be integrated, and the state transition matrix continually computed.

D. State Transition Matrices

1. Inertial Frame

The inertial STM follows from the Laplace transform of equation (13).

$$[\Phi I] = \mathcal{L}^{-1}\left\{ [sI-[FI]]^{-1} \right\} \tag{15}$$

$$[\Phi I] = \begin{bmatrix} 1 & 0 & t & 0 & \frac{1}{b^2}(e^{-bt}+bt-1) & \frac{1}{b^2}(e^{-bt}+bt-1) \\ 0 & 1 & 0 & t & 0 & 0 \\ 0 & 0 & 1 & 0 & \frac{1}{b}(1-e^{-bt}) & 0 \\ 0 & 0 & 0 & 1 & 0 & \frac{1}{b}(1-e^{-bt}) \\ 0 & 0 & 0 & 0 & e^{-bt} & 0 \\ 0 & 0 & 0 & 0 & 0 & e^{-bt} \end{bmatrix} \quad (16)$$

where $t = \Delta t = (t_{k+1} - t_k)$ (17)

2. LOS Frame

In principle, $[\Phi L]$ could be derived by transforms, given plenty of patience. However, it can be derived from $[\Phi I]$ as follows:

$$\underline{XI}_{k+1} = [\Phi I]\underline{XI}_k \quad (18)$$

but

$$\underline{XL}_k = [\Psi_k]\,\underline{XI}_k \Rightarrow \underline{XI}_k = [\Psi_k]^T\underline{XL}_k \quad (19)$$

$$\underline{XL}_{k+1} = [\Psi_{k+1}]\underline{XI}_{k+1} \Rightarrow \underline{XI}_{k+1} = [\Psi_{k+1}]^T\underline{XL}_{k+1} \quad (19a)$$

Substituting (19) and (19a) into (18),

$$[\Psi_{k+1}]^T\underline{XL}_{k+1} = [\Phi I][\Psi_k]^T\underline{XL}_k \quad (20)$$

$$\underline{XL}_{k+1} = [\Psi_{k+1}][\Phi I][\Psi_k]^T\underline{XL}_k \quad (21)$$

or,

$$\underline{XL}_{k+1} = [\Phi L]_k\underline{XL}_k \quad (22)$$

$$[\Phi L]_k = [\Psi_{k+1}][\Phi I][\Psi_k]^T \quad (23)$$

This is an "exact" state transition matrix as opposed to an "approximate" state transition matrix:

$$[\Phi L]_k \approx I + [FL]\Delta t \quad (23a)$$

The former is exact only up to the point that the angular rate, Ω, is linearly varying over the time interval Δt. The latter form is used in a real-time implementation due to the considerably reduced computational requirement.

E. State Noise and Propagation of Variance

While the deterministic differential equations are of the form

$$\dot{\underline{x}} = F\underline{x} \tag{24}$$

The stochastic differential equations are of the form

$$\dot{\underline{x}} = F\underline{x} + G\underline{w} \tag{25}$$

where $\underline{w}$ is a white noise vector.

1. LOS Formulation

The stochastic DE for the estimate $\hat{\underline{XL}}$ of $\underline{XL}$ is:

$$\begin{bmatrix} \dot{D}_s \\ \dot{D}_\ell \\ \dot{V}_s \\ \dot{V}_\ell \\ \dot{a}_s \\ \dot{a}_\ell \end{bmatrix} = \begin{bmatrix} 0 & \Omega & 1 & 0 & 0 & 0 \\ -\Omega & 0 & 0 & 1 & 0 & 0 \\ 0 & 0 & 0 & \Omega & 1 & 0 \\ 0 & 0 & -\Omega & 0 & 0 & 1 \\ 0 & 0 & 0 & 0 & -b & \Omega \\ 0 & 0 & 0 & 0 & -\Omega & -b \end{bmatrix} \begin{bmatrix} D_s \\ D_\ell \\ V_s \\ V_\ell \\ a_s \\ a_\ell \end{bmatrix} + \begin{bmatrix} \hat{D}_\ell & 0 & 0 \\ -\hat{D}_s & 0 & 0 \\ \hat{V}_\ell & 0 & 0 \\ -\hat{V}_s & 0 & 0 \\ \hat{a}_\ell & 1 & 0 \\ -\hat{a}_s & 0 & 1 \end{bmatrix} \begin{bmatrix} \beta \\ \gamma_s \\ \gamma_\ell \end{bmatrix} \tag{26}$$

The reason for the β term is as follows:

The true value of Ω is unknown, but is available only as a measured quantity:

$$\Omega_{meas} = \Omega_{true} + \beta \tag{27}$$

Note that this is not a measurement in the Kalman filter sense, but is a measurement nonetheless. The γ_s and γ_ℓ terms are those random jerque terms, due to target maneuverability, projected onto the s and ℓ axes.

The Q, or "noise", matrix differs for each of the three formulations. For this first formulation,

$$[QL] = E\left[\begin{bmatrix}\beta\\ \gamma_s\\ \gamma_e\end{bmatrix}[\beta\ \delta_s\ \delta_e]\right] = \left[\begin{array}{c|cc} Q_\beta & & \\ \hline & & \\ & Q_{\gamma L} & \end{array}\right] \tag{28}$$

where Q_β = variance (β)

$Q_{\gamma L}$ = spectral matrix due to the Markov process.

The discrete equivalent of the continuous [QL] is

$$[QL_k] = \left[\begin{array}{c|cc} Q_\beta \Delta t^2 & & \\ \hline & & \\ & Q_{\gamma L_k}\Delta t & \end{array}\right] \tag{29}$$

Note that the spectral term builds as Δt because it represents a continuous physical process. On the other hand, the variance term builds as Δt^2 due to the fact that a rotation rate Ω is sampled, and held constant computationally for Δt.

Actually, Q_β is not the same for the two formulations in which LOS propagation of variance is used. For the first formulation, Q_β reflects the error in the rate gyro and the sampling process. For the second formulation, Ω is derived by numerical differencing - normally a horrible practice in a sensitive computation, but less so in this less sensitive propagation of variance application.

Propagation of variance follows:

$$[PL_k]' = [\Phi L_k][PL_k][\Phi L_k]^T + [GL_k][QL_k][GL_k]^T \tag{30}$$

An expanded alternate way of writing this equation follows if we define

$$\underline{g} = [\hat{D}_\ell \quad -\hat{D}_s \quad \hat{V}_\ell \quad -\hat{V}_s \quad \hat{a}_\ell \quad -\hat{a}_s]^T \tag{31}$$

then

$$[PL_{k+1}]' = [\Phi L_k][PL_k][\Phi L_k]^T + \underline{g}(Q_\beta \Delta t)\underline{g}^T + \left[\begin{array}{c|c} 0_{4x4} & 0_{4x2} \\ \hline 0_{2x4} & Q_{\gamma L_k}\Delta t \end{array}\right] \tag{32}$$

2. Inertial Formulation

The system matrix [FI] in the inertial formulation contains no measured quantities as did [FL].

$$\begin{bmatrix} \dot{D}_x \\ \dot{D}_y \\ \dot{V}_x \\ \dot{V}_y \\ \dot{a}_x \\ \dot{a}_y \end{bmatrix} = \begin{bmatrix} 0 & 0 & 1 & 0 & 0 & 0 \\ 0 & 0 & 0 & 1 & 0 & 0 \\ 0 & 0 & 0 & 0 & 1 & 0 \\ 0 & 0 & 0 & 0 & 0 & 1 \\ 0 & 0 & 0 & 0 & -b & 0 \\ 0 & 0 & 0 & 0 & 0 & -b \end{bmatrix} \begin{bmatrix} D_x \\ D_y \\ V_x \\ V_y \\ a_x \\ a_y \end{bmatrix} + \begin{bmatrix} 0 & 0 \\ 0 & 0 \\ 0 & 0 \\ 0 & 0 \\ 1 & 0 \\ 0 & 1 \end{bmatrix} \begin{bmatrix} \gamma_x \\ \gamma_y \end{bmatrix} \tag{33}$$

Here, γ_x and γ_y are the target random jerque terms projected onto the x and y axes. Then

$$[QI] = E\left[\begin{bmatrix} \gamma_x \\ \gamma_y \end{bmatrix} [\gamma_x \gamma_y] \right] = \left[Q_{\delta I} \right] \tag{34}$$

and

$$[Q_{\gamma I_k}] = [Q_{\gamma I_k}\Delta t] \tag{35}$$

Propagation of variance in the inertial frame then follows:

$$[PI_{k+1}]' = [\Phi I][PI_k][\Phi I]^T + \left[\begin{array}{c|c} 0_{4\ x\ 4} & 0_{4\ x\ 2} \\ \hline 0_{2\ x\ 4} & Q_{\gamma I}\Delta t \end{array}\right] \tag{36}$$

3. Projection of the Spectral Matrix onto the Computational Frame

It is a reasonable assumption that the acceleration capability of an aircraft normal to its velocity vector is greater than that along

it velocity vector. Suppose that the Markov spectral matrix is body oriented:

$$[Q_b] = \begin{bmatrix} q_u & 0 \\ 0 & q_v \end{bmatrix} \tag{37}$$

qu is the spectral term along the target velocity vector, while q_v is the term normal to the velocity vector. In that case, $q_u < q_v$. It can be shown that the following is the rotation from $[Q_b]$ from aircraft axes to inertial axes.

$$[Q_{YI}] = \frac{1}{(\hat{v}_x^2+\hat{v}_y^2)} \begin{bmatrix} (\hat{v}_x^2 q_u+\hat{v}_y^2 q_u) & (\hat{v}_x\hat{v}_y q_u-\hat{v}_x\hat{v}_y q_u) \\ (\hat{v}_x\hat{v}_y q_u-\hat{v}_x\hat{v}_y q_u) & (\hat{v}_y^2 q_u+\hat{v}_x^2 q_u) \end{bmatrix} \tag{38}$$

In the same way, $[Q_b]$ is rotated to the LOS axes.

$$[Q_{YL}] = \frac{1}{(\hat{v}_s^2+\hat{v}_\ell^2)} \begin{bmatrix} (\hat{v}_s^2 q_u+\hat{v}_\ell^2 q_u) & (\hat{v}_s\hat{v}_\ell q_u-\hat{v}_s\hat{v}_\ell q_v) \\ (\hat{v}_s\hat{v}_\ell q_u-\hat{v}_s\hat{v}_\ell q_v) & (\hat{v}_\ell^2 q_u+\hat{v}_s^2 q_v) \end{bmatrix} \tag{39}$$

F. Measurements and Measurement Noise

While no measurements are simulated as such in the error analysis mode, it is useful to look at the Kalman measurement equation transformations. In all cases, measurements are made as displacements along the tracker axes.

$$\underline{YL} = [HL]\,\underline{XL} + \underline{v} \tag{40}$$

where

$\underline{v}$ = measurement error

and $$[HL] = \begin{bmatrix} 1 & 0 & 0 & 0 & 0 & 0 \\ 0 & 1 & 0 & 0 & 0 & 0 \end{bmatrix}$$

1. Formulation (A)

$$\underline{\hat{XL}}_{k+1} = [\Phi L_k]\underline{\hat{XL}}_k + [kL_{k+1}]\left(\underline{YL}_{k+1} - [HL][\Phi L_k][\underline{\hat{XL}}_k]\right) \tag{41}$$

Suppose that the radar range variance is given by σ_r^2, and its cross range angular variance is given by $\sigma^2_{\Delta T}$. If the measurement noise covariance matrix is given by

$$[R] = E[\underline{v}\,\underline{v}^T] = \begin{bmatrix} R_{11} & R_{12} \\ R_{21} & R_{22} \end{bmatrix} \tag{42}$$

It can be shown that

$$RL_{11} = \sigma^2 r$$

$$RL_{22} = \left(\frac{\hat{D}_\ell}{\hat{D}_s}\right)^2 \sigma_r^2 + (\hat{D}_s)^2 \sigma^2_{\Delta T} \tag{43}$$

$RL_{12} = RL_{21} = 0$ assuming independence between range and cross range.

2. Formulation (B)

In this case, for the sake of fast and accurate propagation of state, this operation is carried out in inertial coordinates, while propagation of variance takes place in LOS coordinates. (44)

$$\underline{\hat{XI}}_{k+1} = [\Phi I]\underline{\hat{XI}}_k + [\Psi_{k+1}]^T[kL_{k+1}]\left(\underline{YL}_{k+1} - [HL][T_{k+1}][\Phi I]\underline{\hat{XI}}_k\right)$$

The projected inertial state estimate is transformed to form the LOS residual, which is multiplied by a gain [kL] formed by LOS terms. The result is transformed back to the inertial frame. The measurement noise terms are similar to the first formulation, but the cross range angular measurement picks up an additional error: the error in the IMU angular position measurement. Suppose that the variance of this error is given by $\sigma^2_{\Delta A}$.

Then $RL_{11} = \sigma_r^2$

$$RL_{22} = \left(\frac{D_\ell}{\hat{D}_s}\right)^2 \sigma_r^2 + \left(\hat{D}_s\right)^2 \left(\sigma^2_{\Delta T} + \sigma^2_{\Delta A}\right) \tag{45}$$

$$RL_{11} = RL_{22} = 0$$

3. Formulation (C)

Here, both state and variance are propagated in inertial coordinate, while the residual is still in LOS. (46)

$$\underline{\hat{XI}}_{k+1} = [\Phi I]\underline{\hat{XI}}_k + [kI_{k+1}][T]^T \left(\underline{YL}_{k+1} - [HL][\P_{k+1}][\Phi I]\underline{\hat{XI}}_k\right)$$

In this case, the gain [kI] is formed from inertial terms, so the noise terms in equation (45) still apply, but rotated into the inertial frame.

$$[RI] = \begin{bmatrix} (\cos^2 A)r_{11} + (\sin^2 A)r_{22} & (\cos A)(\sin A)(r_{11} - r_{22}) \\ (\cos A)(\sin A)(r_{11} - r_{22}) & (\cos^2 A)r_{22} + (\sin^2 A)r_{11} \end{bmatrix} \tag{47}$$

where

$$r_{11} = \sigma_r^2$$

$$r_{22} = \left(\frac{\hat{D}_\ell}{\hat{D}_s}\right)^2 \sigma_r^2 + (\hat{D}_s)^2(\sigma^2_{\Delta T} + \sigma^2_{\Delta A})$$

$$r_{11} = r_{22} = 0$$

and

$$\begin{bmatrix} \hat{D}_s \\ \hat{D}_\ell \end{bmatrix} = [T]^T \begin{bmatrix} \hat{D}_x \\ \hat{D}_y \end{bmatrix} \tag{48}$$

It should be noted here that while some of these noise terms are getting a bit complicated, the filter is still fully coupled. The truth model will show the effects of approximations.

G. Kalman Gain

1. LOS Gain

The Kalman gain, given by

$$[kL_{k+1}] = [PL_{k+1}]'[HL]^T \left([HL][PL_{k+1}]'[HL]^T + [RL]\right)^{-1} \tag{49}$$

can be simplified, considering the form of [HL]

$$[kL_{k+1}] = \begin{bmatrix} pl'_{11} & pl'_{12} \\ pl'_{21} & pl'_{22} \\ pl'_{31} & pl'_{32} \\ pl'_{41} & pl'_{42} \\ pl'_{51} & pl'_{52} \\ pl'_{61} & pl'_{62} \end{bmatrix} \begin{bmatrix} (pl'_{11} + RL_{11}) & (pl'_{12} + RL_{12}) \\ (pl'_{21} + RL_{21}) & (pl'_{22} + RL_{22}) \end{bmatrix}^{-1} \tag{50}$$

2. Inertial Gain

In the same way,

$$[kI_{k+1}] = \begin{bmatrix} pi'_{11} & pi'_{12} \\ pi'_{21} & pi'_{22} \\ pi'_{31} & pi'_{32} \\ pi'_{41} & pi'_{42} \\ pi'_{51} & pi'_{52} \\ pi'_{61} & pi'_{62} \end{bmatrix} \begin{bmatrix} (pi'_{11} + RI_{11}) & (pi'_{11} + RI_{12}) \\ (pi'_{21} + RI_{21}) & (pi'_{22} + RI_{22}) \end{bmatrix}^{-1} \tag{51}$$

H. A Posteriori Covariance

When the Kalman gain is optimally computed, the short form covariance may be used.

$$[P_{k+1}] = (I - [k_{k+1}][H])[P'_{k+1}] \tag{52}$$

This form will also be used in the sub-optimal filters.

However, the truth model uses the Joseph form to compute the true covariance resulting from a sub-optimally formed gain.

$$[P_{k+1}] = (I - [k_{k+1}][H])[P'_{k+1}](I - [k_{k+1}][H])^T + [K_{k+1}][R_{k+1}][k_{k+1}]^T \quad (53)$$

V. Means of Filter Performance Evaluation

A. Numerical Values

1. Reference Accuracy

Formulation A requires a rate gyro, while formulations B and C require an IMU. The values chosen for rate gyro rate error standard deviation, σ_β, and IMU angular position error standard deviation, $\sigma_{\Delta A}$, were chosen to yield approximately equal estimation accuracy for the decoupled filters when the target trajectory is parallel to an axis in the inertial computational frame.

$$\sigma_\beta = 5 \text{ mr./sec.} \tag{54}$$

$$\sigma_{\Delta A} = 2 \text{ mr.} \tag{55}$$

All secondary reference error sources were neglected. Specifically, IMU drift was neglected due to the short time duration of individual anti-aircraft encounters.

2. Measurement Error

Measurements, in the Kalman Filter sense, include radar range error, σ_R, and cross range error, $\sigma_{\Delta T}$. Nominal values were chosen as

$$\sigma_R = 5 \text{ m.} \tag{56}$$

$$\sigma_{\Delta T} = 1 \text{ mr.} \tag{57}$$

3. Markov Acceleration Model Parameters

The standard deviation in target acceleration was chosen to be $\sigma_{ac} = 2 \text{ m/sec}^2$, and the Markov time constant to be $\tau = 5$ sec. From this follows the Markov spectral terms:

$$q_u = \frac{2\sigma^2_{ac}}{\tau} \tag{58}$$

$$q_u = 4\, q_u \tag{59}$$

The u and v terms correspond to the target vector respectively. The above quantities were chosen based upon previous experience where a solutional mode Kalman Filter was processing actual flight data.

B. Target Trajectories

Even to the extent to which the target state estimation problem has been simplified to this point, it is difficult to draw conclusions applicable to all target trajectories. Since a primary objective has been to examine the impact of decoupling in I or LOS coordinates, two trajectories were chosen: both of which are a non-accelerating straight line fly-by, but one is parallel to an axis of the fixed computational frame, while the other is set at 45° to the axis. Both are shown in Figure V-1.

Test Trajectories

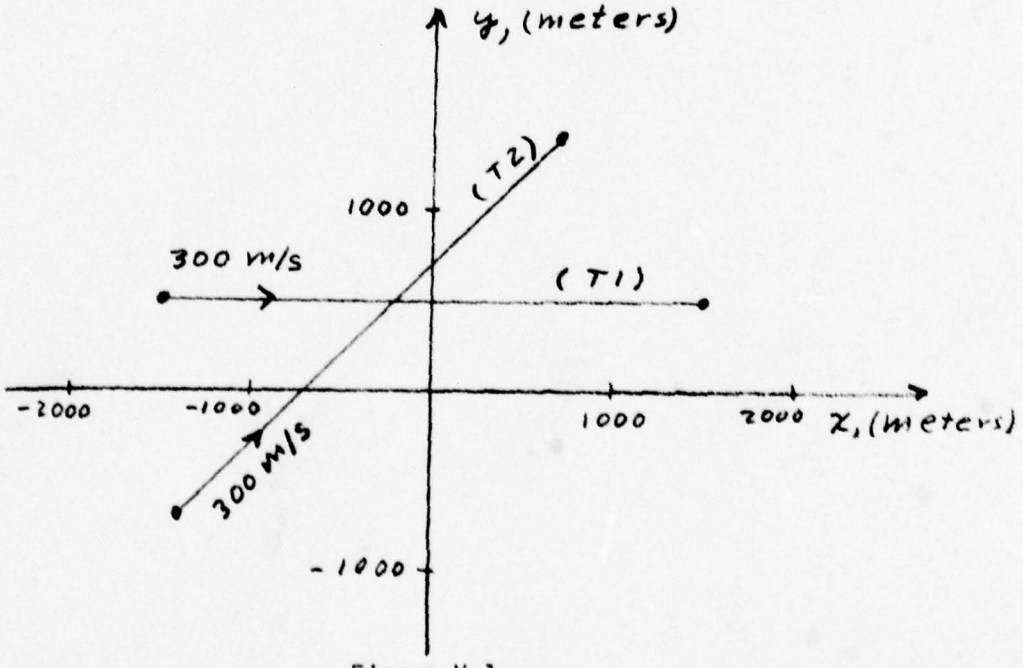

Figure V-1

C. Truth Model

Given the form of the Kalman Filter estimation equation,

$$\hat{\underline{x}}_{k+1} = \Phi_k \hat{\underline{x}}_k + K_{k+1}(\underline{y}_{k+1} - H_{k+1}\Phi_k \hat{\underline{x}}_k) \tag{60}$$

If the optimal Kalman gain, K_{k+1}, computed according to the equation

$$K_{k+1} = P_{k+1}' H_{k+1}^T (H_{k+1} P'_{k+1} H_{k+1}^T + R_{k+1})^{-1} \tag{61}$$

When all of the Kalman Filter equations precisely describe the given problem, then the a posteriori covariance is given by

$$P_{k+1} = (I - K_{k+1}H_{k+1})P'_{k+1} \cdot \tag{62}$$

In practice, if the gain is not optimal due to inadvertent mismodeling or due to purposeful sub-optimization, then the following Joseph form a posteriori equation reflects the measurement incorporation regardless of how K_{k+1} was obtained:

$$P_{k+1} = (I - K_{k+1}H_{k+1})P'_{k+1}(I - K_{k+1}H_{k+1})^T + K_{k+1}R_{K+1}K_{k+1}^T \tag{63}$$

This last equation is the essence of the truth model. The complete truth model, however, incorporates propagation of variance according to the same correct dynamics and state noise error sources found in the sub-optimal filter. The truth model concept is shown below.

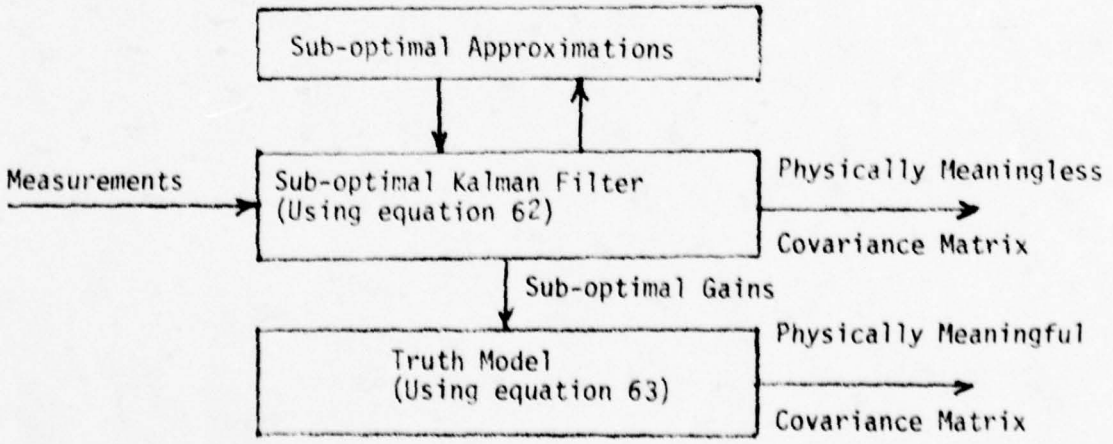

Figure V-2

All truth model computations are carried out in fixed cartesian coordinates to obtain the accuracy of an exact state transition matrix.

D. Error Statistics at the Target

While the covariance matrix produced by the truth model is correct to the extent that the various model parameters are realistic, it does not directly convey the information of interest, which is the likelihood of hitting a target. What is required is the position error ellipse at the target which applies at the time when the projectile reaches the target.

1. Projection of Covariance

Following the K^{th} measurement at time t_k, the truth model covariance matrix, P_k, exists. It is most conveniently projected ahead in time in a fixed cartesian frame as follows:

$$PP_k = [\Phi I(TF)][P_k][\Phi I(TF)]^T \tag{64}$$

The closed form state transition matrix is given for any time interval, t, by equation (16). In this application, the time to be substituted into ΦI is the projectile time of flight. The simple time of flight expression used here is

$$TF_k = \frac{RP_k}{B - \left(\frac{C}{2}\right) RP_k \quad B} \tag{65}$$

where

$B = 1200$ m/s

$C = 0.007$ (m sec)$^{-1/2}$

This time of flight is a function of range which is, of course, a function of time of flight. Projected range follows from

$$\underline{XP}_k = [\Phi I(TF_k)]\underline{XI}_k \tag{66a}$$

and

$$RP_k = [DP^2_{XK} + DP^2_{YK}]^{1/2} \tag{66b}$$

Equations (65) and (66) are solved iteratively to produce the time of flight required in equation (64). DP_{XK} and DP_{YK} in (66b) are the first two terms in the projected inertial state vector, $\underline{XP}_k$.

2. Error Ellipse

All random variables within the Kalman Filter and Truth Model are assumed to be Gaussian. In two dimensional space, the curve of equal probability density is an ellipse, given by

$$\underline{XP}^T P^{-1} \underline{XP} = c^2 \tag{67}$$

Here $\underline{XP}$ is a two vector, $\underline{XP} = [DP_x \; DP_y]^T$, and P is the 2x2 position covariance matrix extracted from equation (64).

The constant c^2 follows a chi-square distribution with two degrees of freecom. If c = 1.180, equation (67) describes a parabola about the target such that the projectile is equally likely to fall within the ellipse as it is to fall outside of the ellipse. The ellipses shown in the results are then the "50%" ellipses.

3. Performance Criteria

The error ellipse about the target varies as a function of time for any given filter formulation. It is desirable to reduce all of this projected data to a single scalar figure of merit to facilitate the comparison of one formulation to another. In fact, two are used which are as follows.

a) Sum Square Error

If PP_k is the projected covariance from the measurement at time k, then the x direction and y direction variances are, respectively

$$\sigma^2_{XK} = PP_{K_{1,1}} \tag{68}$$

$$\sigma^2_{YK} = PP_{K_{2,2}} \tag{69}$$

The sum square error in both directions, over NM measurements is then

$$SSE = \sum_{k=1}^{NM} (\sigma^2_{XK} + \sigma^2_{YK}) \tag{70}$$

the mean square error is then

$$MSE = \frac{1}{NM} \sum_{k=1}^{NM} (\sigma^2_{XK} + \sigma^2_{YK}) \tag{71}$$

It will be of interest, for instance, to observe successive increments in error if more and more sub-optimal approximations are incorporated into a given formulation.

b) RSS Error Ratio (ζ)

Another performance criterion relates the performance of a particular formulation to a theoretical "best" possible formulation.

Suppose, as before, the projected position various are σ^2_{XK} and σ^2_{YK}. The root sum square error is then

$$RSS_K = \sqrt{\sigma^2_{XK} + \sigma^2_{YK}} \tag{72}$$

Furthermore, suppose that the RSS position error of the "best" filter at the same time is

$$RSS^*_K = \sqrt{\sigma^{2*}_{XK} + \sigma^{2*}_{YK}} \tag{73}$$

Then the average ratio of these RSS errors is

$$\zeta = \frac{1}{NM} \sum_{K=1}^{NM} \frac{RSS^*_K}{RSS_K} \tag{74}$$

Naturally, since any practical formulation can only approach the ideal, $RSS_K > RSS^*_K$ and

$$0 < \zeta < 1. \tag{75}$$

What is the "best", or ideal, filter? For our purposes it will be defined as a fully coupled filter containing no approximate computations, and making perfect measurements. The sole source of an error ellipse, or RSS_K^*, is the uncertainty due to uncertain target maneuverability. The ideal filter is, in this case, computed in fixed inertial coordinates due to the availability of an exact state transition matrix.

4. Run Sequence

In order to compute the above performance criteria, the following sequence is followed.

a) Establishment of Reference

The reference consists of a file, BREF, containing the sequence RSS_K^*, $1 \leq K \leq NM$. This reference is unique to a given trajectory and target model. So long as these do not change, the reference file, once established, need not be changed.

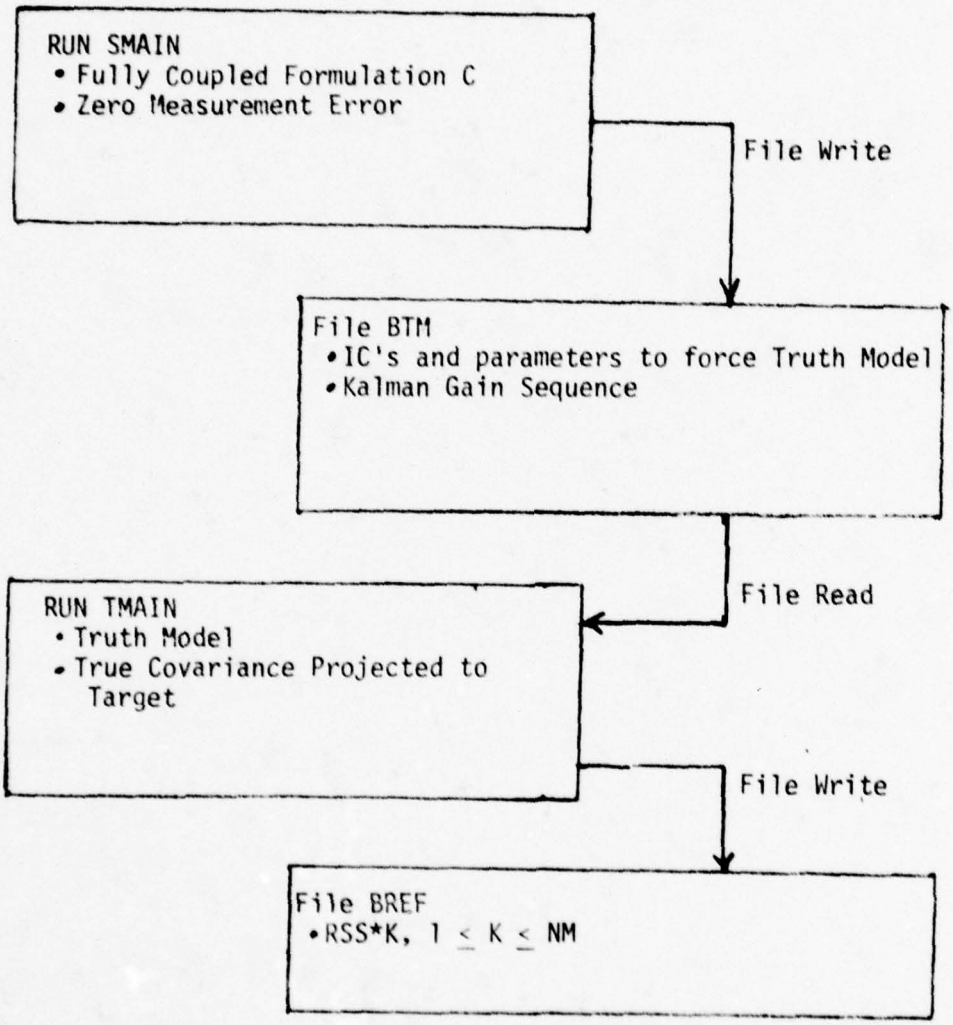
RUN SMAIN
• Fully Coupled Formulation C
• Zero Measurement Error
File Write
File BTM
•IC's and parameters to force Truth Model
•Kalman Gain Sequence
File Read
RUN TMAIN
• Truth Model
• True Covariance Projected to Target
File Write
File BREF
•RSS*K, 1 ≤ K ≤ NM

Figure V-3

b) Sub-Optimal Run and Evaluation

To perform this sequence, program SMAIN simulates the sub-optimal filter, then TMAIN computes the true covariance and then the performance criteria.

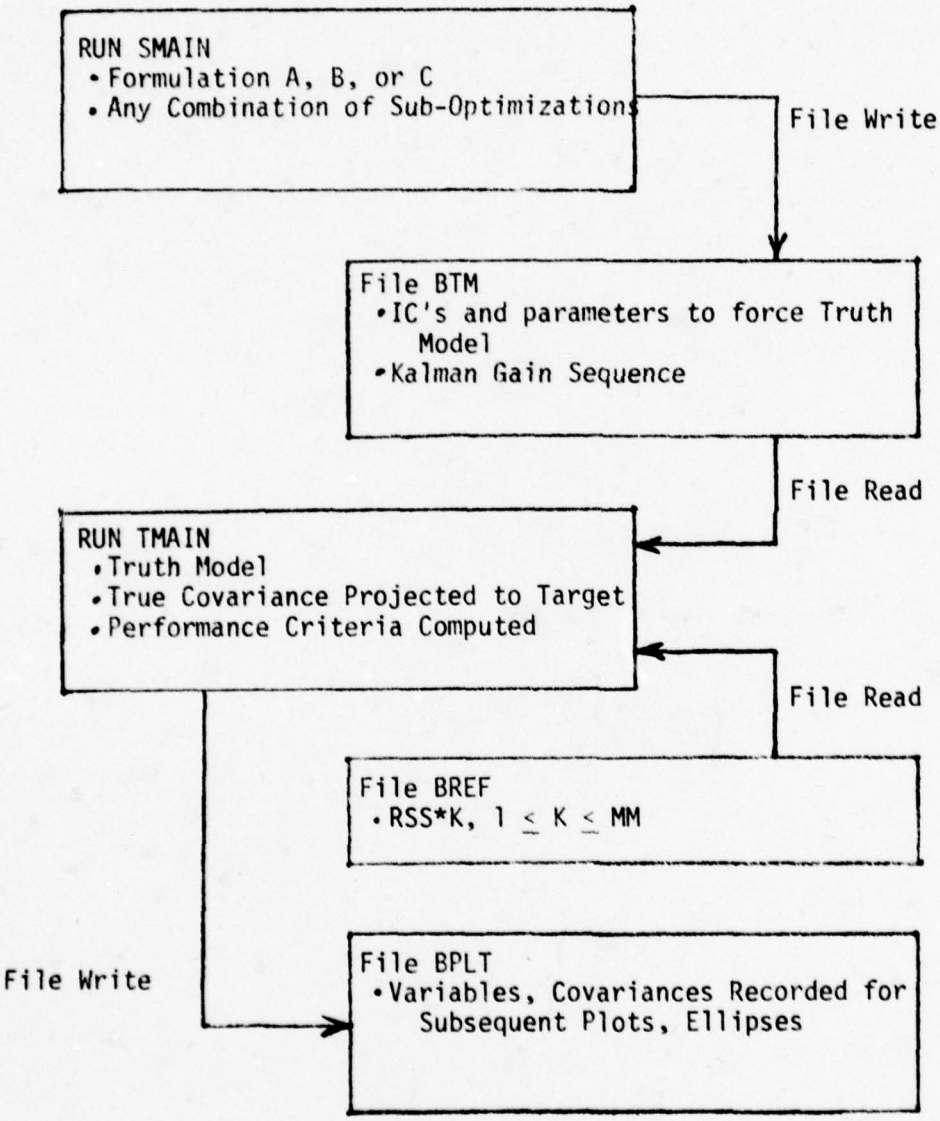

VI. Results

A. Sub-Optimization Sequence

For each of the three formulations considered, it is possible to start with a "perfect" filter, yielding estimation error due only to target maneuverability, then to see the amount of error added at each step along the way to a real-time implemented sub-optimal filter.

1. Formulation (A)

In formulation A, both state and variance are propagated in LOS coordinates. The sub-optimization steps are as follows:

- "perfect", or reference filter
- Introduction of rate gyro error, σ_β
- Approximation of state transition matrix by first two terms of a Taylor series

$$\Phi_L \tilde{=} I + F_L \Delta t \tag{76}$$

- Decoupling of covariance. In order to accomplish a real-time solution, decoupling is required where covariances between position, velocity, and acceleration in the s direction and those in the ℓ direction are assumed to be zero. Decoupling in this line of sight axis will be abbreviated LOS DEC.

2. Formulation (B)

In this formulation, propagation of state takes place in inertial (I) coordinates, and propagation of variance in LOS coordinates. The sub-optimization steps are as follows:

- "perfect", or reference filter
- Introduction of IMU angular measurement error, $\sigma_{\Delta A}$
- Numerical differencing of IMU position to produce rates

required for state transition matrix

- Approximate STM:

$$\Phi_L = I + F_L \Delta t$$

- Decoupling of covariance matrix in LOS coordinates (LOS DEC)

3. Formulation (C)

Here, both state and variance are propaged in inertial coordinates. Recall that the state transition matrix may use written in closed form, without approximation. The sub-optimization stops are as follows:

- "perfect", or reference filter
- Introduction of IMU angular measurement error
- Decoupling of covariance matrix in inertial (I) coordinates (I DEC)

B. *Fully Coupled Sensitivities to Measurement Error*

The conditions under which the following sensitivities were computed are as follows:

- Trajectory #1 (10 second fly-by at 300 m/s, 500 m range at cross-over)
- 8 Hz measurement rate
- Single propagation of state and variance in between each measurement
- All previously outlined sub-optimization steps are in effect with the exception of decoupling.

Referring to Figures VI-1, VI-2, and VI-3, the following observations may be made

- The percent increase in mean square error takes as a baseline the reference filter.

- Apparent in formulation A and B is a lower limit of 2.6% below which the error increase will not fall as measurement error approaches zero. This error is due to the first order $\Phi_L \cong I + F_L \Delta t$ approximation.
- No such limit is observed for formulation C where an exact state transition matrix is available.
- The limit in A and B is not a fundamental limitation, but is a function of the order of the state transition matrix (STM) approximation and the time interval over which the approximate STM is effective. In other words, there is considerable flexibility in modifying this limit.
- Note the approximately equivalent accuracy for $\sigma_\beta = 5$ mr/s in A and $\sigma_{\Delta A} = 2$ mr in B. These numbers will form the baseline for comparisons to follow.

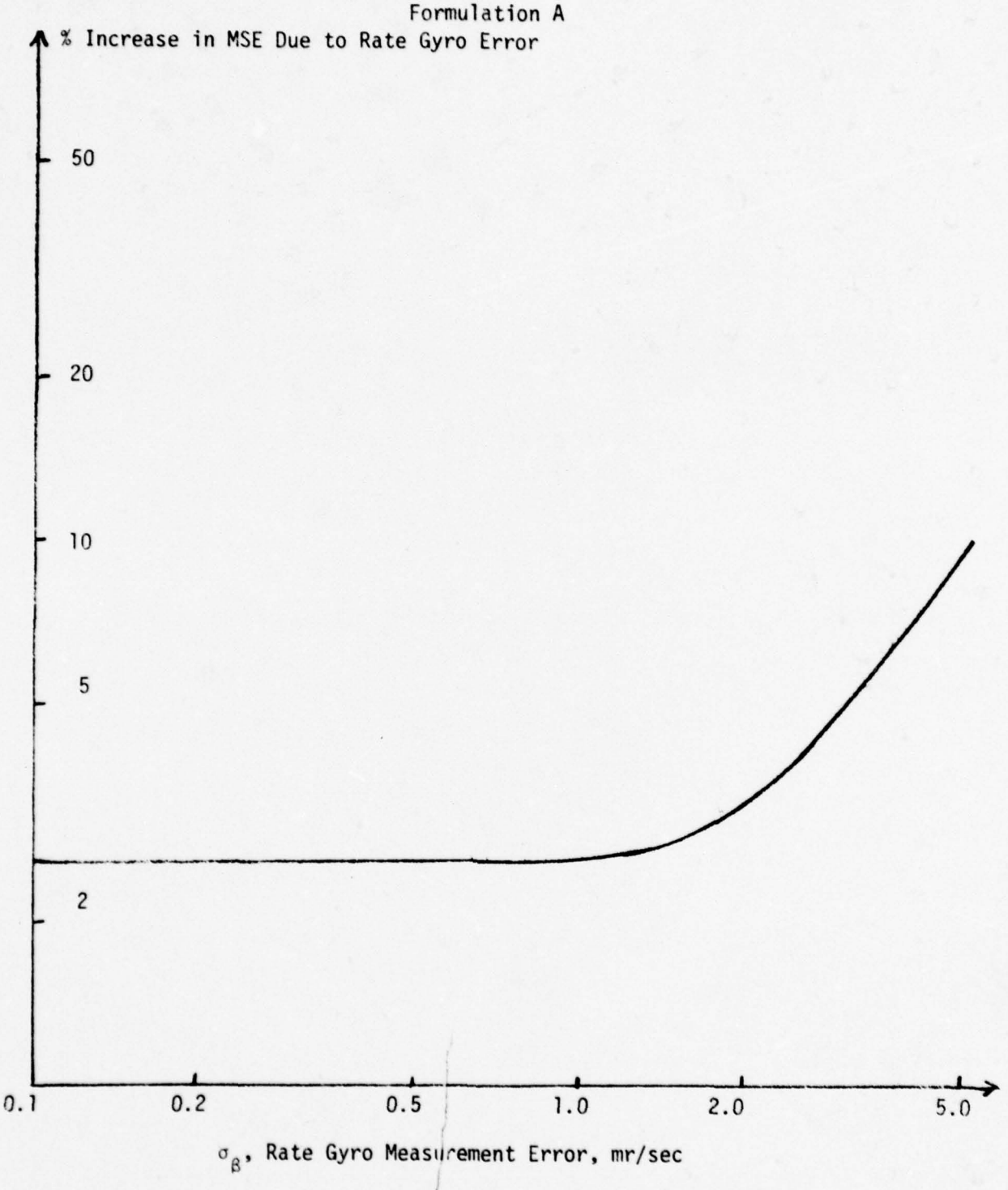
Formulation A
% Increase in MSE Due to Rate Gyro Error
50
20
10
5
2
0.1
0.2
0.5
1.0
2.0
5.0
σ_β, Rate Gyro Measurement Error, mr/sec

Figure VI-1

Formulation B

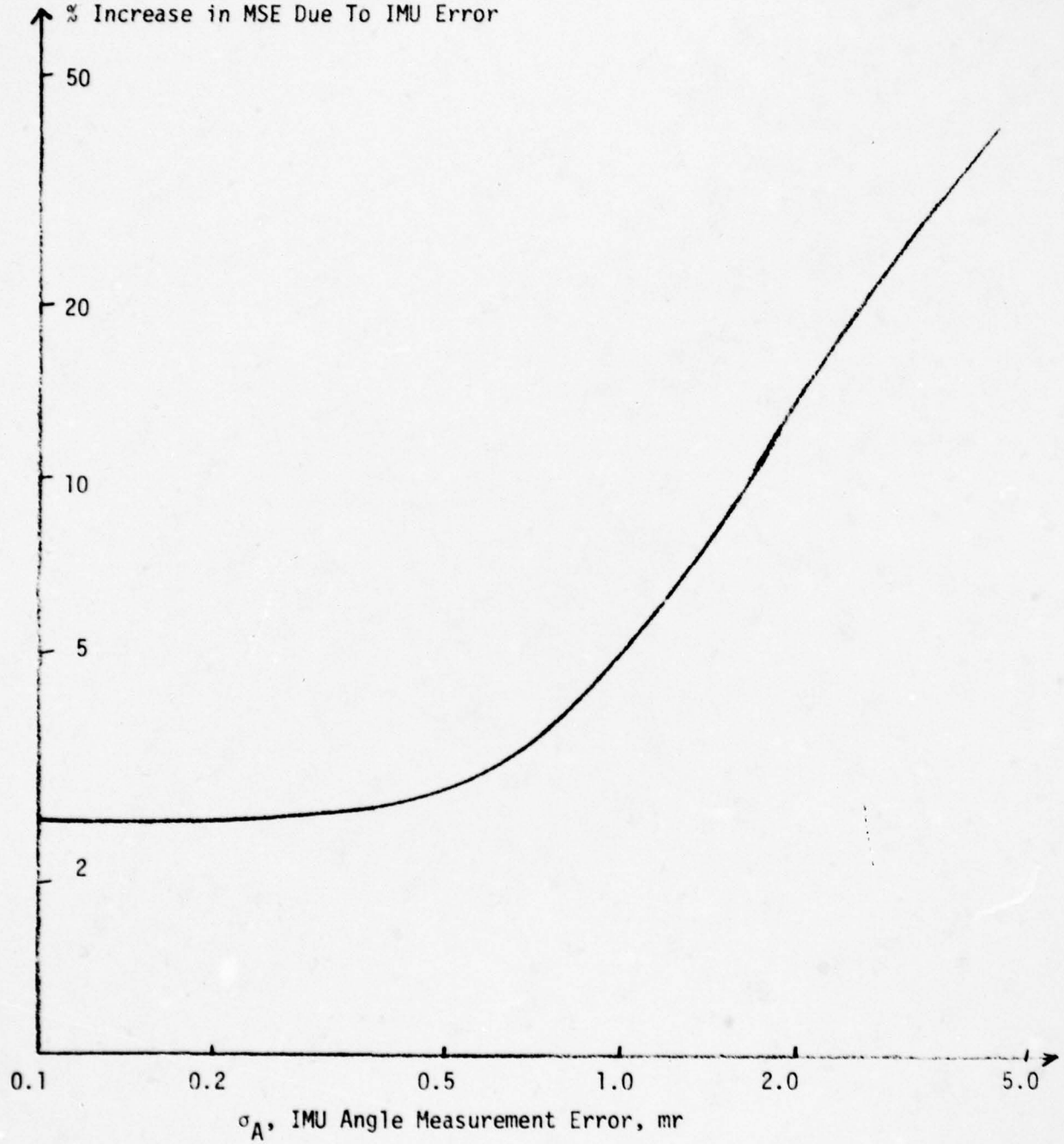

Figure VI-2

Formulation C

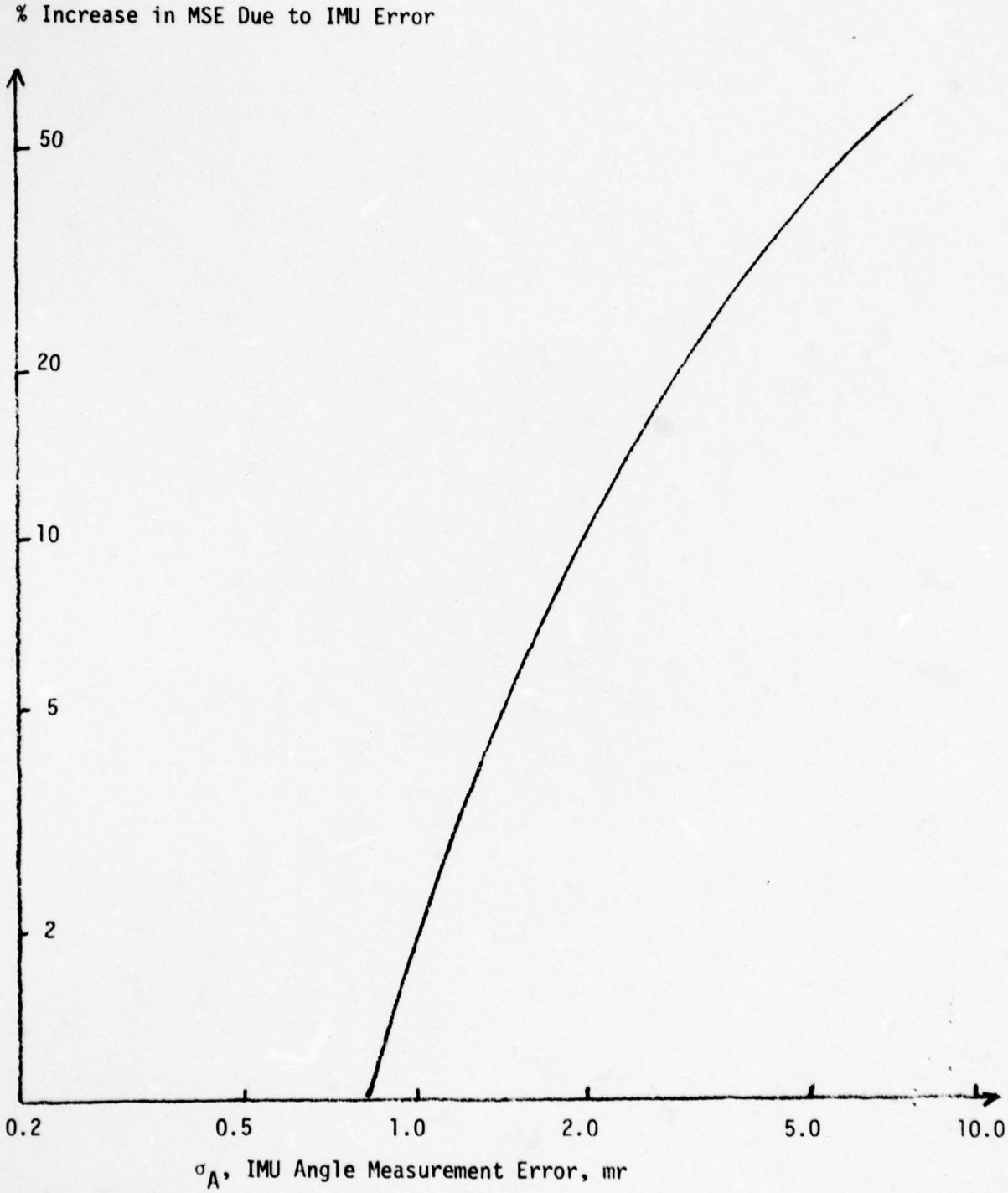

Figure VI-3

C. Added Error in Real Filters

Referring to Figure VI-4, it may be seen the error contributions of each of several steps from the perfect measurement reference filter to the real-time decoupled filter. The following observations will help in interpreting the figure.

- The baseline error is due only to the target maneuver uncertainty.
- Rate gyro and IMU errors were chosen to provide approximately equivalent performance in formulations A and C, trajectory #1.
- These results are not general. They are to some extent trajectory dependent.
- Recall that trajectory #1 is parallel to an axis of the inertial computational frame, while trajectory #2 is at 45° to the axes. When variance is propagated in LOS coordinates, as in A and B, there is naturally no difference in results in comparing these two trajectories.
- When variance is propagated in the inertial frame, a greater penalty is paid due to decoupling when the target is flying at 45° to the axes. More will be said about decoupling in section VI.D.
- The error contribution due to the approximate computation of the LOS STM can be reduced by a higher order approximation or multiple propagation steps in between measurements.
- The error due to numerical differencing in B required to form angular rates does not appear in the figure. The derived angular rate is needed only in producing some STM terms for propagation of variance, because state is propagated in inertial coordinates. The use of the derived rates is in such an

uncritical computation that the added error is only 0.03%. An analytical solution for this last figure is difficult. Rather, a random number generator corrupted IMU angular position measurement before deriving rates. This result is then the result of a Monte Carlo simulation.

D. Computation of Kalman Gain: Comparison of LOS Coordinates Versus Inertial Coordinates

Figure VI-4, in the previous section, showed a marked difference in added error when decoupling is performed in LOS coordinates as compared to inertial coordinates. In order to understand the reasons for this difference, it is probably most easily done by examining graphical results.

1. Position Variance

Figure VI-5 shows for trajectory #1 the variance in LOS range ($\sigma_{D_s}^2$), cross range ($\sigma_{D_\ell}^2$), and the covariance (σ_{D_s,D_ℓ}). The trajectory period is 10 seconds, and the filter transient is substantially complete in two seconds. Figure VI-6 shows the corresponding quantities in inertial (I) coordinates. Recall from Figure V-1 that trajectory #1 consists of of a straight line fly-by parallel to the inertial x axis, crossing the y axis at a range of 500m at 5 seconds. The I position variances are then σ^2_x and σ^2_y while the covariance is $\sigma_{x,y}$. These plots are often taken from terms of the LOS and I covariance matrices, respectively, when the filters are not yet decoupled.

The variances exhibit the typical Kalman Filter pattern: growth during intermeasurement periods, and abrupt drops at measurement

Percent Increase in Mean Square Error Due to Sub-Optimization

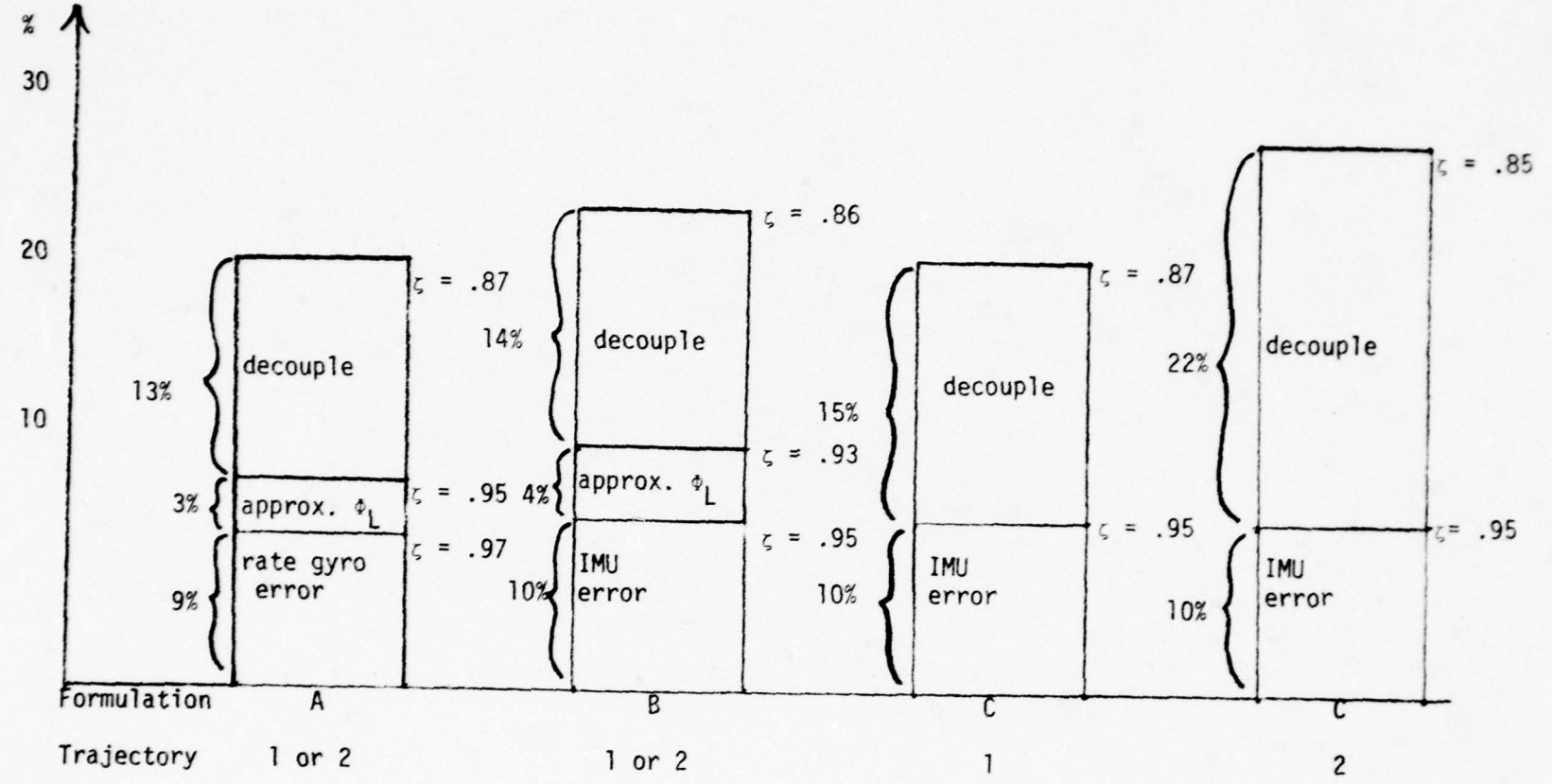

Figure VI-4

times. Before decoupling, the sum square uncertainty is much the same for LOS and I:

$$(\sigma^2_{D_s}(t) + \sigma^2_{D_\ell}(t)) \approx (\sigma^2_{D_x}(t) + \sigma^2_{D_y}(t)) \tag{78}$$

the notable difference is that in general, the LOS covariance is much less than the I counterpart.

$$|\sigma_{D_s D_\ell}| < |\sigma_{D_x,D_y}| \tag{79}$$

A small covariance indicates that the error ellipse is closely aligned to the coordinate axes. Figure VI-7,8,9,10, 11 show a time sequence of LOS position error ellipses demonstrating the near alignment of the position ellipses with the LOS axes. While LOS ellipses were plotted, I ellipses could have been. Prior to decoupling, they look essentially the same.

The reason for this alignment is as follows. The error ellipses have a natural tendency to grow parallel to the aircraft axes due to the aircraft's greater acceleration uncertainty normal to its velocity vector in comparison to the uncertainty along the velocity vector. However, the measurements made by the radar are made in range (along the s axis) and cross range (along the ℓ axis). Due to this measurement geometry, the a posterior position error ellipses are continually realigned to the tracker (LOS) axes. The implications of this alignment will become apparent in the following sections.

Now, consider plots for the same quantities for trajectory #2. Figure V-1 shows that this trajectory makes a 45° angle with the I axes. First of all, the plots of $\sigma^2_{D_s}$, $\sigma^2_{D_\ell}$, σ_{D_s,D_ℓ} are identically the same for T2 as they were for T1. The rotating LOS coordinates have

no absolute inertial reference, so T1 and T2 look the same in the LOS frame. However, Figure VI-12 shows a considerable change in $\sigma^2_{D_x}$, $\sigma^2_{D_y}$, and σ_{D_x,D_y} for T2 as compared to T1 in Figure VI-6.

Figures VI-13,14,15,16,17 shows the sequence of LOS (essentially the same as I) position ellipses for trajectory #2. As was the case for T1, the T2 ellipses are substantially aligned to the tracker axes.

2. Kalman Gains of Fully Coupled Filters

When the matrix inversion is carried out in the Kalman Gain equation (equation 50,51). The gain is as follows.

$$K = \frac{1}{[(p'_{11}+r_{11})(p'_{22}+r_{22})-(p'_{12}+r_{12})^2]} \begin{bmatrix} p'_{11} & p'_{12} \\ p'_{21} & p'_{22} \\ p'_{31} & p'_{32} \\ p'_{41} & p'_{42} \\ p'_{51} & p'_{52} \\ p'_{61} & p'_{62} \end{bmatrix} \begin{bmatrix} (p'_{22}+r_{22}) - (p'_{12}+r_{12}) \\ -(p'_{12}+r_{12}) \quad (p'_{11}+r_{11}) \end{bmatrix} \quad (80)$$

The LOS position gains are interpreted as follows:

(Modification of $\hat{D}s$) = $(K_{1,1})$(range residual)

(Modification of $\hat{D}\ell$) = $(K_{2,1})$(range residual)

(Modification of $\hat{D}_s$) = $(K_{1,2})$ (cross range residual)

(Modification of $\hat{D}\ell$) = $(K_{2,2})$(cross range residual)

Figure VI-18 shows plots of the LOS position gains for trajectory #1. Although range and cross range measurements are essentially simultaneous, suppose the measurement in range precedes that of cross range. First, the range measurement decreases $\hat{D}s$ uncertainty via $K_{1,1}$. From the

figure, the decrease in $\hat{D}_\ell$ due to range measurement is negligible because $K_{2,1}$ is small. However, at crossover, the cross range accuracy increases (see equation 43), so the $K_{1,2}$ term is significant in further reducing $\hat{D}_s$ uncertainty. Finally, cross range reduces $\hat{D}_\ell$ via $K_{2,2}$

It is interesting to look at the $K_{1,2}$ term. From equation (80), with $r_{1,2} = 0$,

$$K_{1,2} = \frac{r_{11}p'_{12}}{[(p'_{11}+r_{11})(p'_{22}+r_{22}) - p'^2_{12}]} \qquad (81)$$

While $p_{12} = \sigma_{s,\ell}$ is always small, Figure VI-5 shows that it reaches its maximum at crossover. Simultaneously, cross range measurement error, r_{22}, reaches a minimum at crossover. The net result is the significant $K_{1,2}$ at crossover. The reason for the interest in $K_{1,2}$ is that it is the most important of the terms lost when the filter is decoupled.

A similar line of reasoning can be applied to the position gains in inertial coordinates. Figure VI-19 shows that in this case, both cross terms $K_{1,2}$ and $K_{2,1}$ are significant. Both will be lost to decoupling.

Now, consider trajectory #2 in comparison with trajectory #1. For the reason tha the LOS covariance terms are identical for T1 and T2, the Kalman gains are also the same for T1 and T2. However, the inertial position gains for T2, shown in Figure VI-20 are substantially different than those for T1 in Figure VI-19. Again there are significant, but different cross terms $K_{1,2}$ and $K_{2,1}$ to be lost to decoupling. The implications at this point are as follows:

- LOS position gains are, to saome extent, trajectory independent

- The trajectory dependence of inertial gain cross terms suggests that upon their loss in decoupling, the error introduced will be greater for some trajectories than for others.

So far, only the four position gains have been discussed. There are also velocity gains which correct velocity estimates based upon position measurements, and acceleration gains which correct acceleration estimates based upon position measurements. The effects apparent in the position gains are also present, to a somewhat lesser extent, in the velocity and acceleration gains. The velocity and acceleration gain counterparts of the previous position gain plots are included and summarized as follows:

Figure	Title
VI-21	T1 & T2 LOS Velocity Gains
VI-22	TL I Velocity Gains
VI-23	T2 I Velocity Gains
VI-24	T1 & T2 LOS Acceleration Gains
VI-25	T1 I Acceleration Gains
VI-26	T2 I Acceleration Gains

3. Kalman Gains of Decoupled Filters

Decoupling is performed to reduce computation in order to permit real-time gain computation. In the three dimensional solution, a fully coupled filter has 45 different terms, while a decoupled filter has only 18.

Decoupling assumes statistical independence in uncertainties from one computational axis to another. That is, $\sigma_{Ds,D\ell} = 0$, $\sigma_{Ds,V\ell} = 0$, etc. The elimination of covariance terms implies that error ellipses are parallel to coputational axes. As it has been seen, the position error ellipses are nearly aligned to the LOS axes, so that it may be concluded that the pragmatic decoupling decision is more in keeping with the physical reality of the LOS frame than the I frame. It is for this reason that Figure VI-4 shows greater error introduced by I decoupling than by LOS decoupling.

When the target is flying parallel to the I axes, its acceleration uncertainty tends to rotate the error ellipses away from the tracker axes toward the I axes inbetween measurement times. This is relatively favorable to I decoupling. However, when the trajectory is at 45° to the I axes, the resulting growth in covariance cross terms is relatively unfavorable to I decoupling. Hence, the difference in T1 and T2 decoupling error in formulation C, Figure VI-4. Again, the LOS gains are the same for T1 and T2, so the error introduced by decoupling is the same for both.

When the state vectors are composed as they are in this report, decoupling result in the zeroing of covariance matrix terms whose row plus column sum is odd. This causes the square matrix in equation (80) to become diagonal. All of the Kalman Gain cross terms are then eliminated, leaving only $K_{1,1}$, $K_{2,2}$, $K_{3,1}$, $K_{4,2}$, $K_{5,1}$, and $K_{6,2}$.

When LOS is decoupled as shown in Figure VI-27, only $K_{1,1}$ and $K_{2,2}$ remain of the position gains. Note that in comparison with

the undecoupled gains in Figure VI-18, the important $K_{1,2}$ term is lost, but $K_{1,1}$ and $K_{2,2}$ are substantially unchanged. However, Figure VI-28 shows the I decoupled gains where $K_{1,2}$ and $K_{2,1}$ are lost, but in comparison with Figure VI-19, the remaining $K_{1,1}$ and $K_{2,2}$ have been considerably changed. In addition, Figure VI-29 shows that T2 I decoupled gains differ from T1 I decoupled gains. The implications of these results are as follows:

- For both I and LOS, information is lost in the loss of the $K_{1,2}$ term, with the inevitable loss in estimation accuracy.
- Since $K_{1,1}$ and $K_{2,2}$ remain essentially unchanged in deoupling LOS, the possibility exists that the lost $K_{1,2}$ could be approximated through equation (81) by use of an empirical relation for the uncomputed p'_{12}. The generation of empirical relations appears feasible due to the trajectory independent nature of the LOS covariance matrix, and due to the relatively minor changes in that covariance matrix due to decoupling.
- For just the opposite reasons, the generation of approximate gain terms lost in I decoupling would appear to be quite difficult.

Again, the results in the velocity and acceleration gains are similar to those seen in the position gains. A summary of the graphical results is as follows:

Figure	Title
VI-30	T1 & T2 LOS Decoupled Velocity Gains
VI-31	T1 I Decoupled Velocity Gains
VI-32	T2 I Decoupled Velocity Gains
VI-33	T1 & T2 LOS Decoupled Acceleration Gains

Figure		Title
VI-34	T1	I Decoupled Acceleration Gains
VI-35	T2	I Decoupled Acceleration Gains

4. Projected Position Error Ellipses

While the computed Kalman Filter position, velocity, and acceleration uncertainty all have a bearing on the ultimate probability of hitting the target, the projected position ellipse conveys the most information in this regard. As described in Chapter V, a projected ellipse is constructed such that the projectile is equally likely to land inside or outside the ellipse.

Figure VI-36,37,38,39,40 show the sequence of projected position ellipses resulting from the decoupled LOS filter acting on trajectory #2. The ellipse is relatively large at T = 2 because the filter is just finishing its transient. By the time of cross over, T = 5, the ellipse is quite small due to the high quality cross range measurement due to short range to the target. Finally, by T = 10, the ellipse is again large, partially due to the degrading cross range accuracy, but primarily due to the long flight time as the projectile is now catching up to a departing target.

Finally, Figure VI-41,42,43,44,45 show the same sequence resulting from the I decoupled filter. The line of sight axes are shown on the figures, but are not used computationally. Note the generally larger ellipses in this sequence relative to the last sequence, showing the poorer accuracy due to decoupling in inertial coordinates.

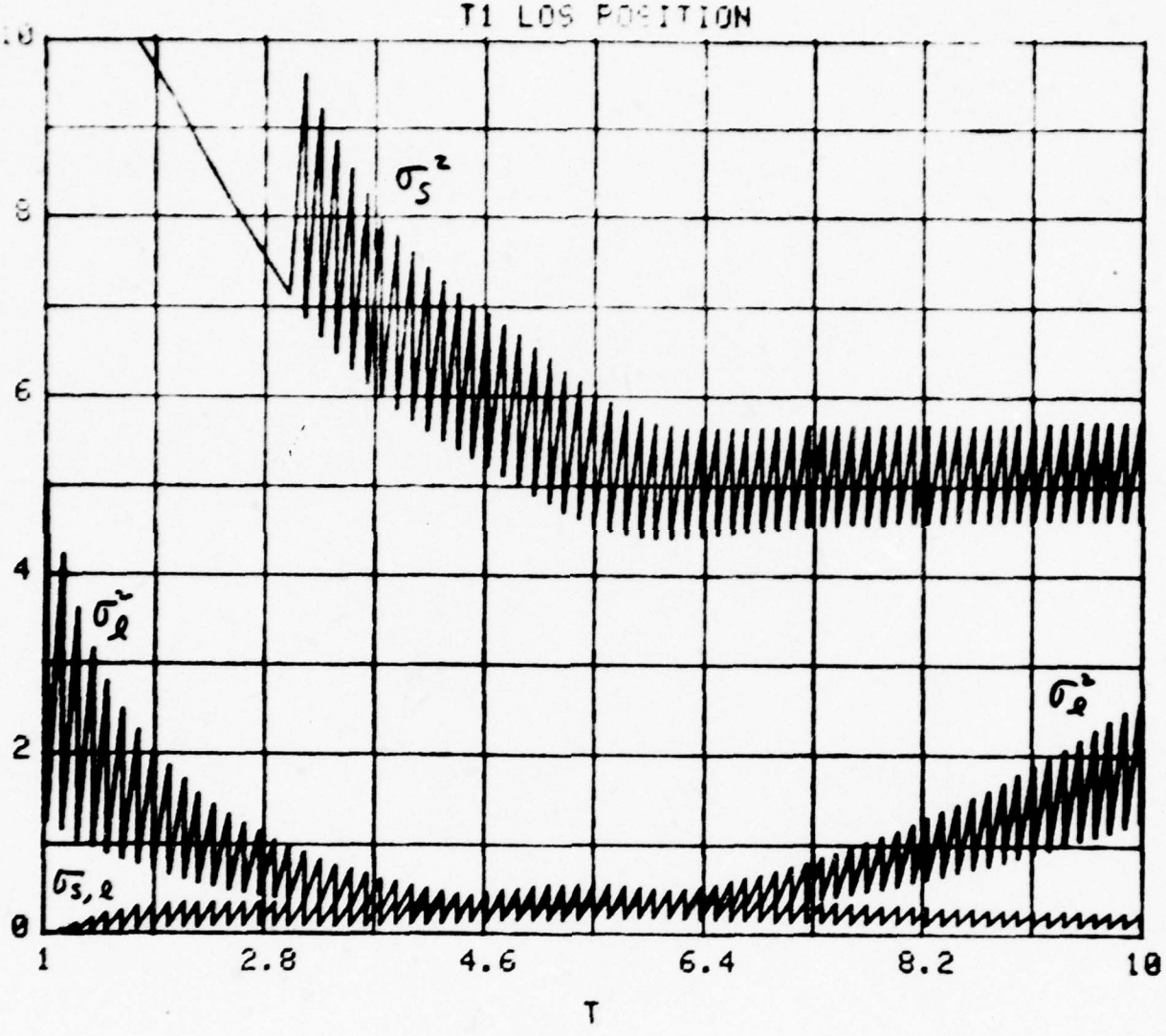
T1 LOS POSITION
σ_s^2
σ_ℓ^2
σ_ℓ^2
$\sigma_{s,\ell}$
8
6
4
2
0
1
2.8
4.6
6.4
8.2
10
T

FIGURE VI - 5

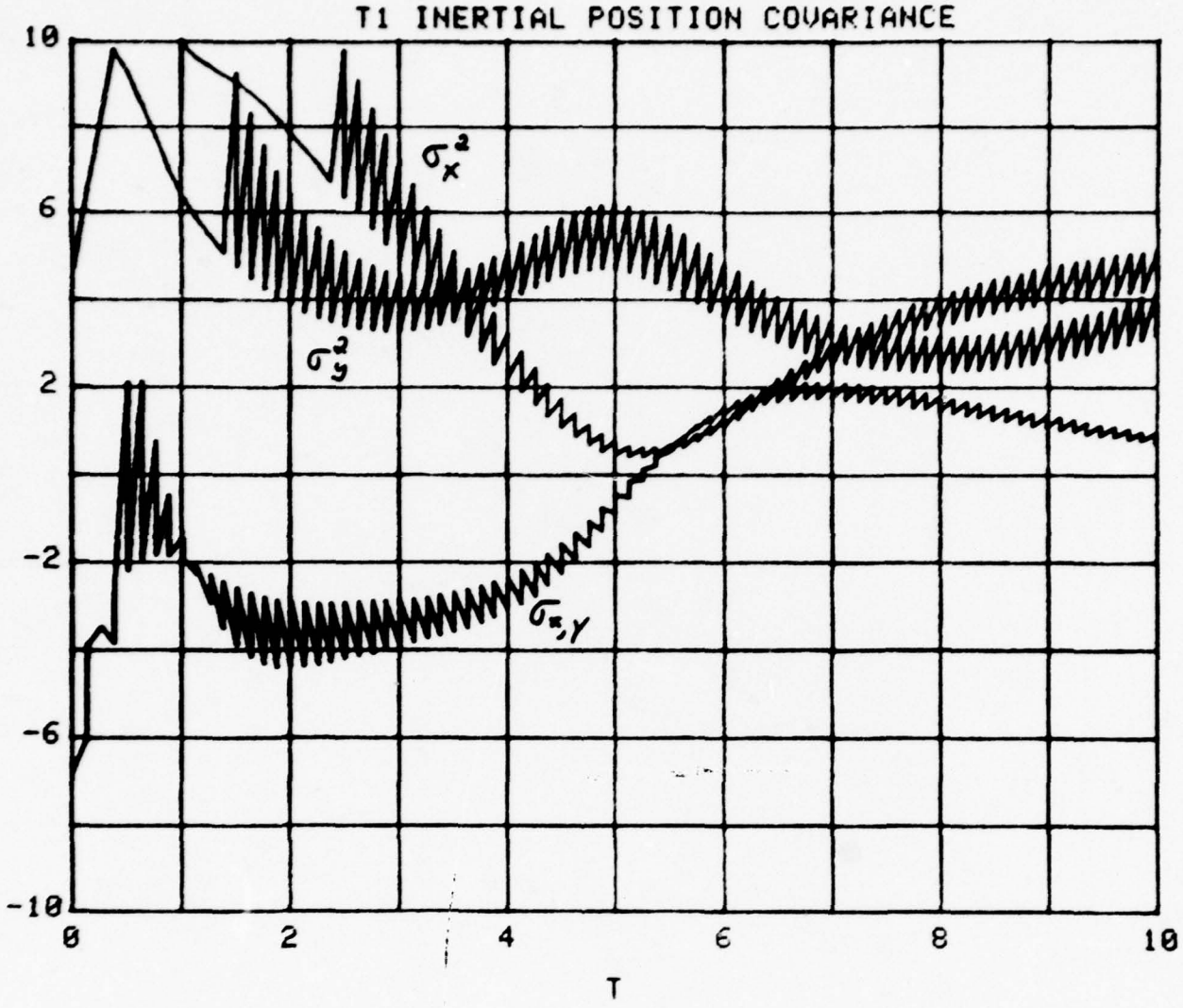
T1 INERTIAL POSITION COVARIANCE
10
6
2
-2
-6
-10
0
2
4
6
8
10
T
σ_x^2
σ_y^2
$\sigma_{x,y}$

FIGURE VI - 6

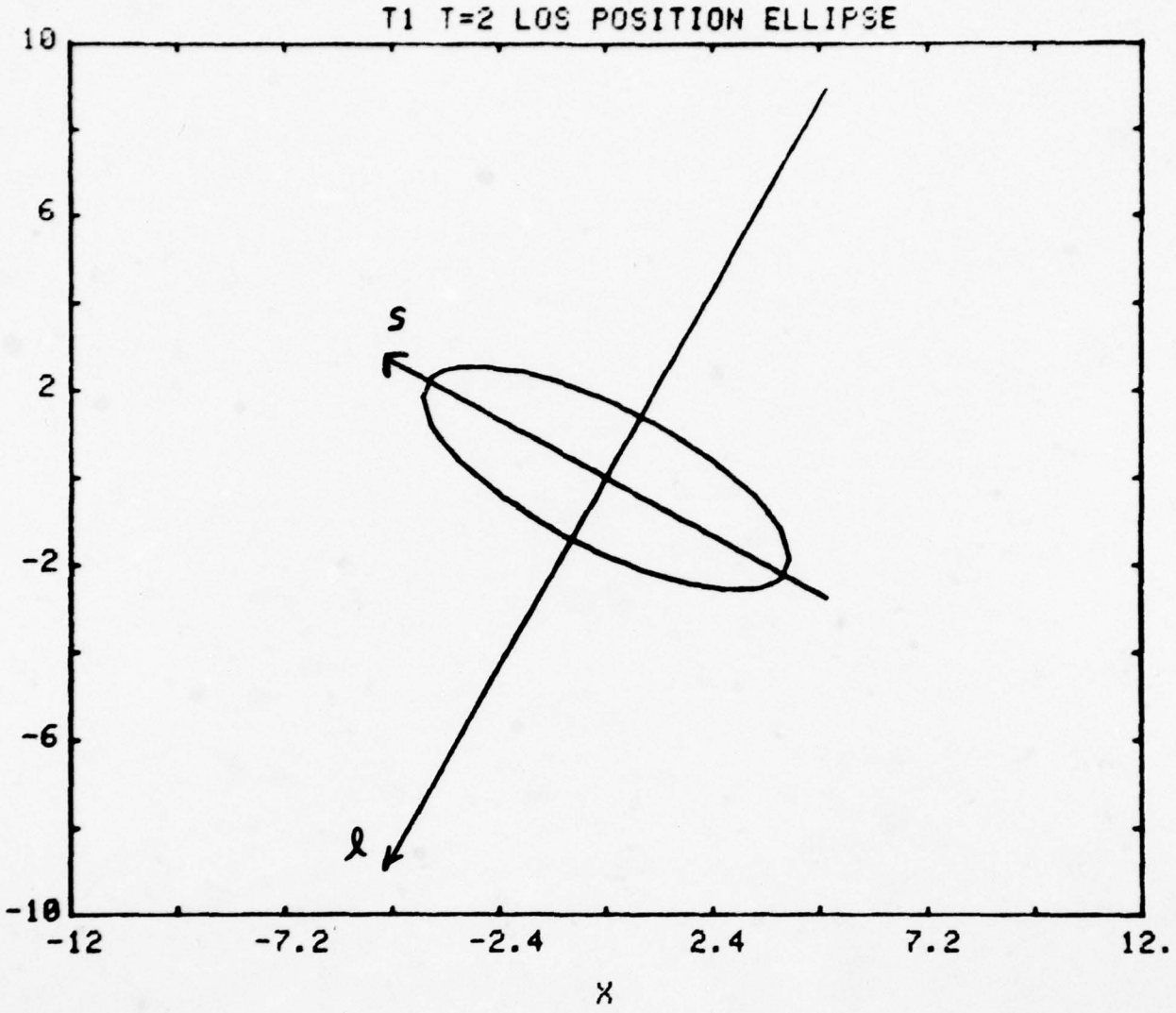

FIGURE VI - 7

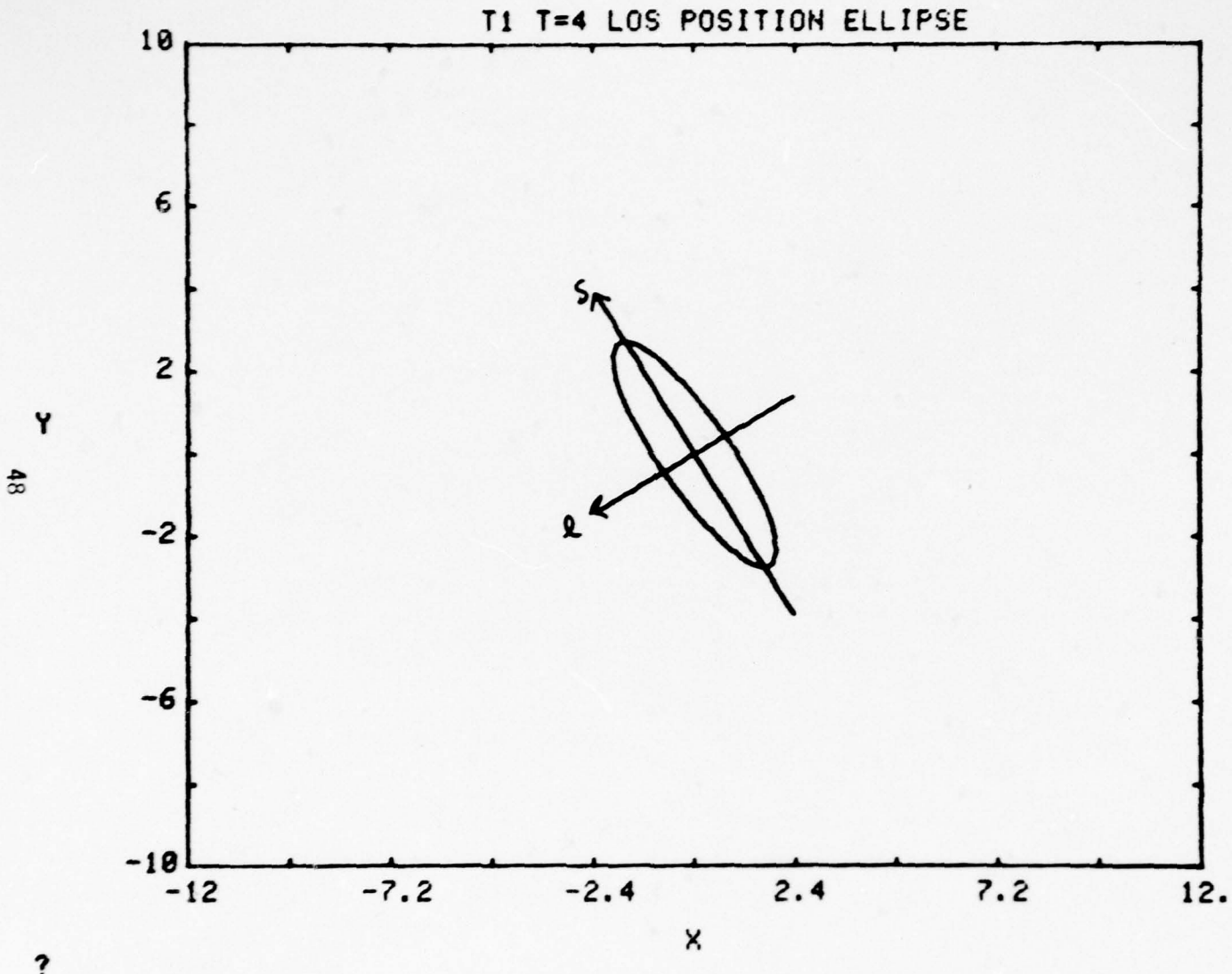

FIGURE VI - 8

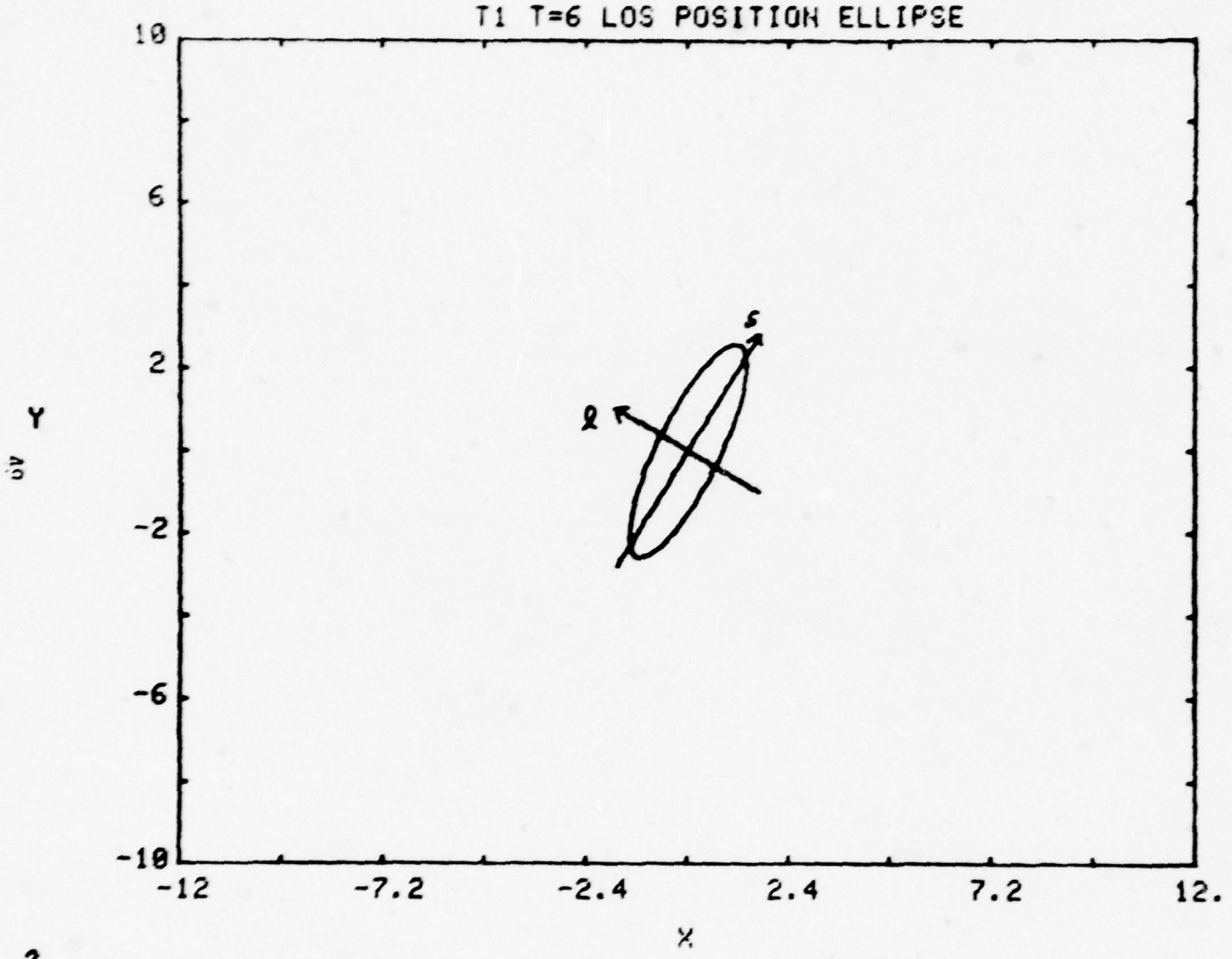

?

FIGURE VI - 9

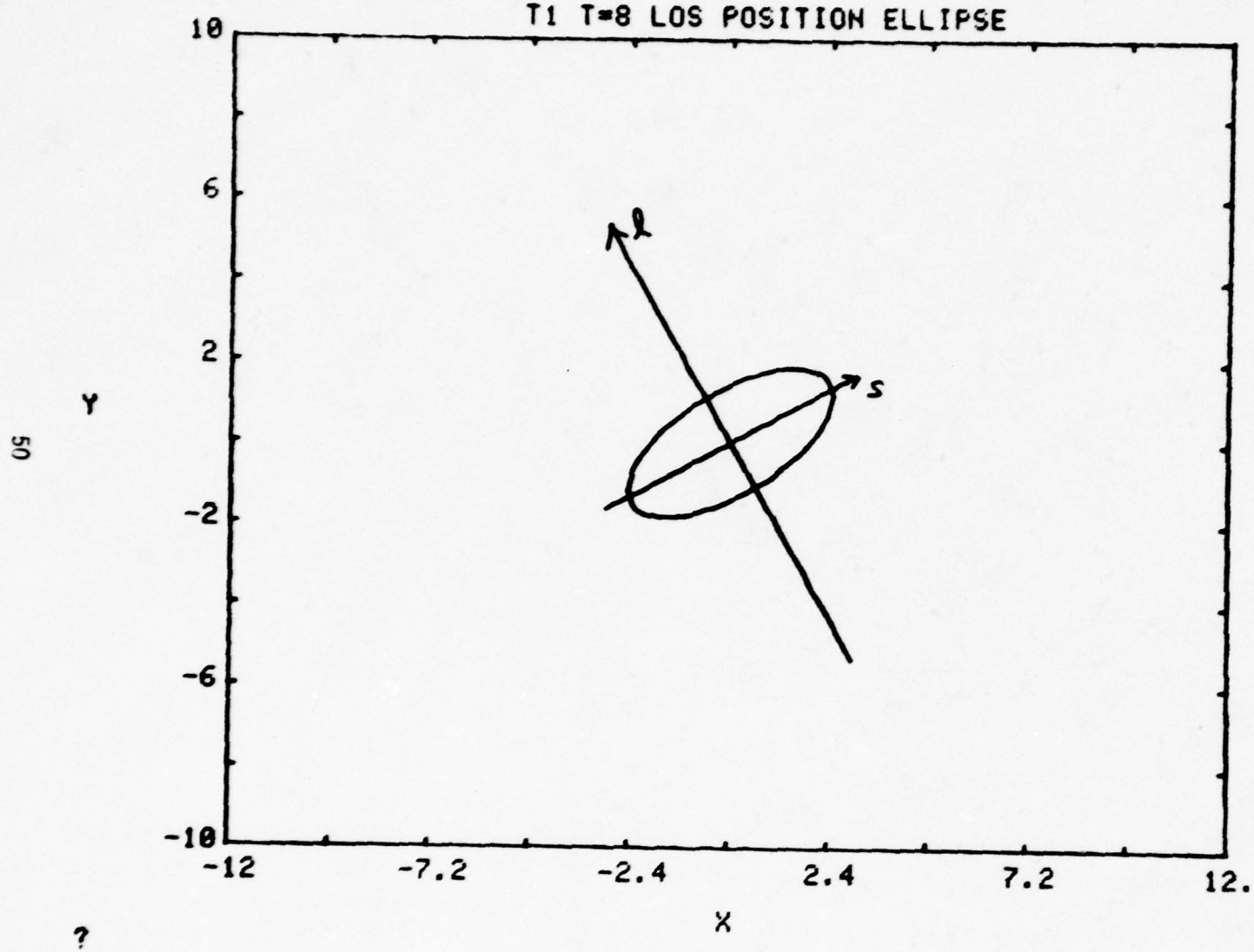

FIGURE VI - 10

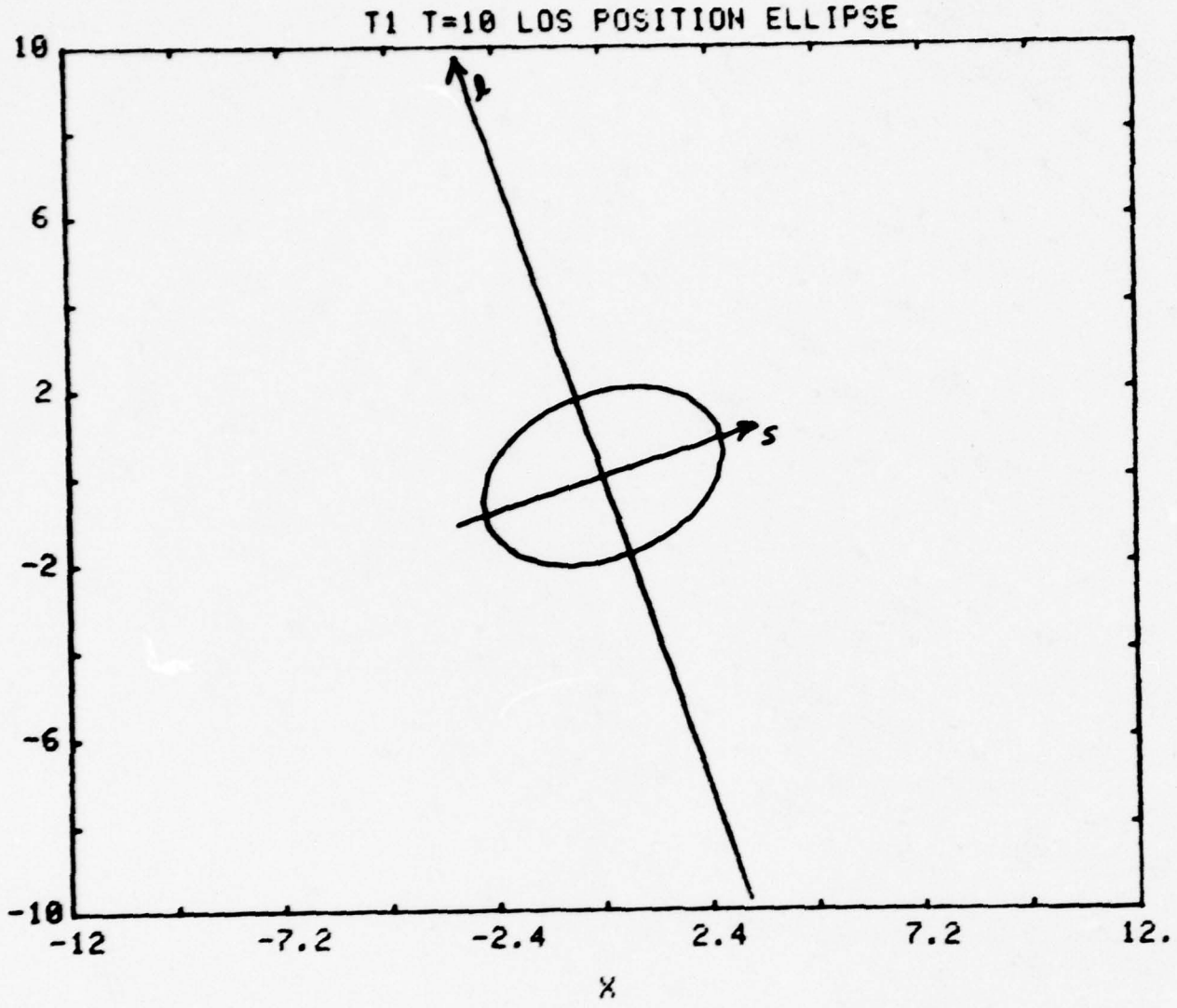

FIGURE VI - 11

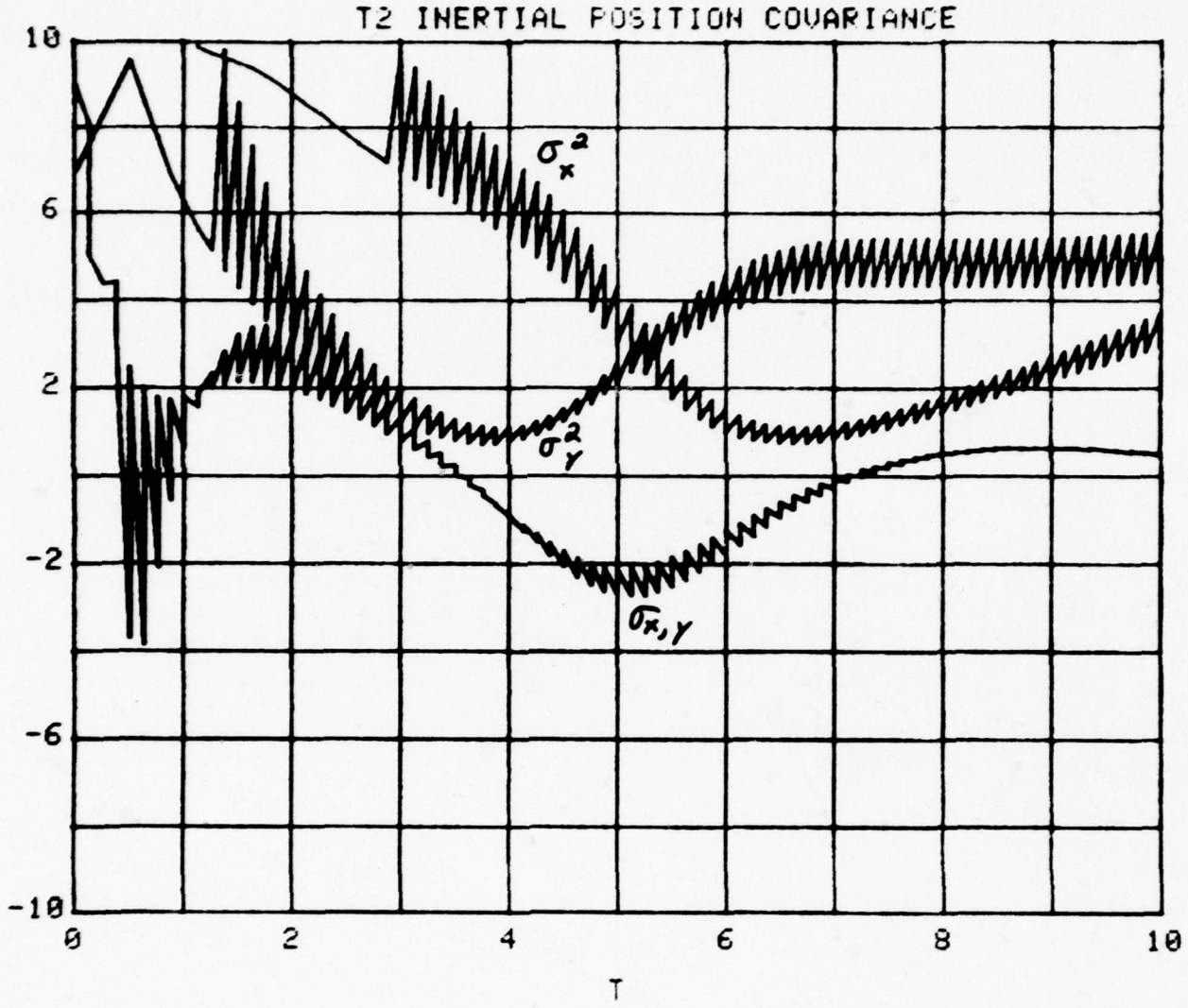
T2 INERTIAL POSITION COVARIANCE
10
6
2
-2
-6
-10
0
2
4
6
8
10
T
σ_x^2
σ_y^2
$\sigma_{x,y}$

FIGURE VI - 12

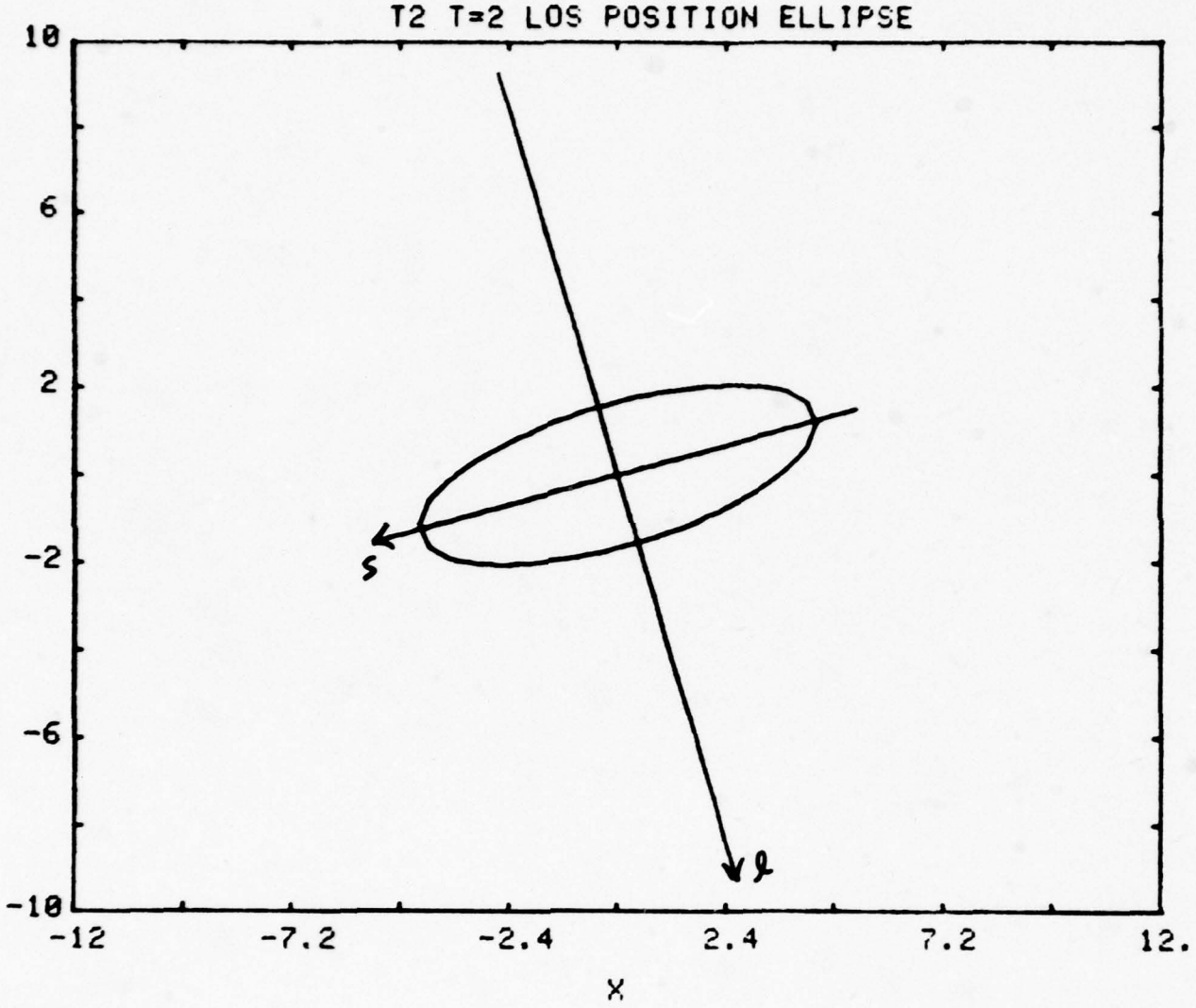

FIGURE VI - 13

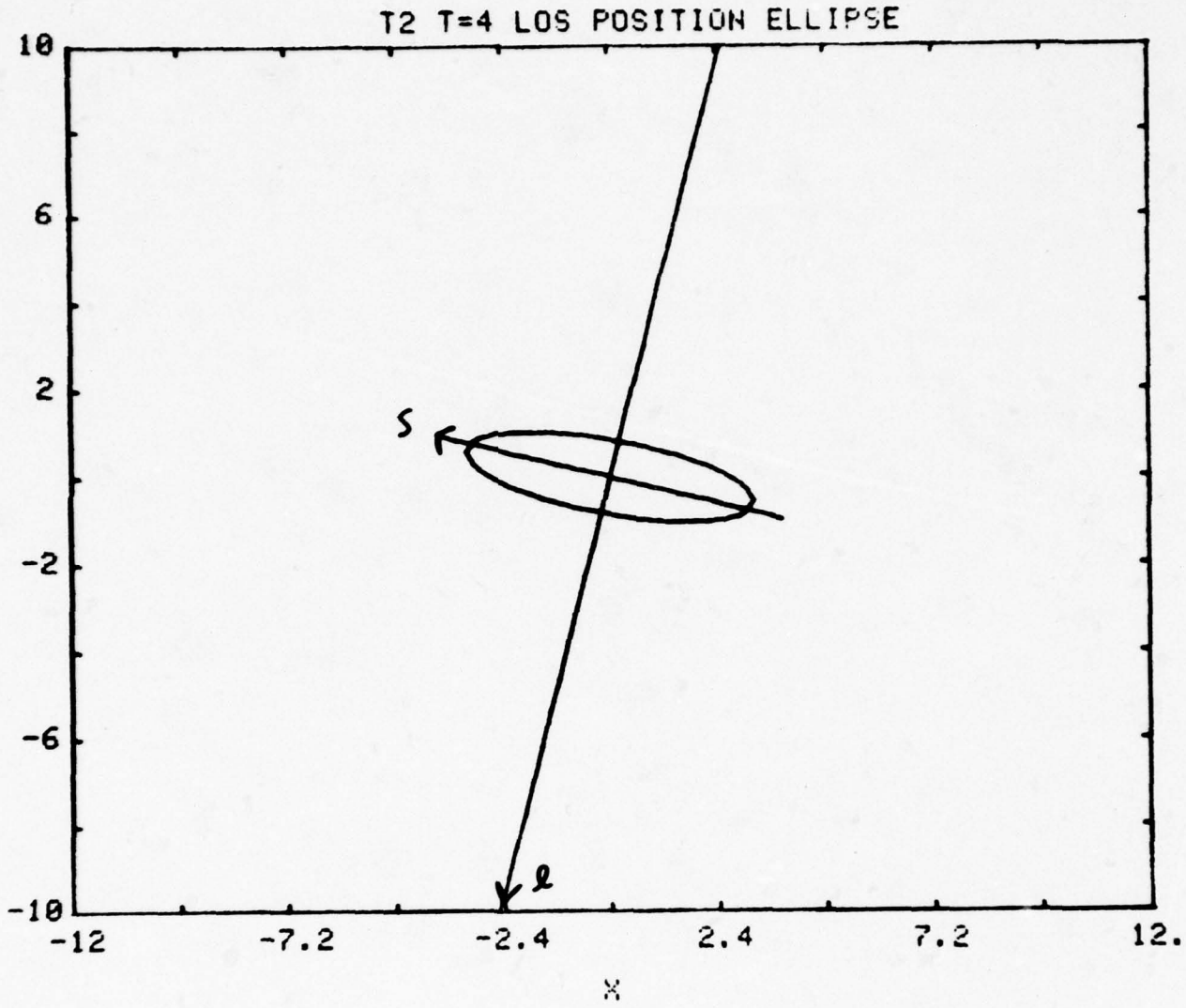

FIGURE VI - 14

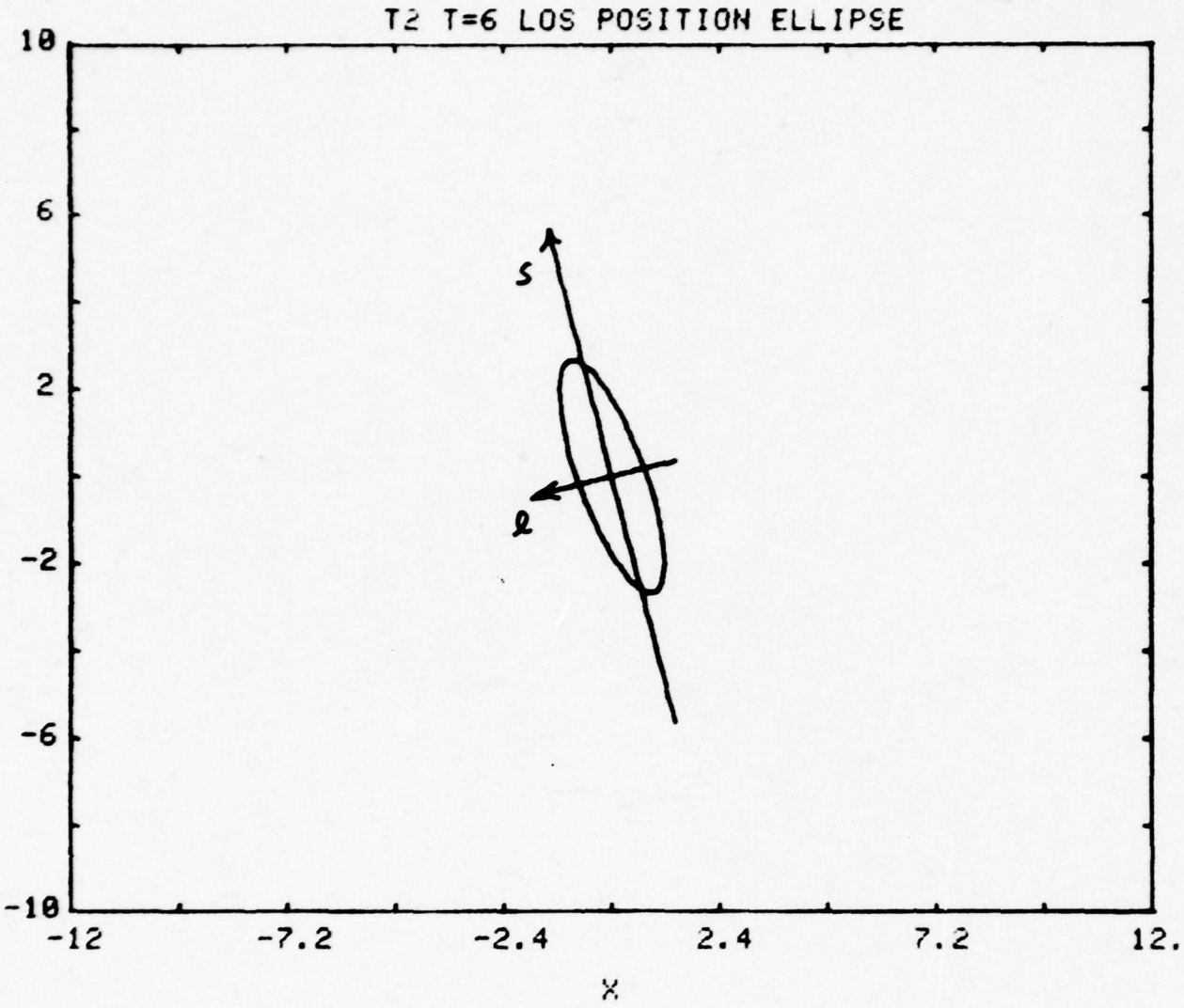

FIGURE VI - 15

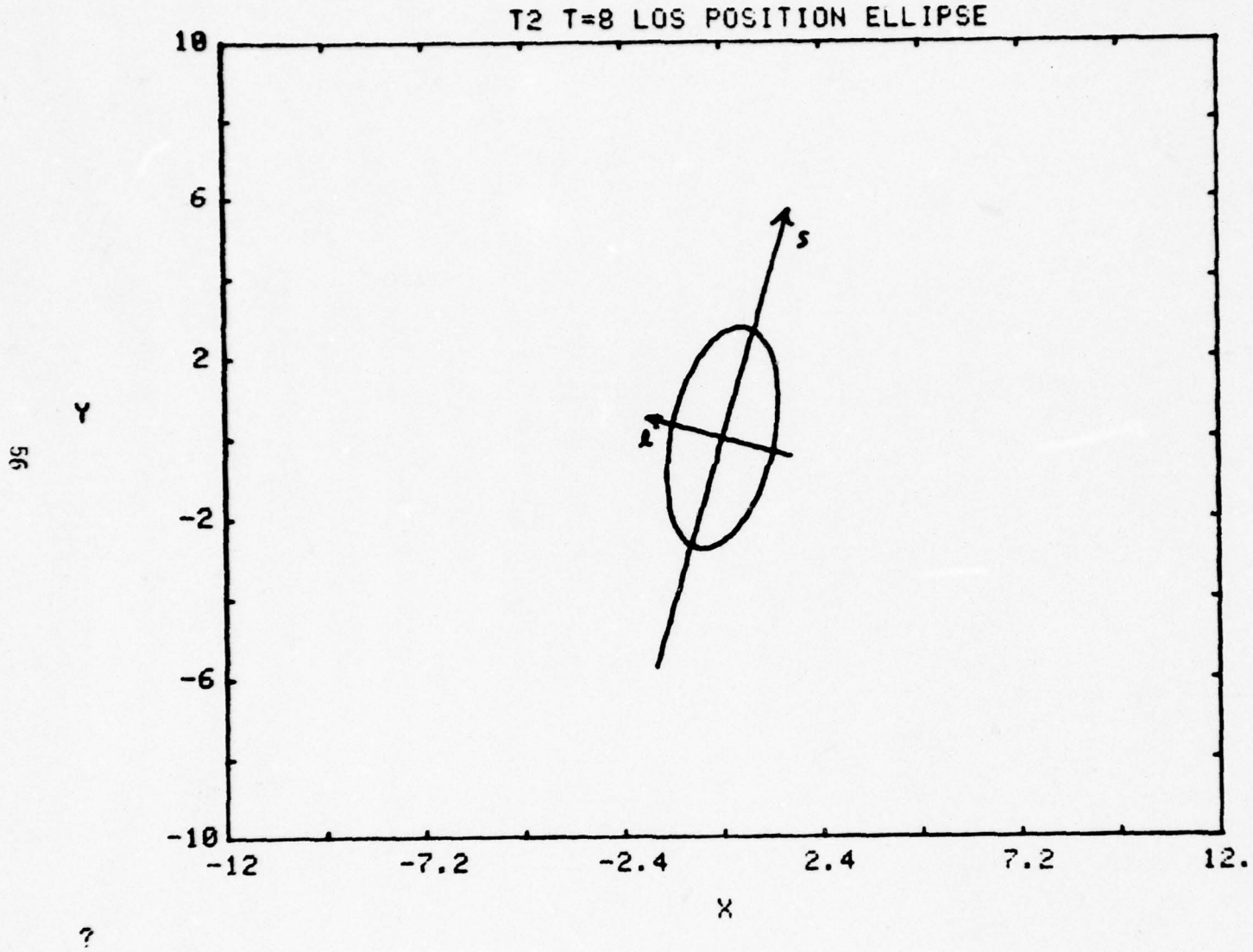

FIGURE VI - 16

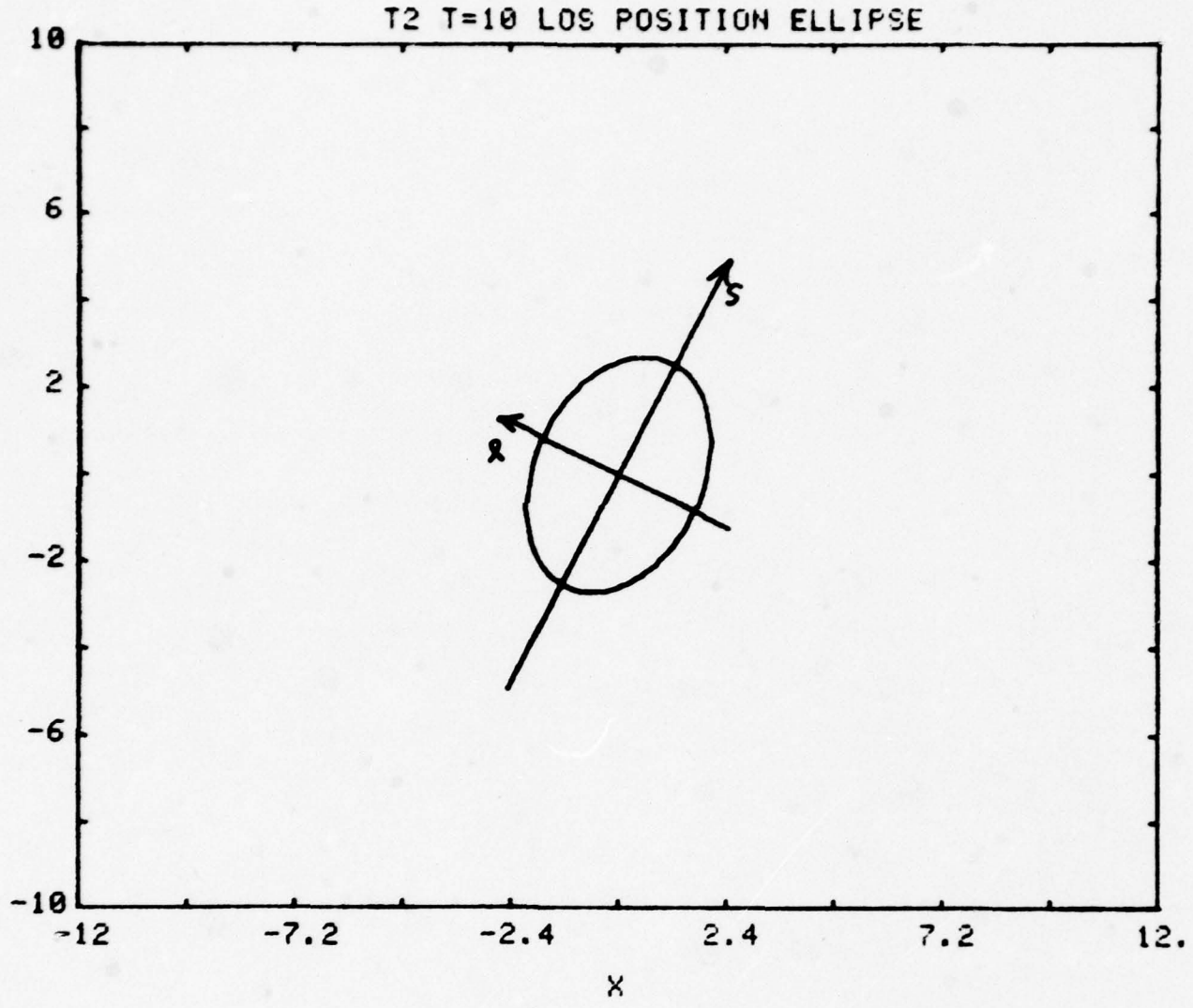

FIGURE VI - 17

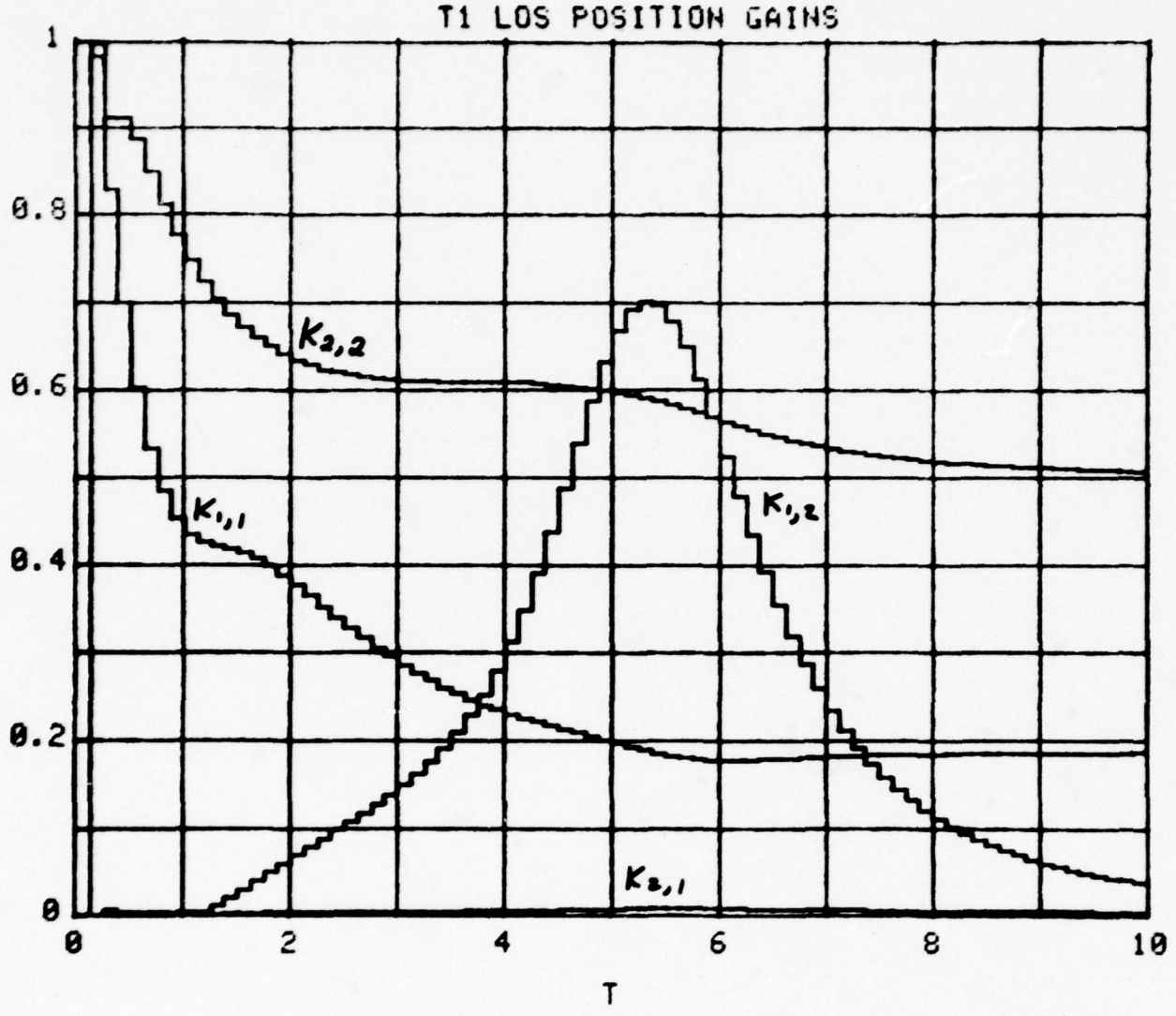

?

FIGURE VI - 18

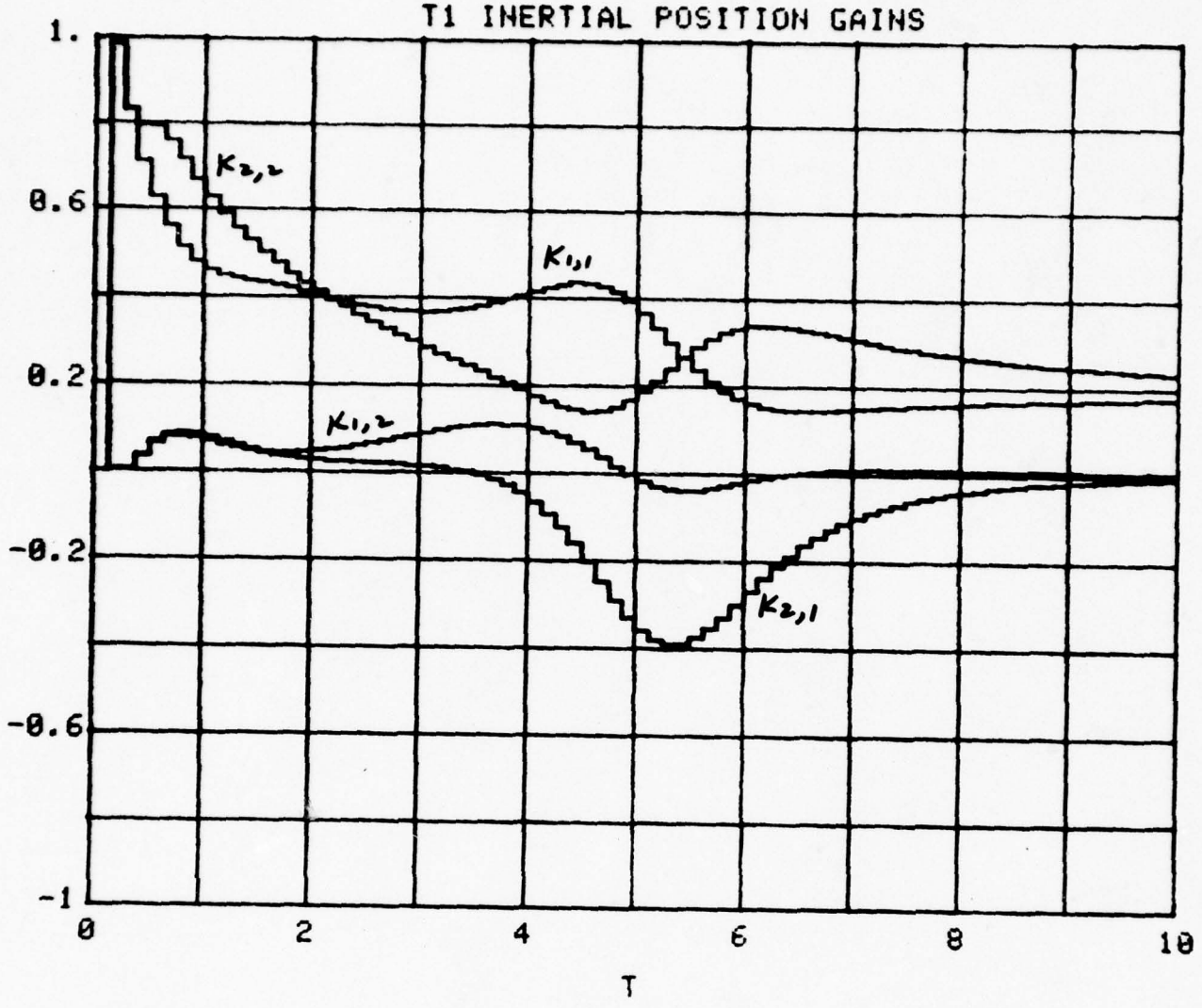
T1 INERTIAL POSITION GAINS
1.
0.6
0.2
-0.2
-0.6
-1
0
2
4
6
8
10
T
K2,2
K1,1
K1,2
K2,1

FIGURE VI - 19

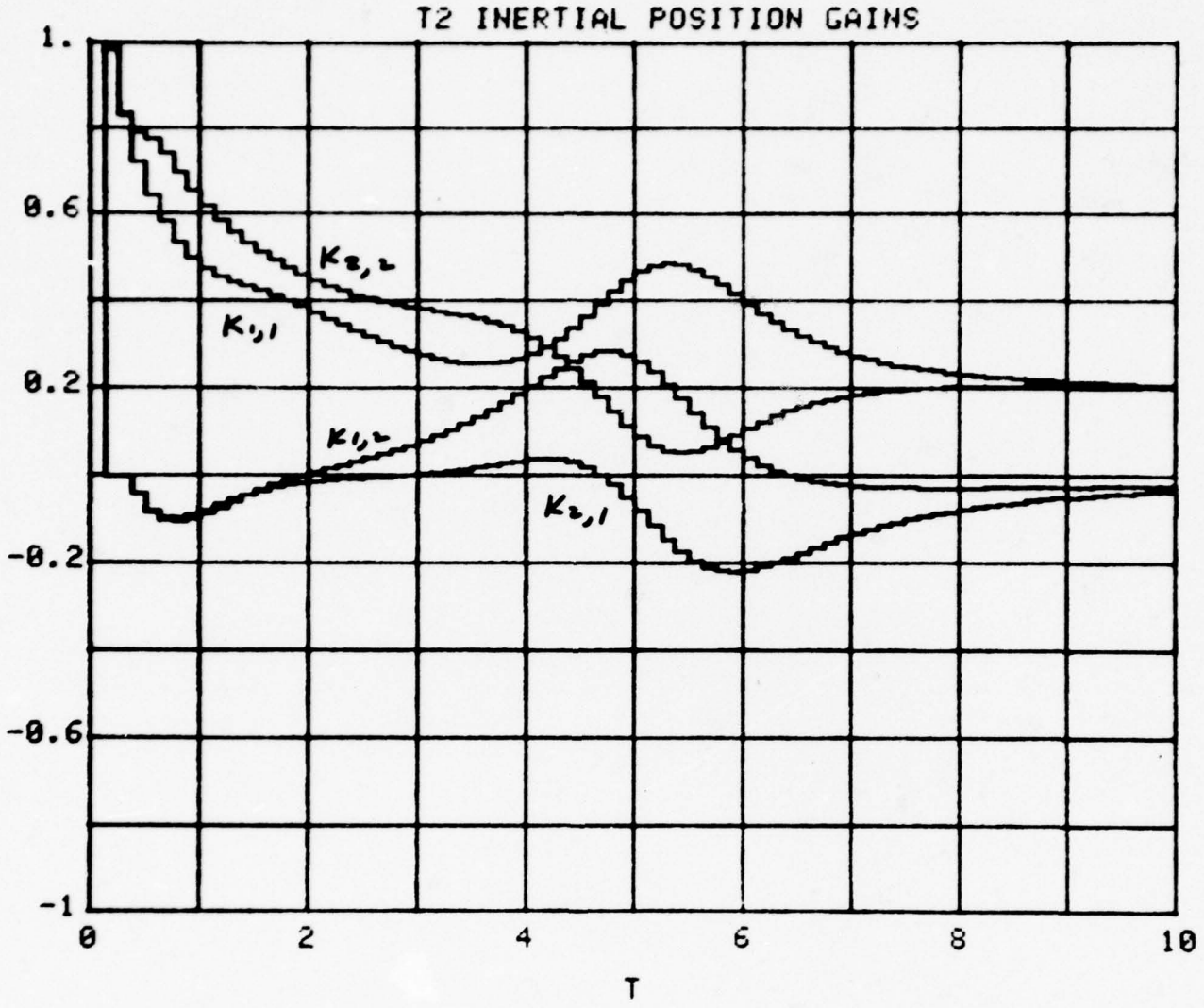
T2 INERTIAL POSITION GAINS
1.
0.6
0.2
-0.2
-0.6
-1
0
2
4
6
8
10
T
K2,2
K1,1
K1,2
K2,1

FIGURE VI - 20

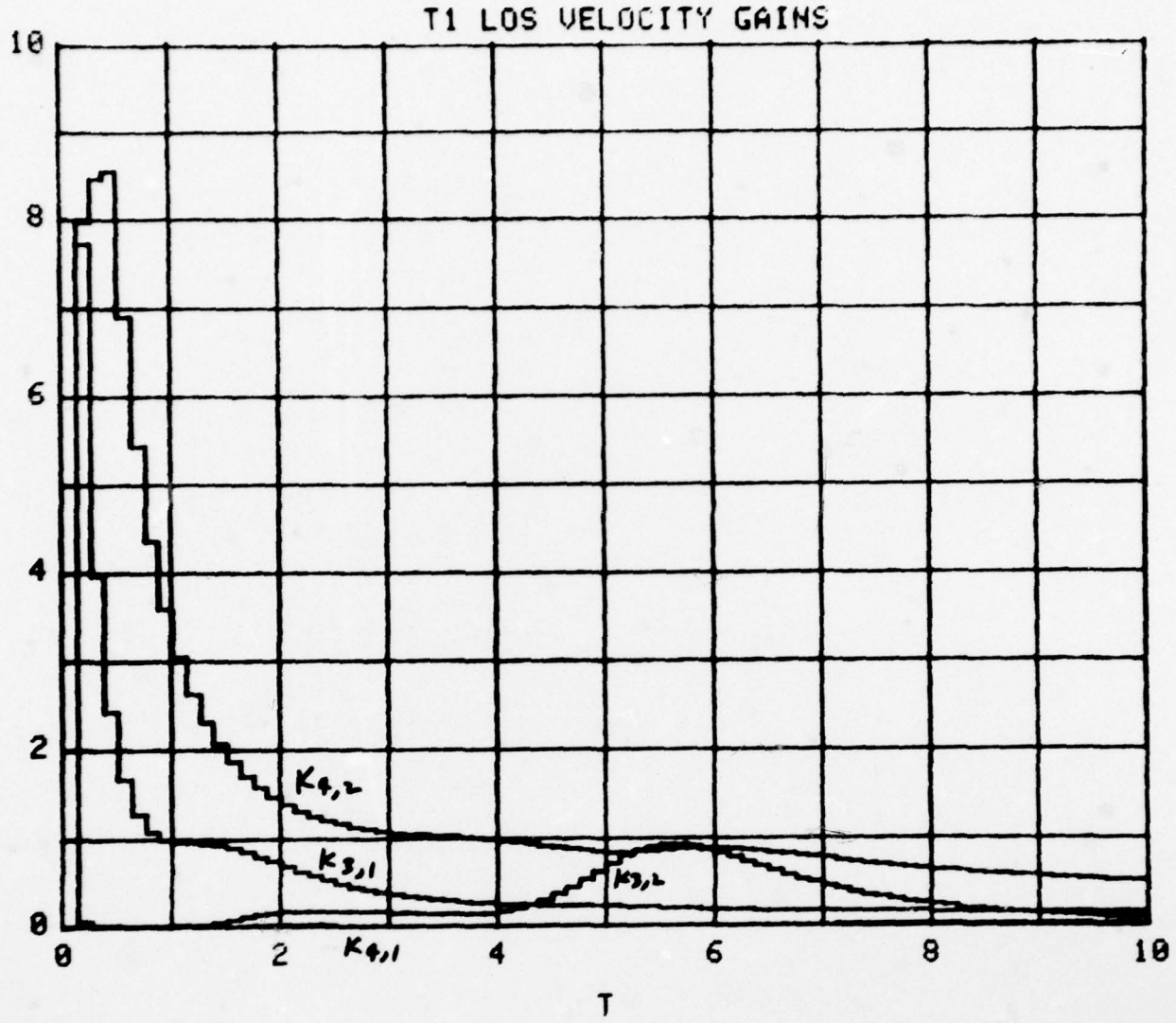

FIGURE VI - 21

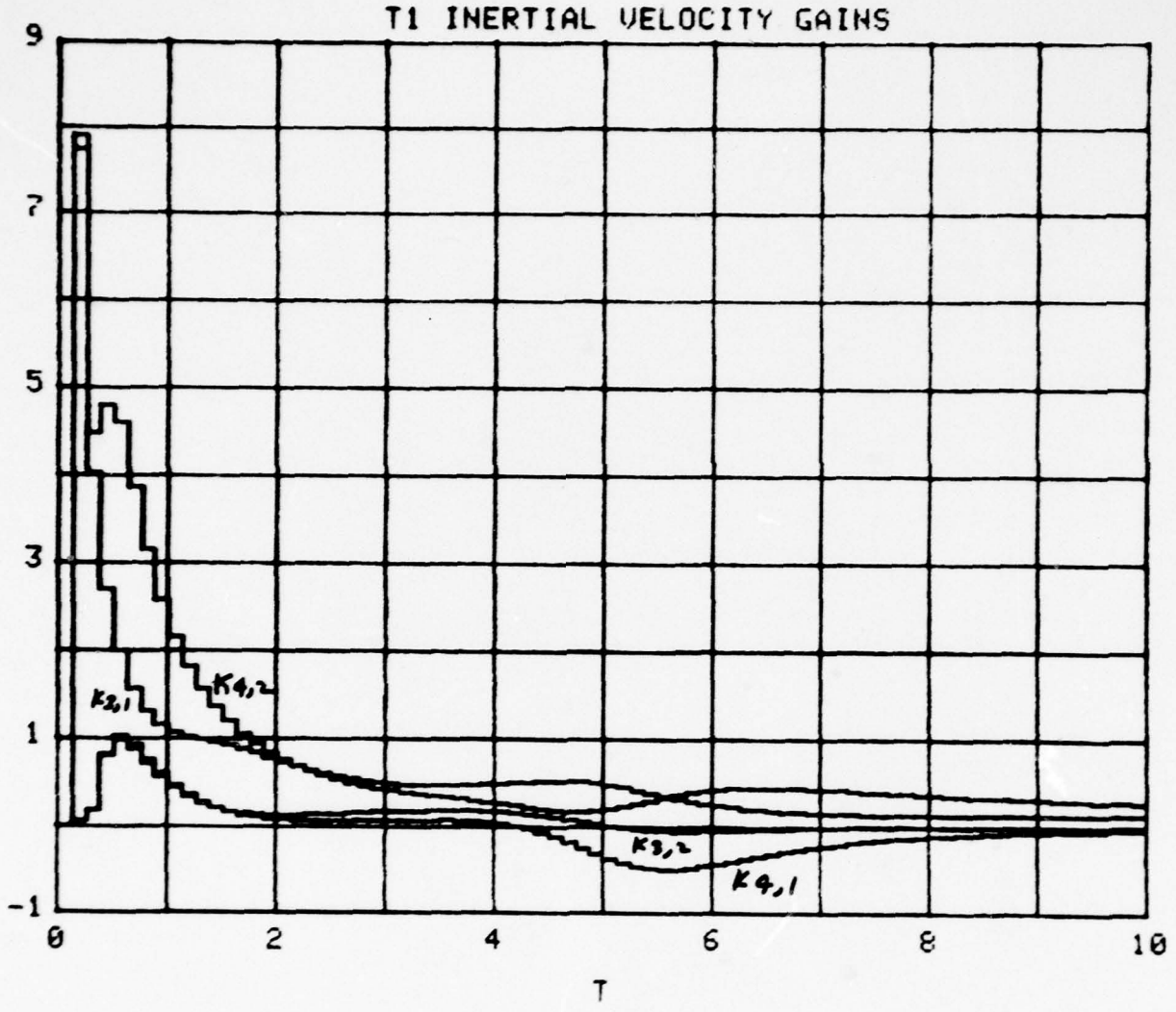

FIGURE VI - 22

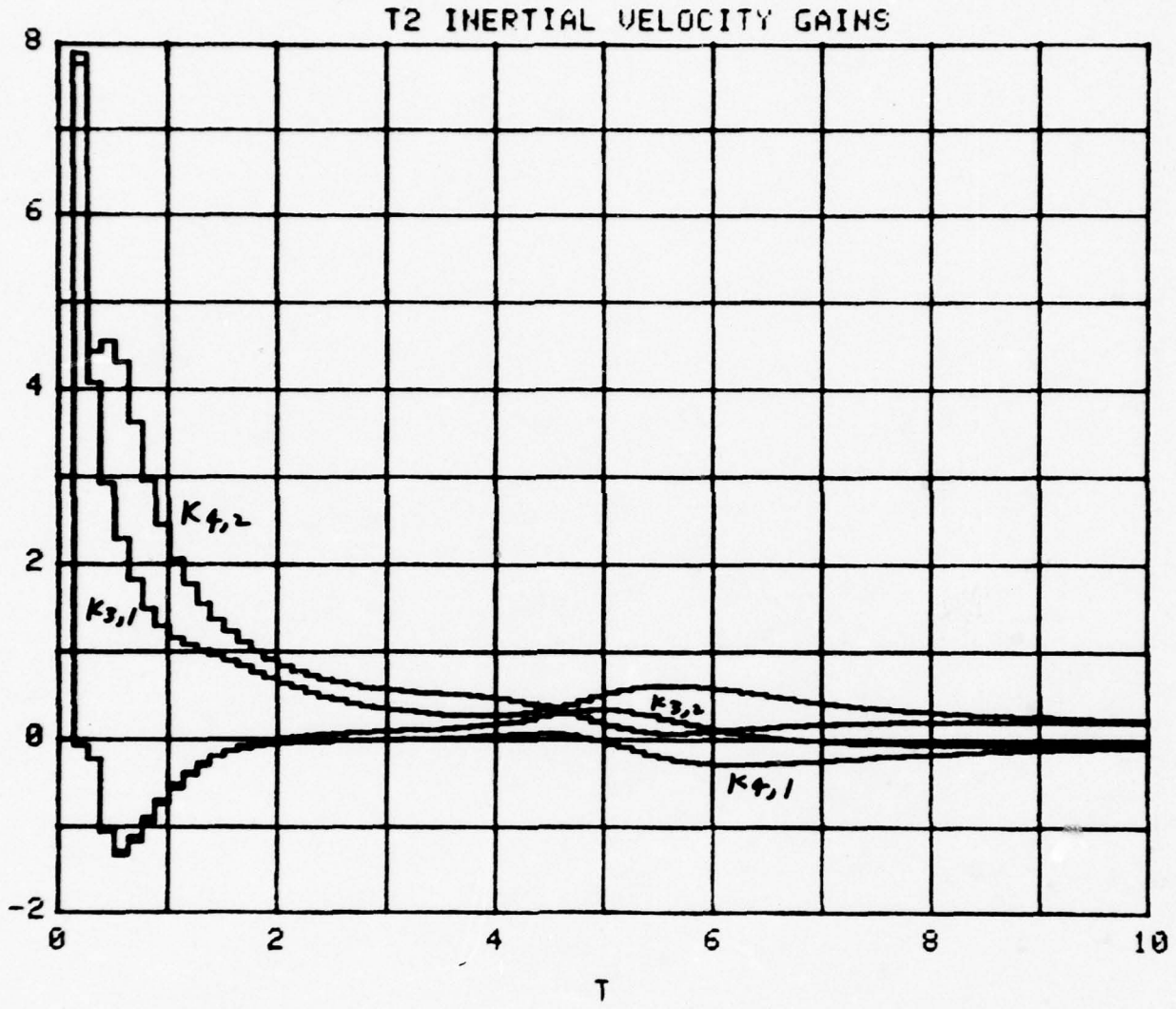

FIGURE VI - 23

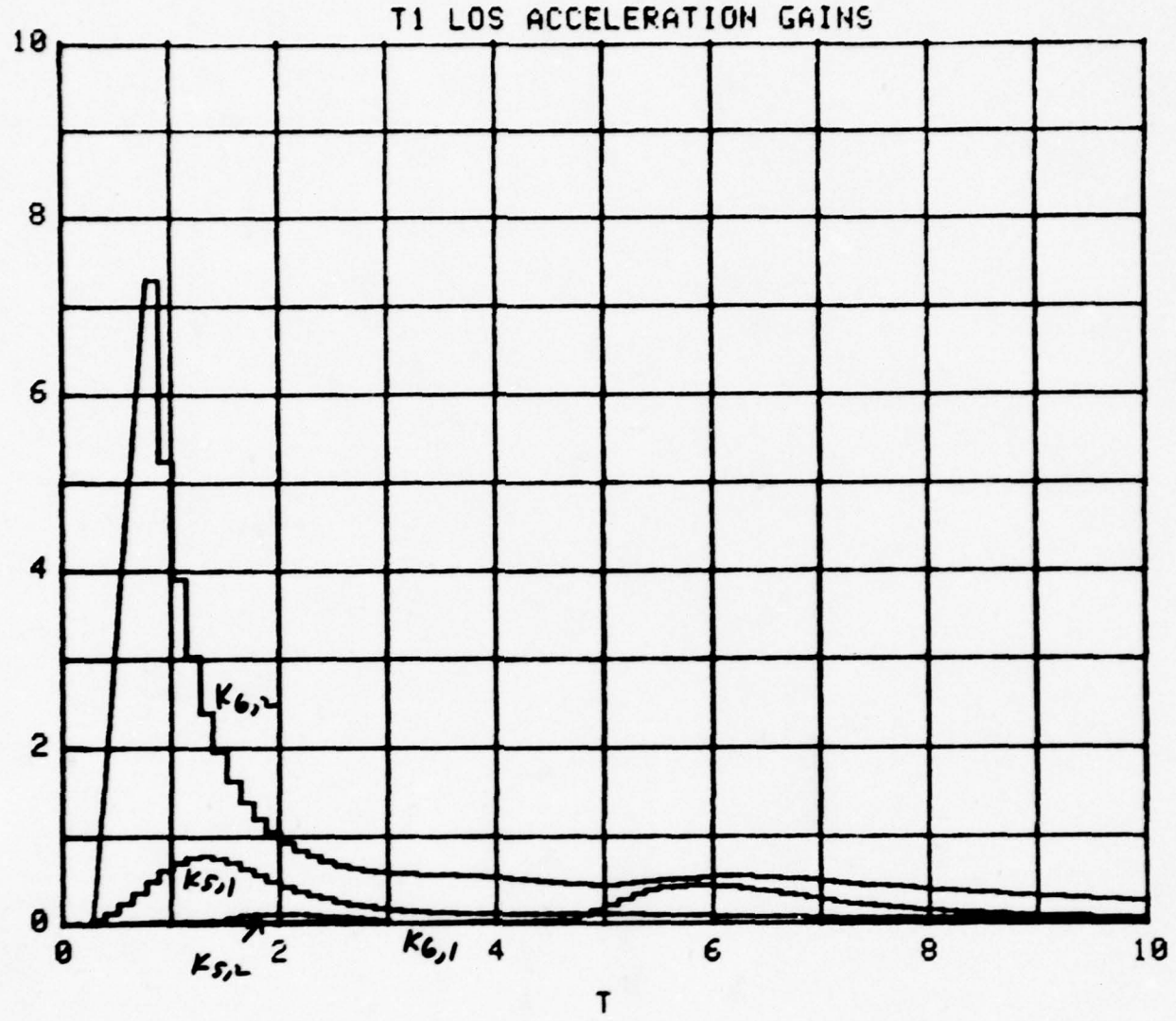

FIGURE VI - 24

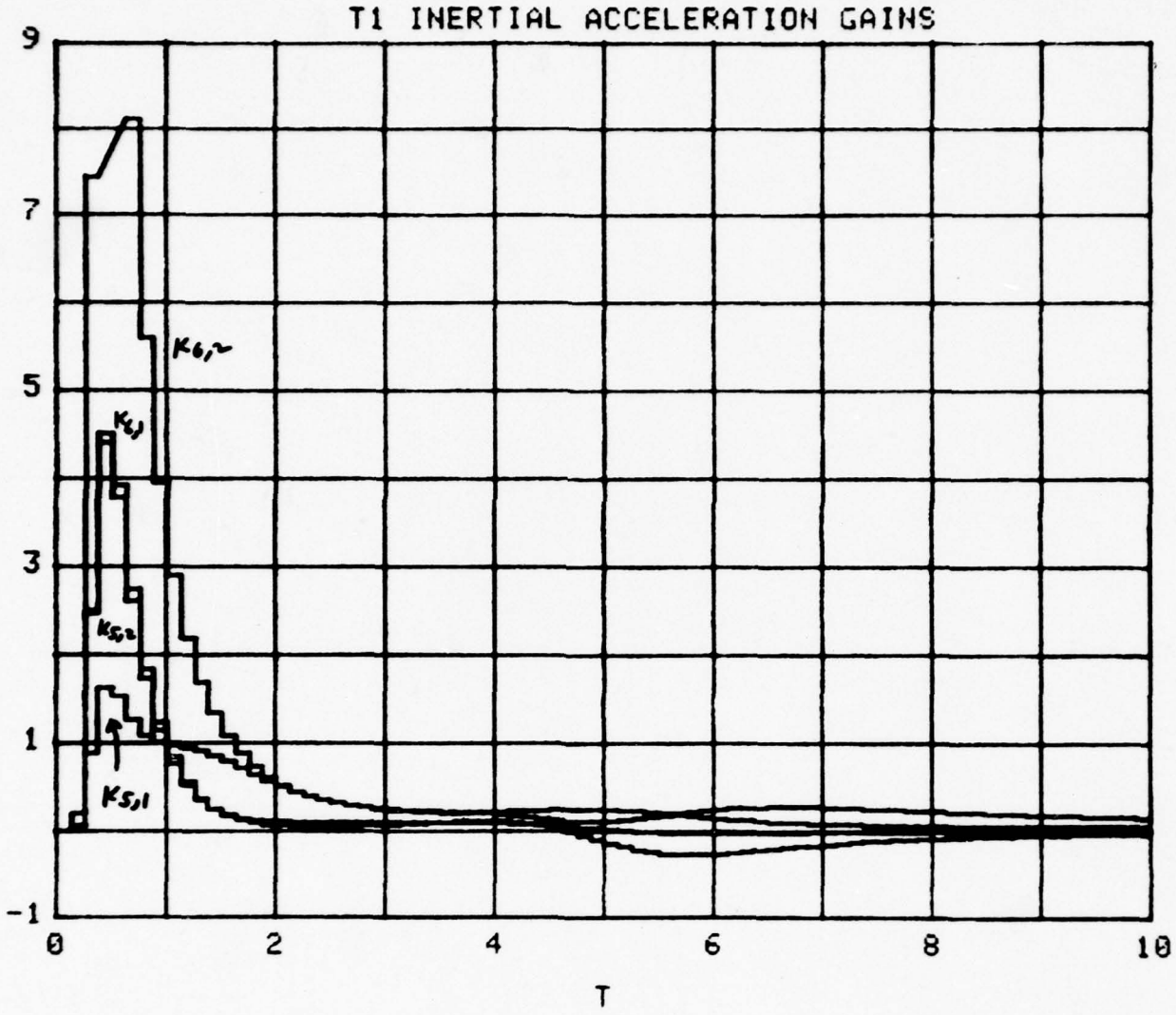
T1 INERTIAL ACCELERATION GAINS
9
7
5
3
1
-1
0
2
4
6
8
10
T
K6,2
K6,1
K5,2
K5,1

FIGURE VI - 25

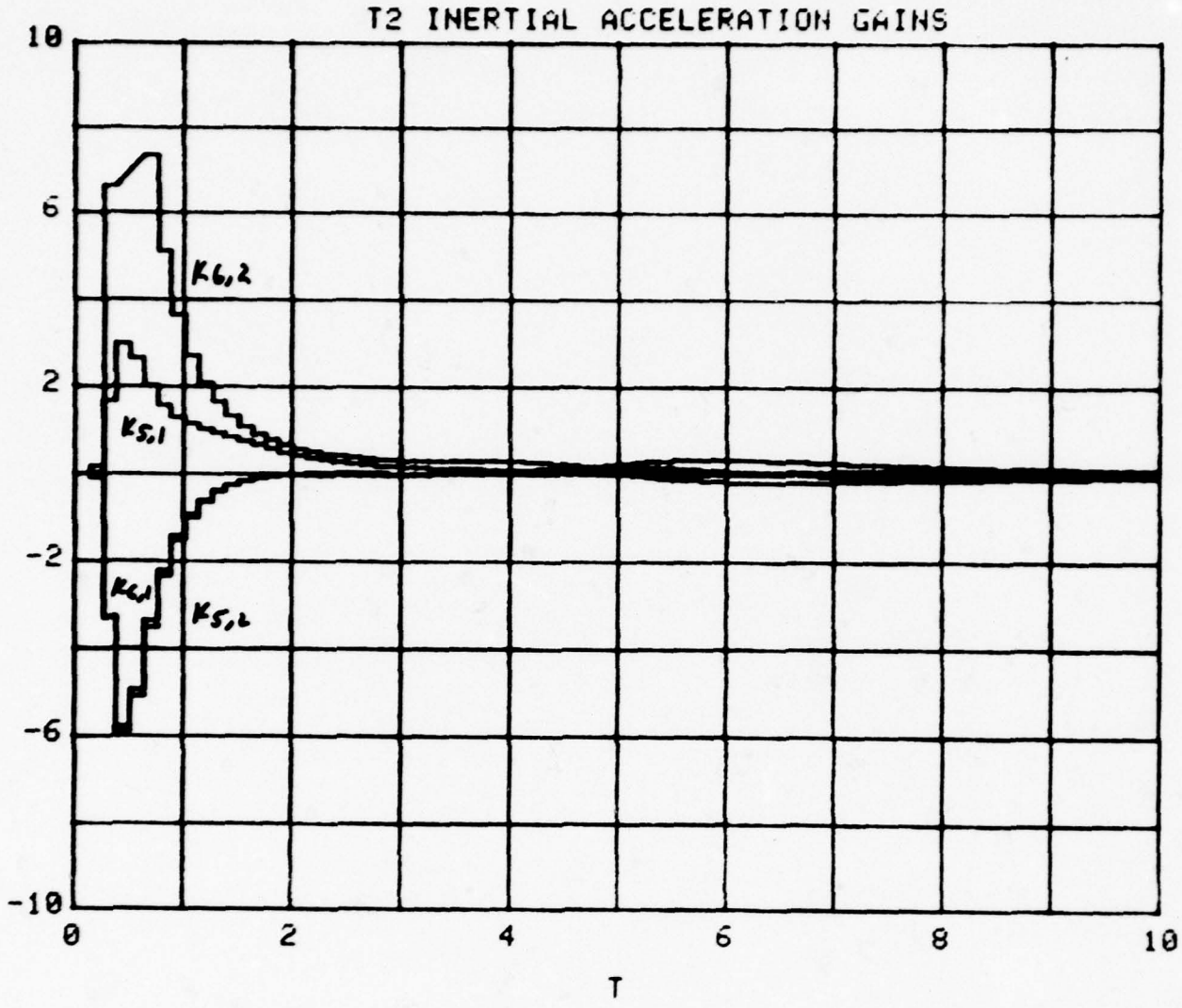
T2 INERTIAL ACCELERATION GAINS
10
6
2
-2
-6
-10
0
2
4
6
8
10
T
K6,2
K5,1
K6,1
K5,2

FIGURE VI - 26

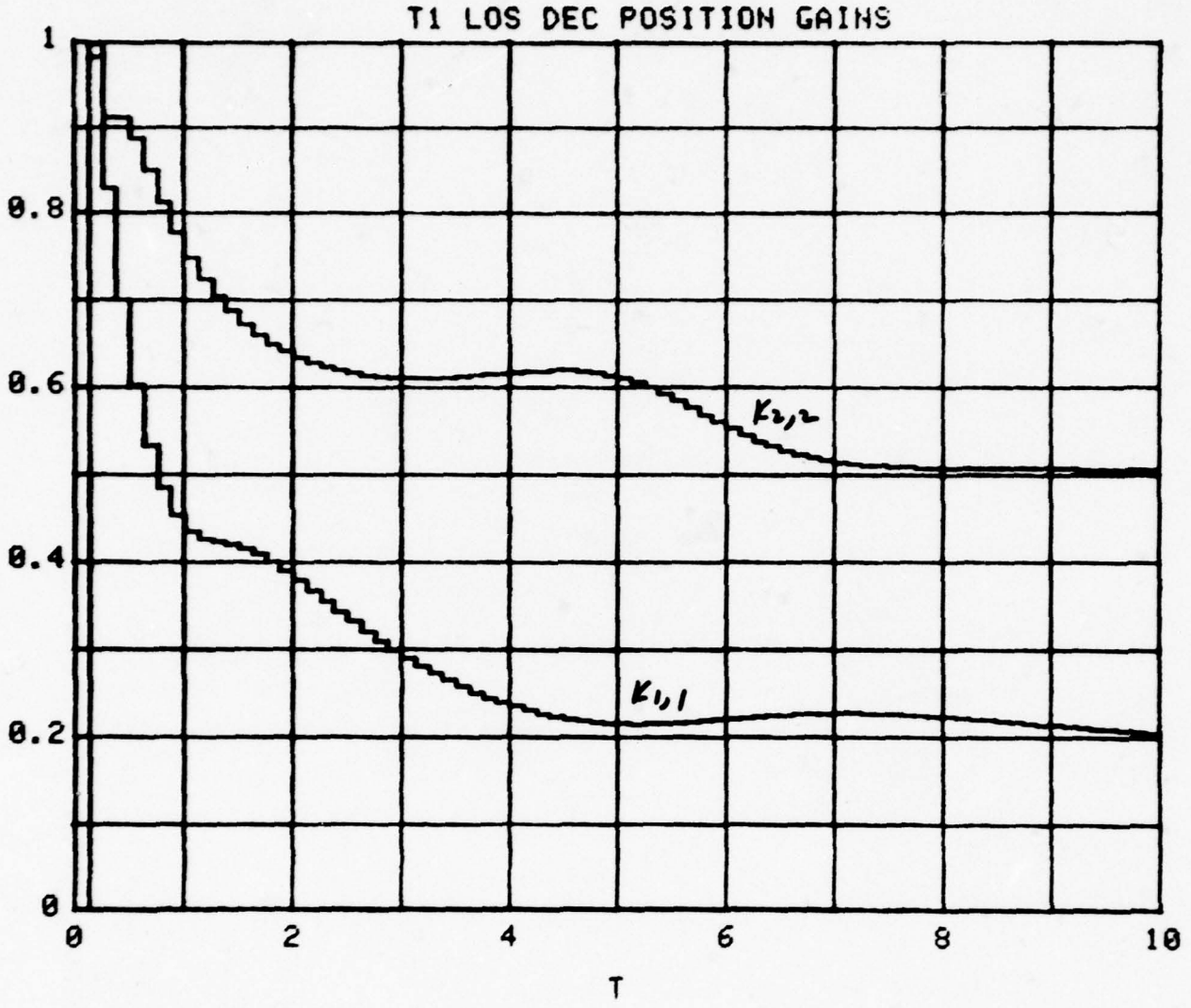

FIGURE VI - 27

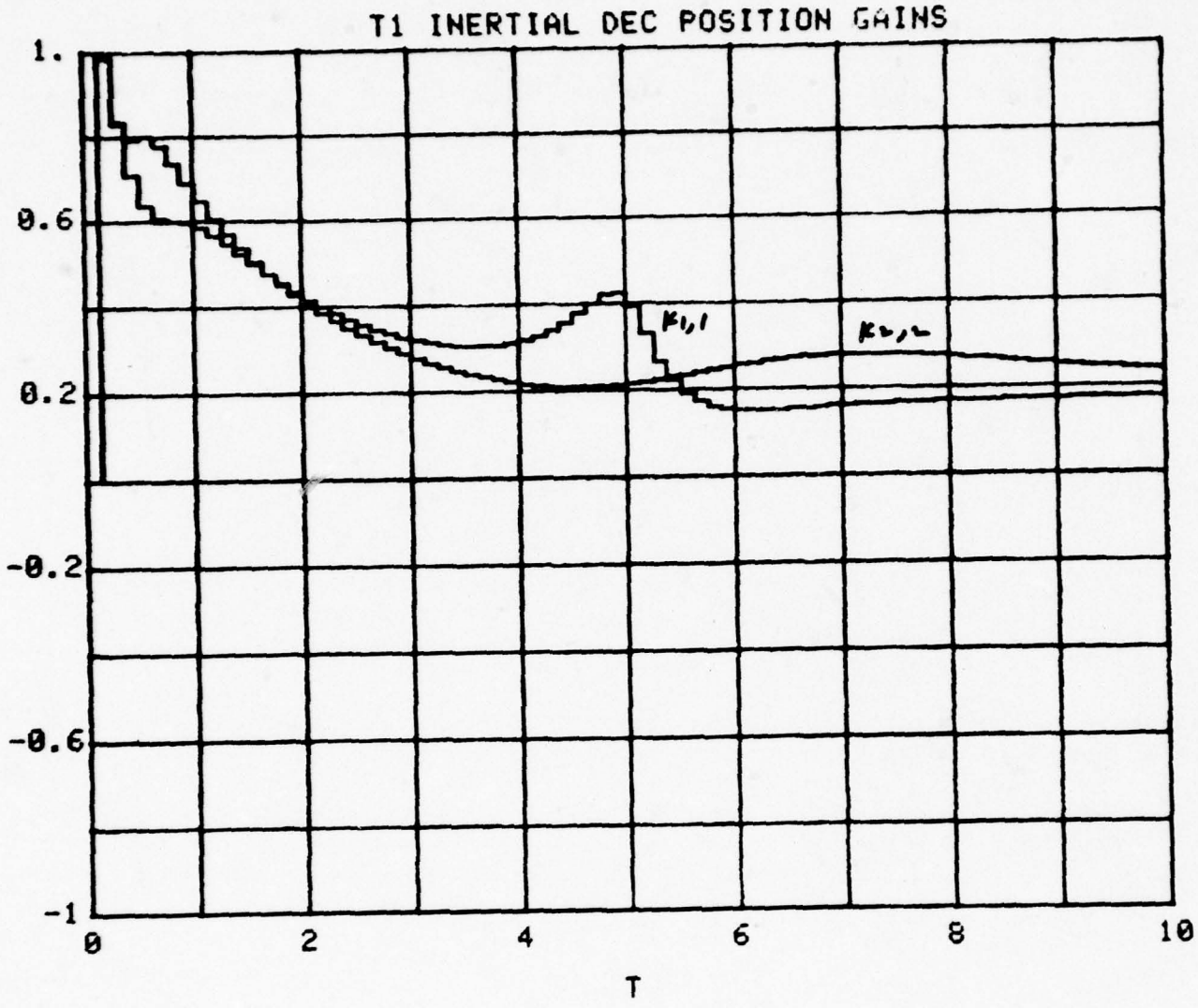
T1 INERTIAL DEC POSITION GAINS
1.
0.6
0.2
-0.2
-0.6
-1
0
2
4
6
8
10
T
K1,1
K2,1

?

FIGURE VI - 28

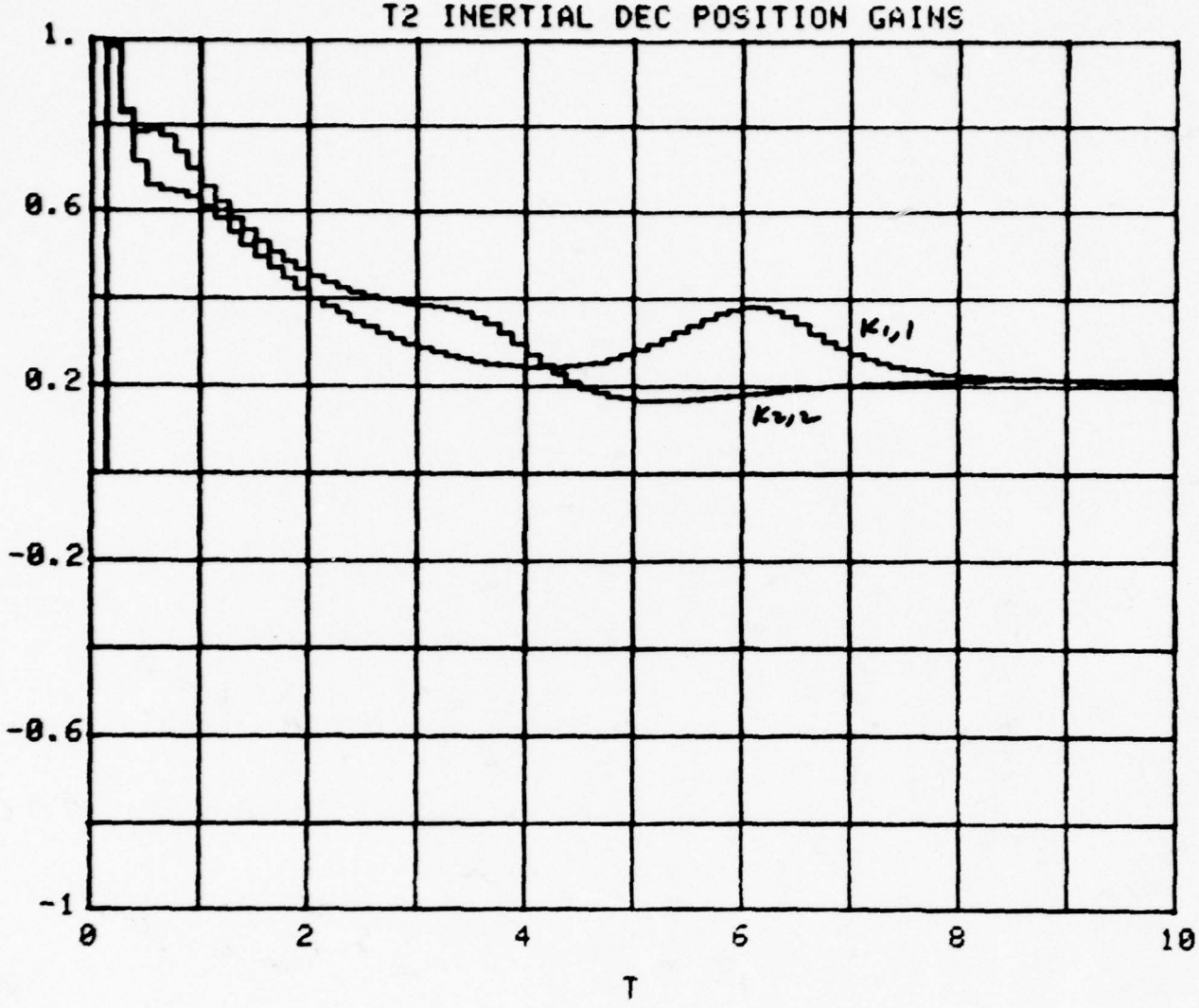
T2 INERTIAL DEC POSITION GAINS
1.
0.6
0.2
-0.2
-0.6
-1
0
2
4
6
8
10
T
K1,1
K2,2

FIGURE VI - 29

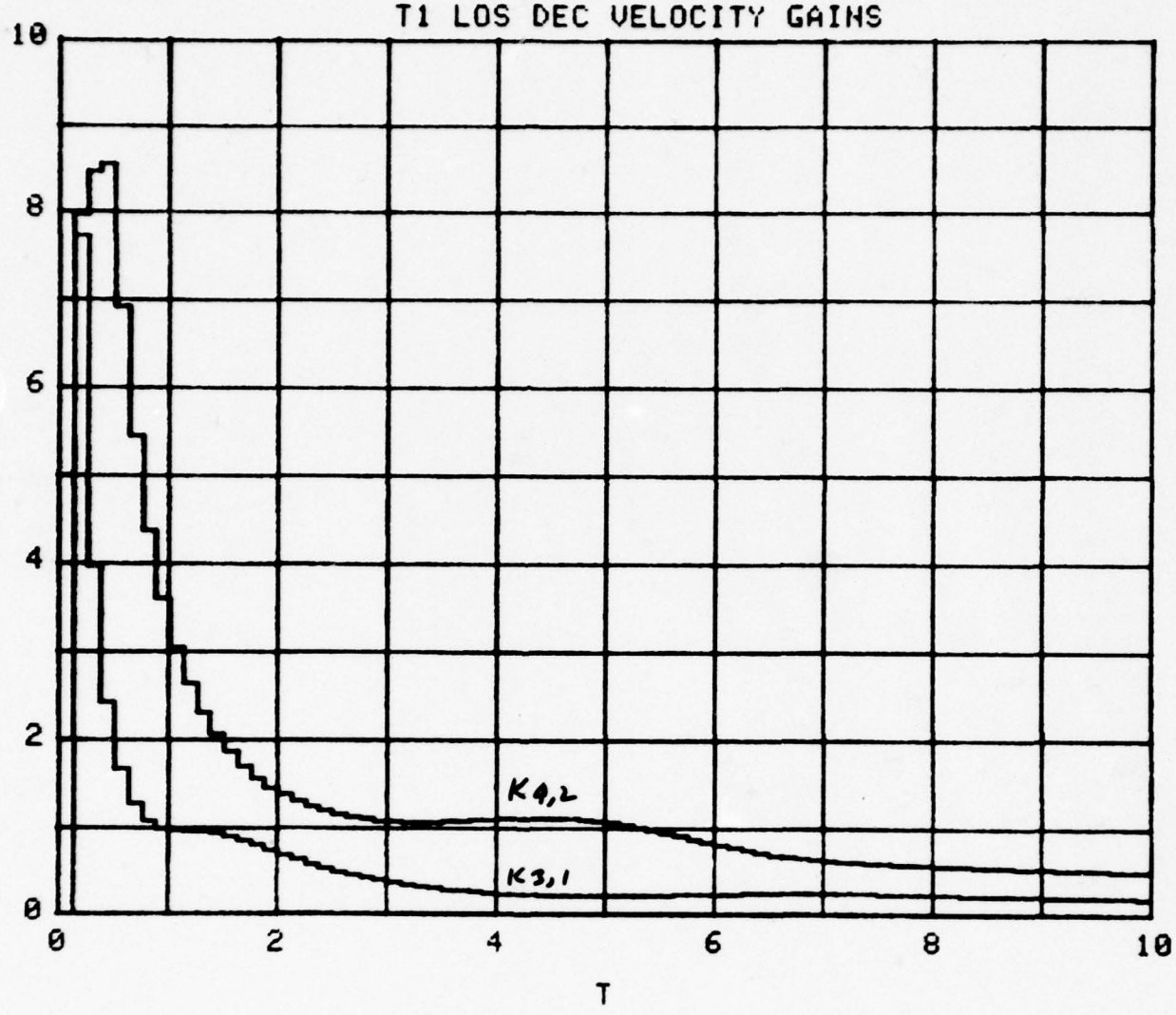

FIGURE VI - 30

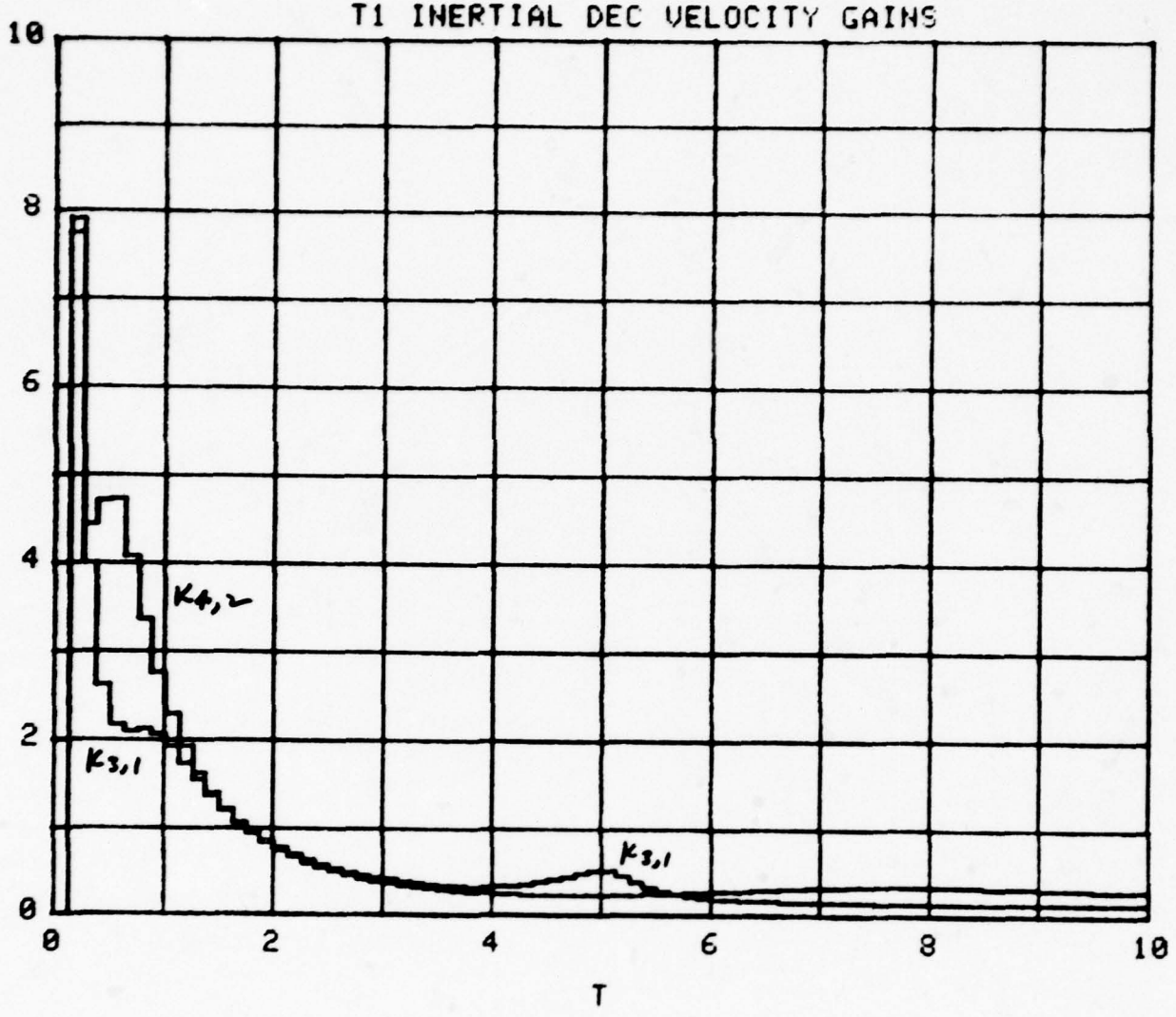
T1 INERTIAL DEC VELOCITY GAINS
10
8
6
4
2
0
0
2
4
6
8
10
T
K4,2
K3,1
K3,1

FIGURE VI - 31

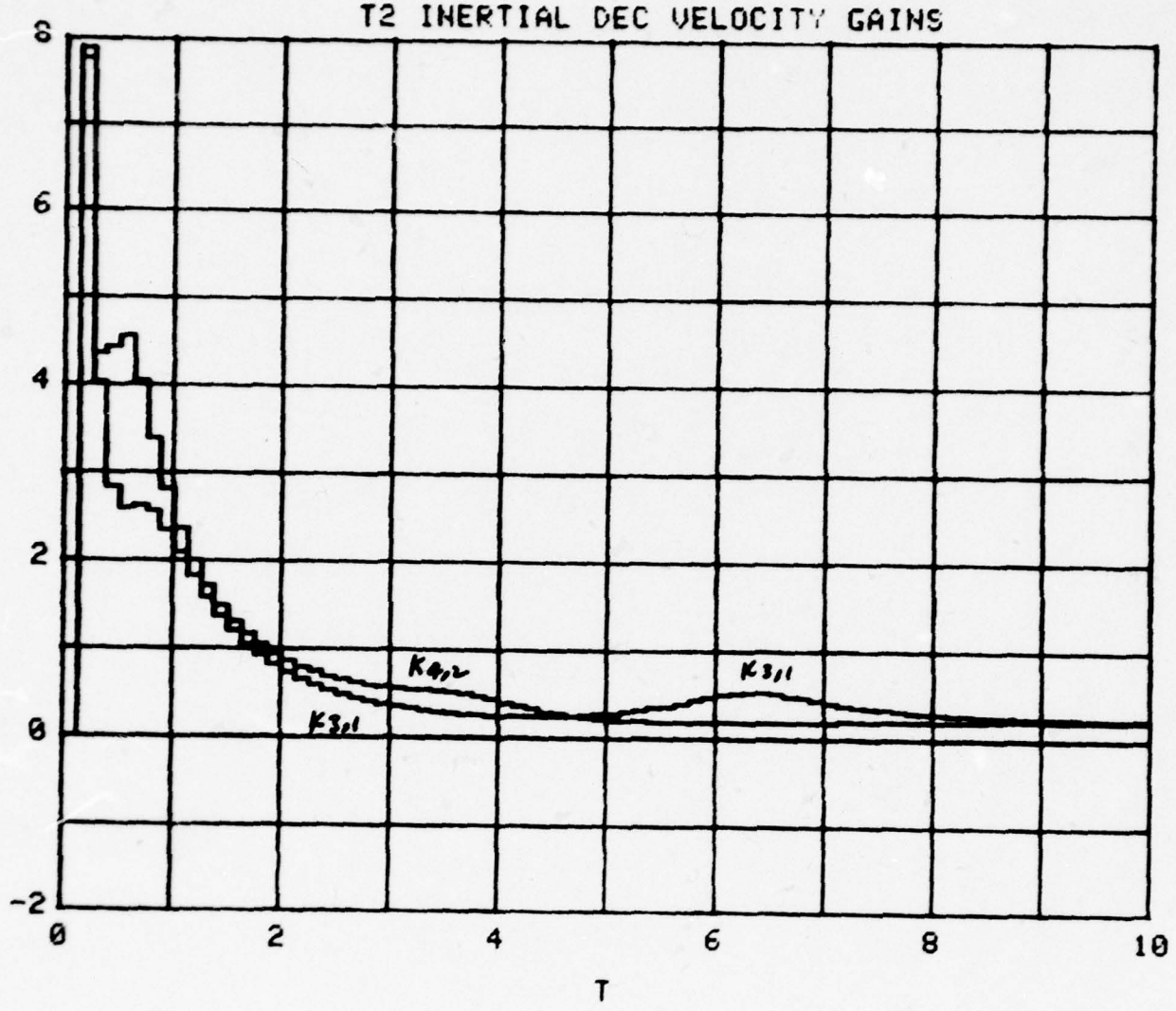

FIGURE VI - 32

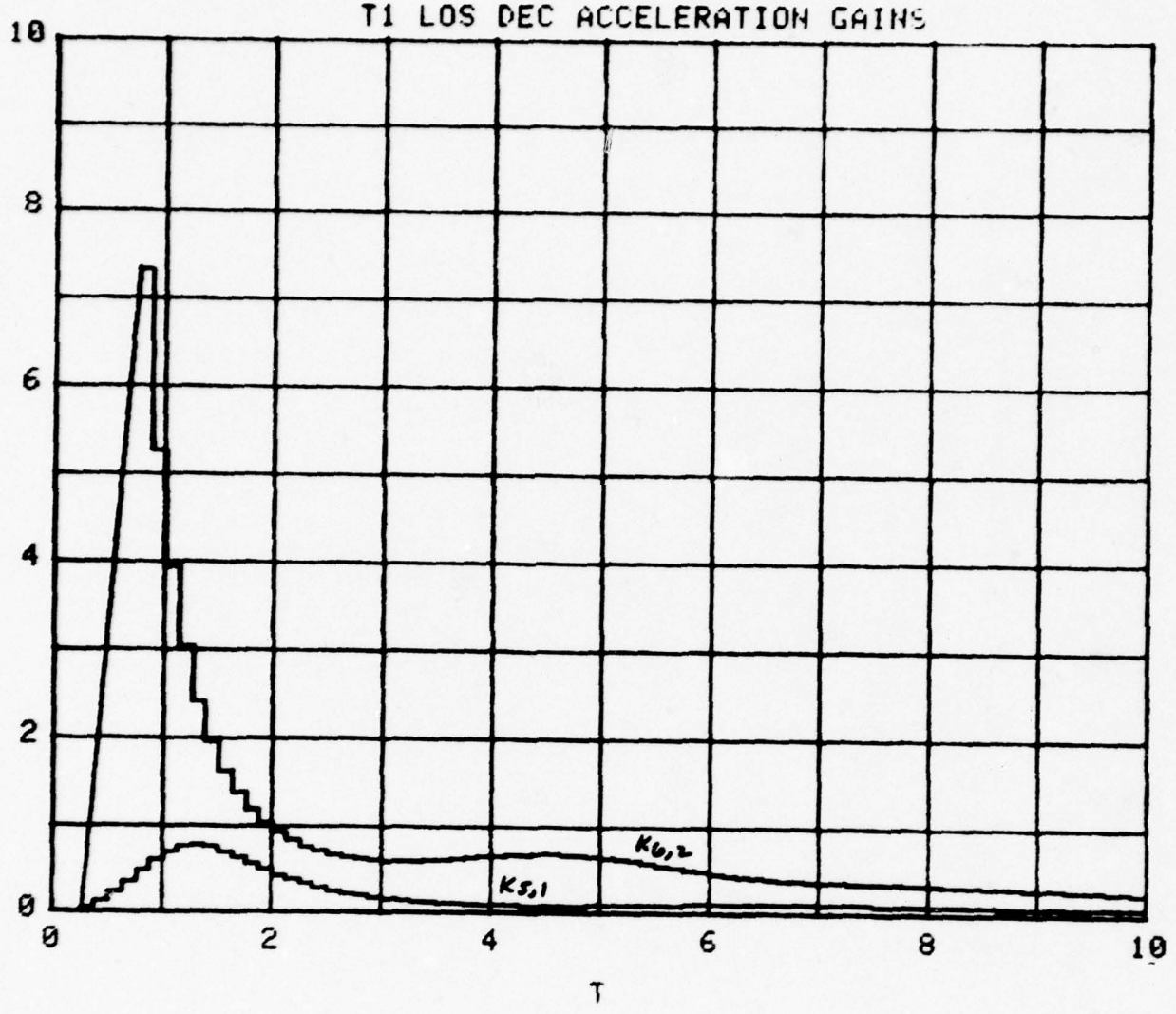

FIGURE VI - 33

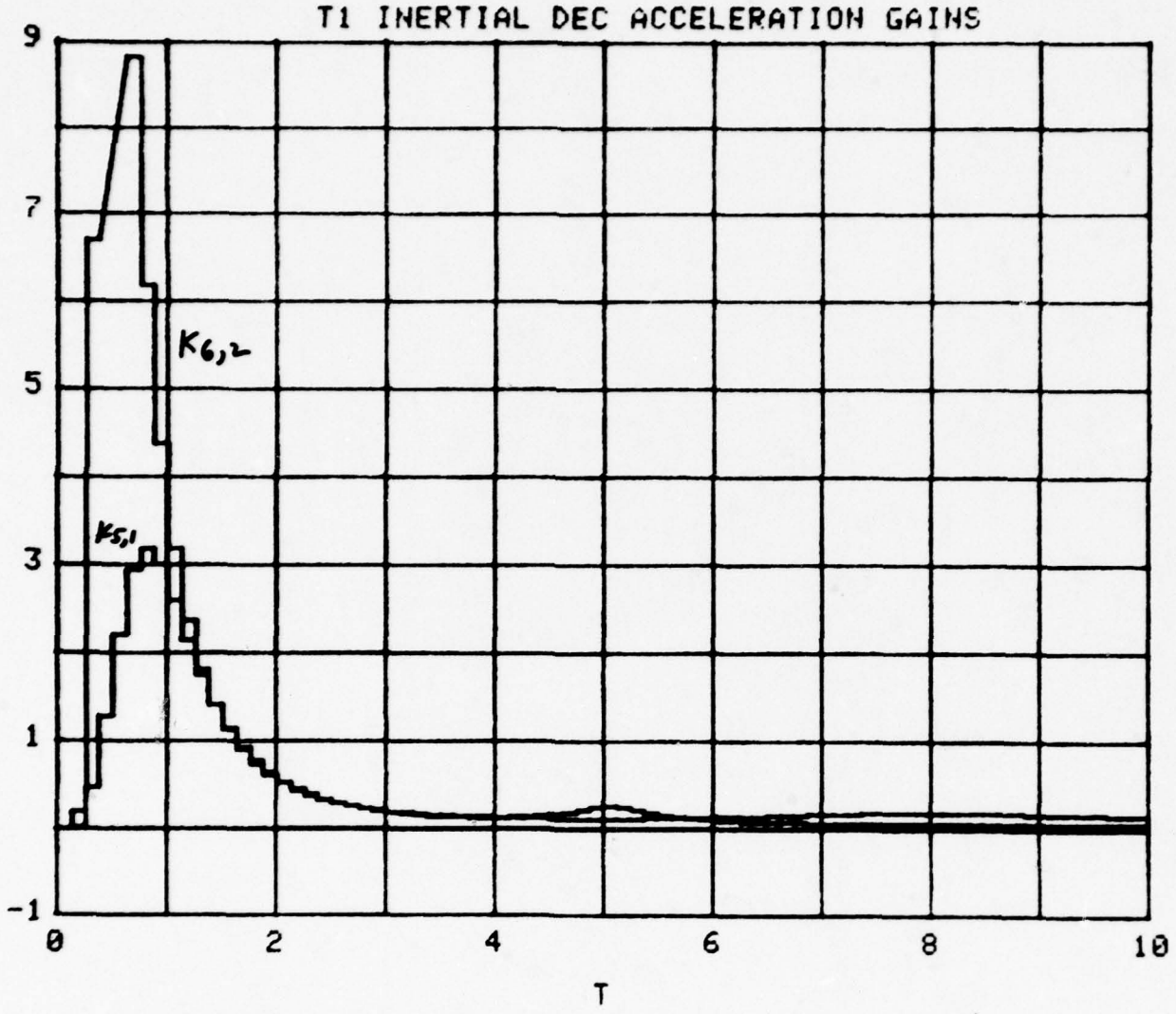
T1 INERTIAL DEC ACCELERATION GAINS
9
7
5
3
1
-1
0
2
4
6
8
10
T
K6,2
K5,1

FIGURE VI - 34

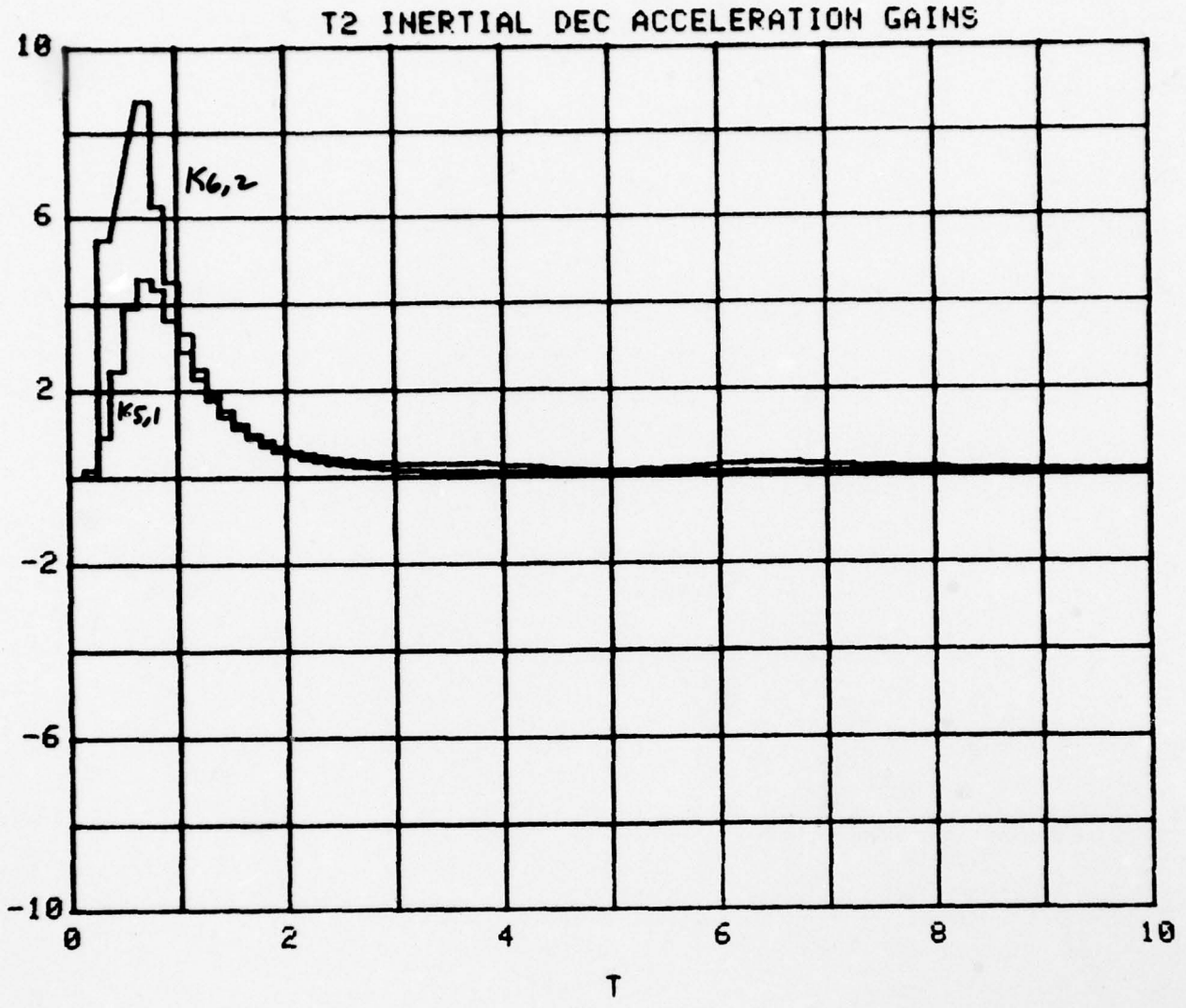
T2 INERTIAL DEC ACCELERATION GAINS
10
6
2
-2
-6
-10
0
2
4
6
8
10
T
K6,2
K5,1

FIGURE VI - 35

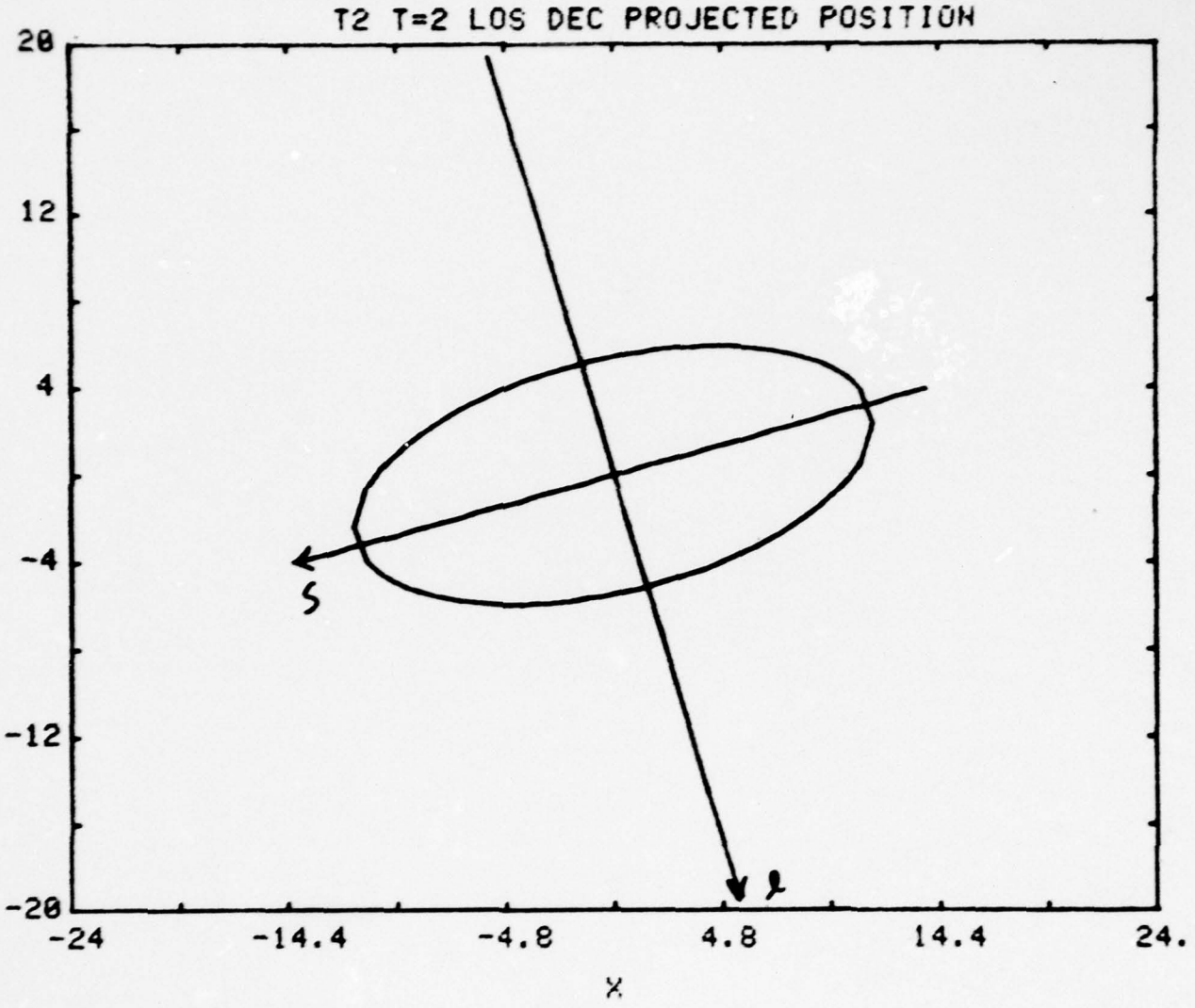
T2 T=2 LOS DEC PROJECTED POSITION
20
12
4
-4
-12
-20
Y
-24
-14.4
-4.8
4.8
14.4
24.
X
S
I

FIGURE VI - 36

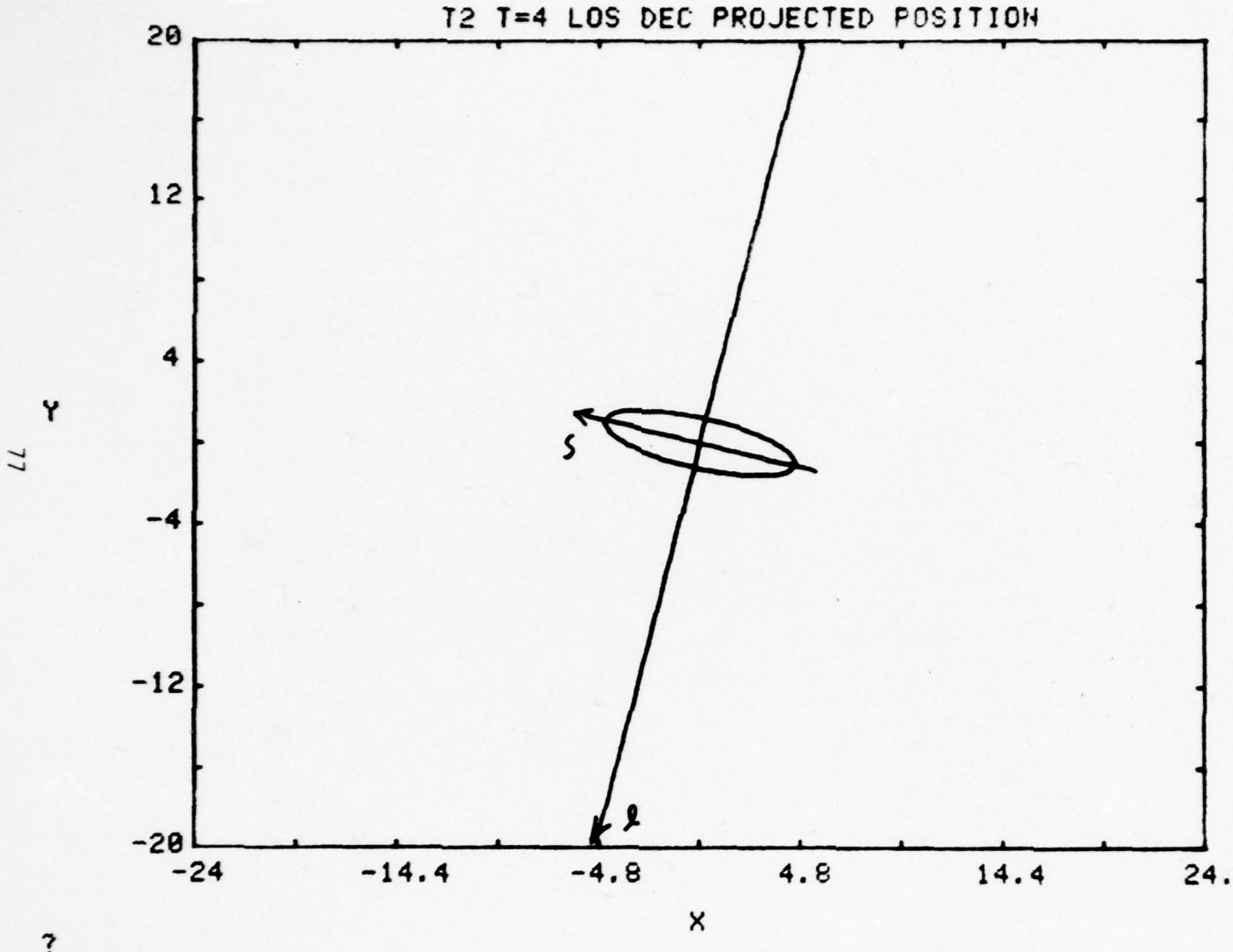
T2 T=4 LOS DEC PROJECTED POSITION
20
12
4
-4
-12
-20
Y
-24
-14.4
-4.8
4.8
14.4
24.
X
S
l

FIGURE VI - 37

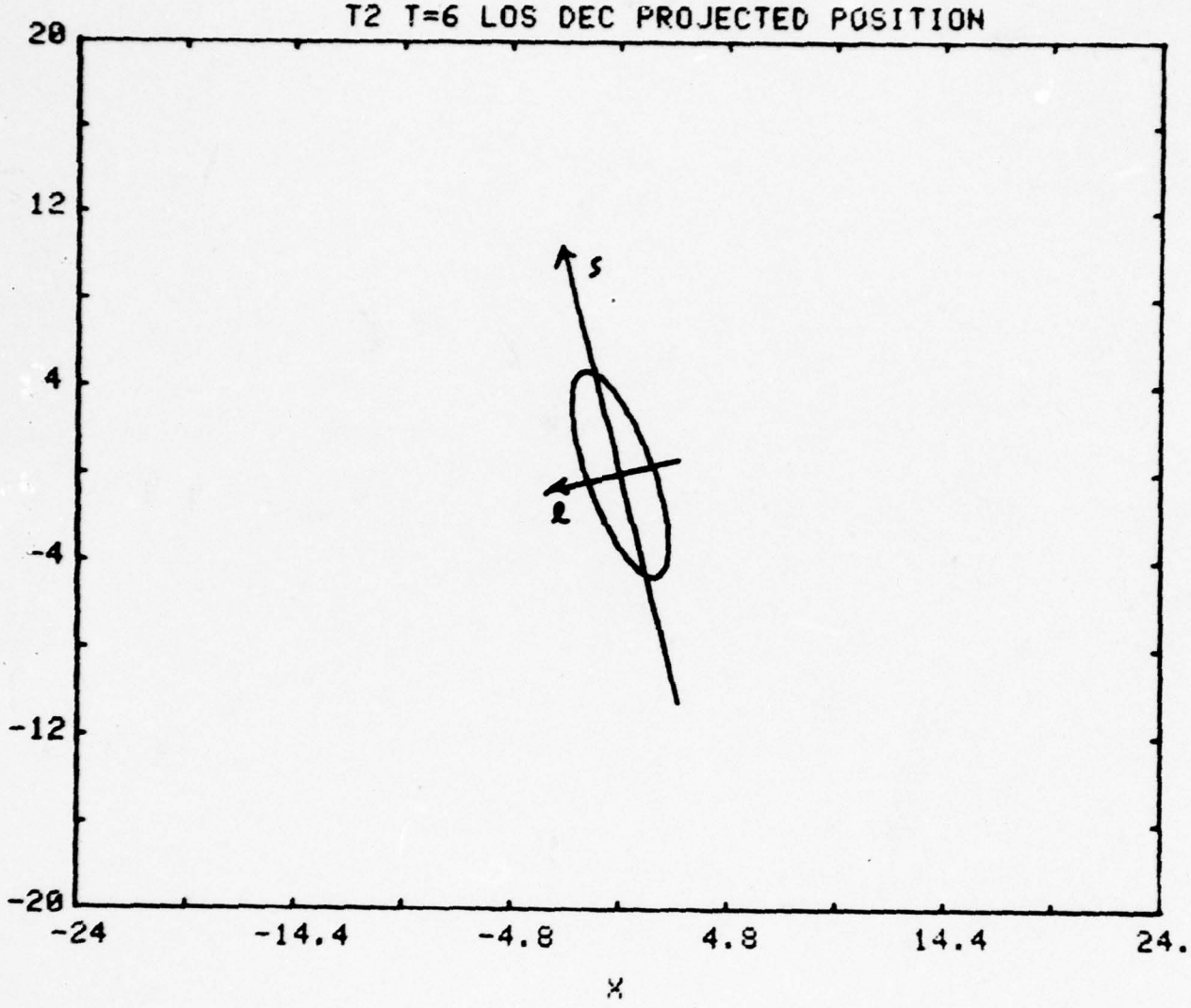
T2 T=6 LOS DEC PROJECTED POSITION
20
12
4
-4
-12
-20
-24
-14.4
-4.8
4.8
14.4
24.
Y
X
S
R

FIGURE VI - 38

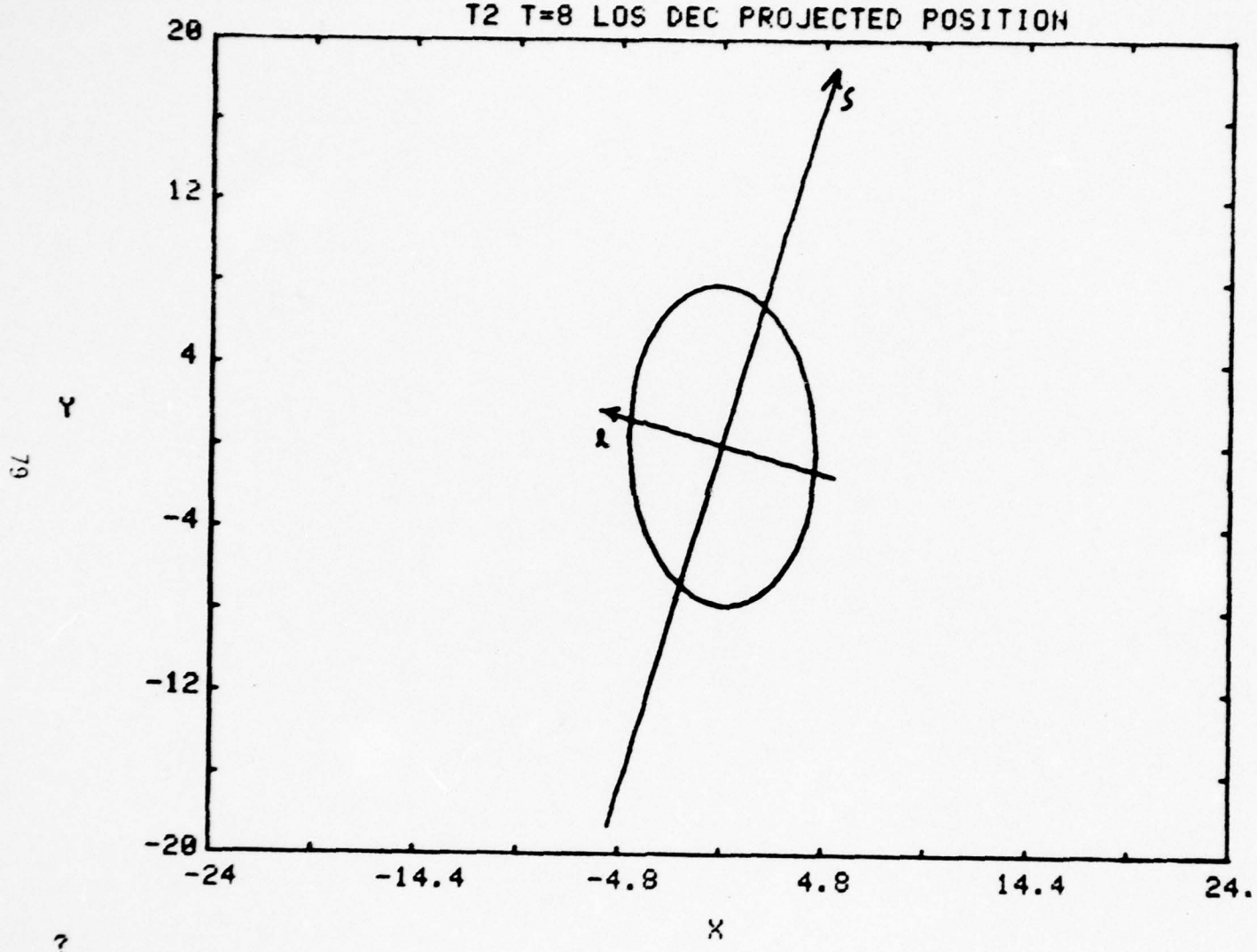
T2 T=8 LOS DEC PROJECTED POSITION
20
12
4
-4
-12
-20
Y
-24
-14.4
-4.8
4.8
14.4
24.
X
S
R

FIGURE VI - 39

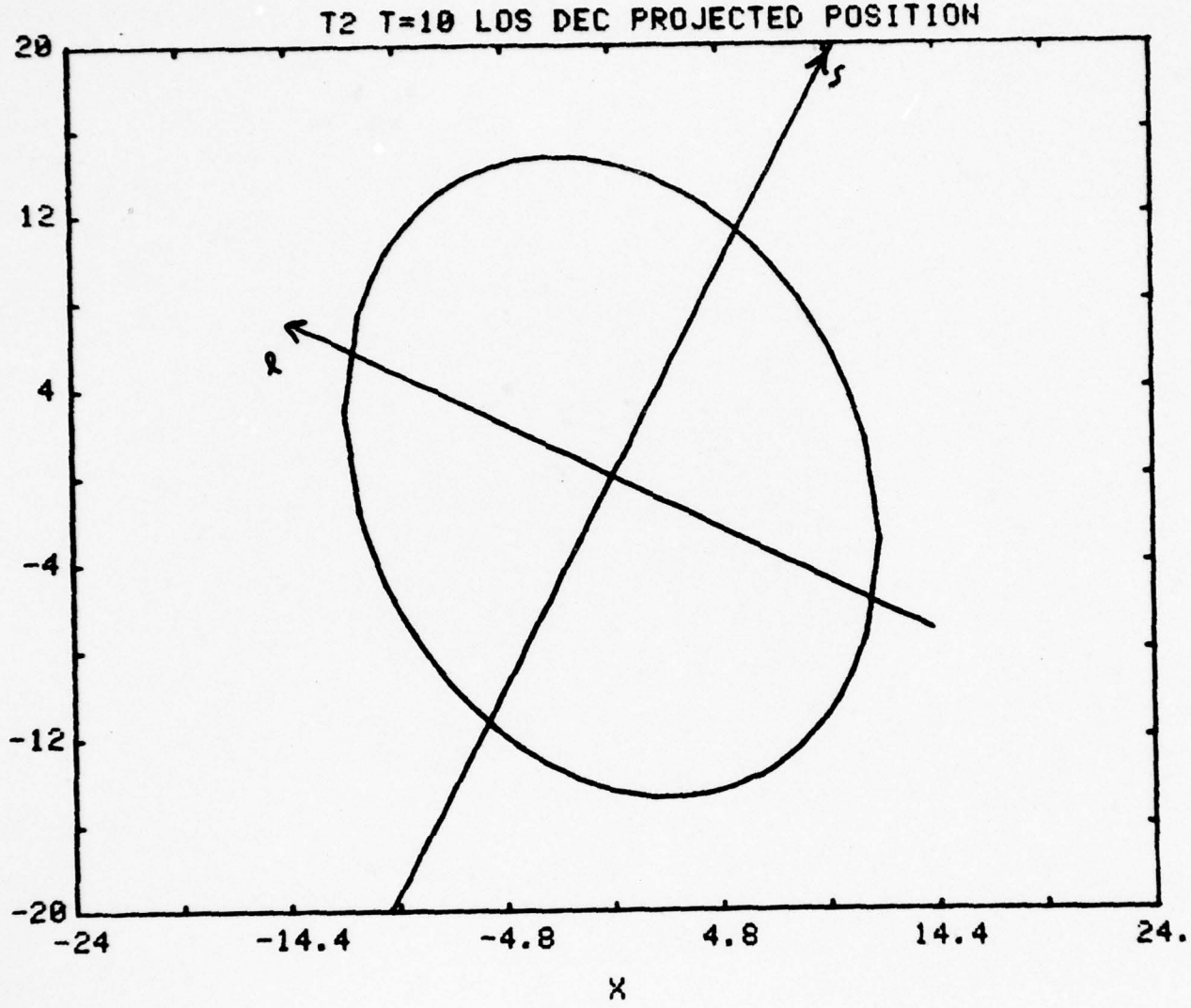
T2 T=10 LOS DEC PROJECTED POSITION
20
12
4
-4
-12
-20
-24
-14.4
-4.8
4.8
14.4
24.
S
R
Y
X

FIGURE VI - 40

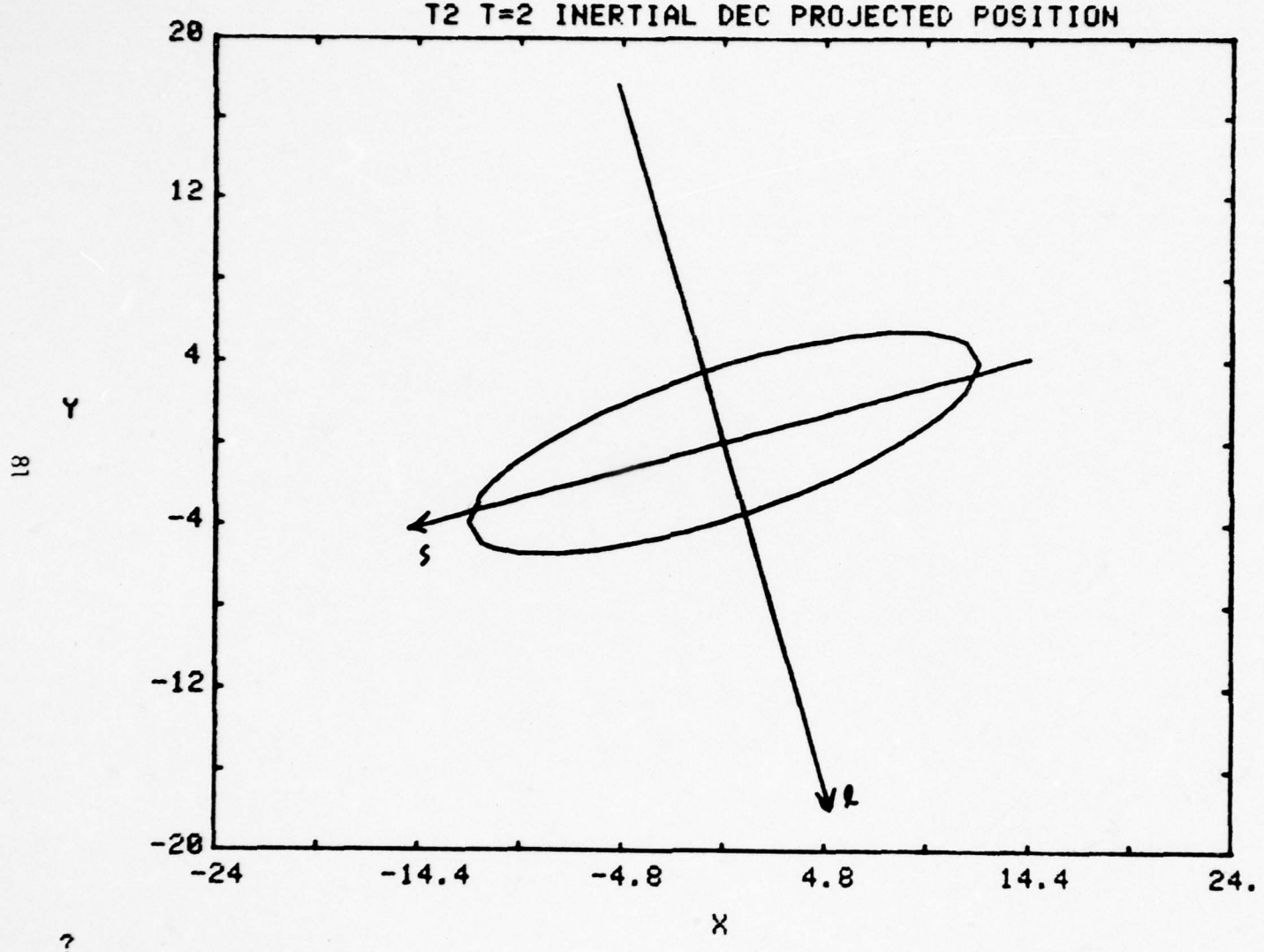
T2 T=2 INERTIAL DEC PROJECTED POSITION
20
12
4
-4
-12
-20
-24
-14.4
-4.8
4.8
14.4
24.
Y
X
S
L

FIGURE VI - 41

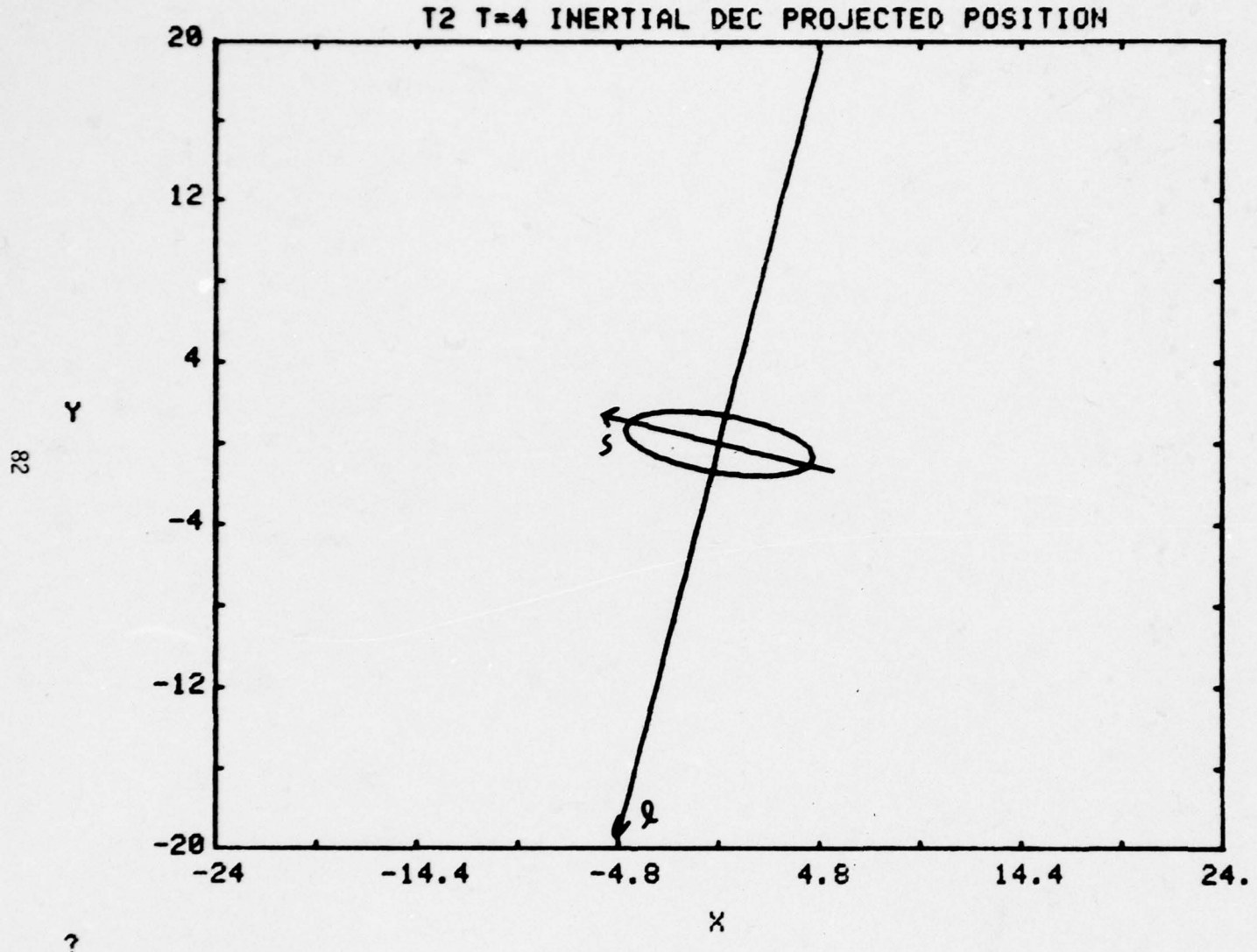
T2 T=4 INERTIAL DEC PROJECTED POSITION
20
12
4
-4
-12
-20
-24
-14.4
-4.8
4.8
14.4
24.
Y
X
S
L

FIGURE VI - 42

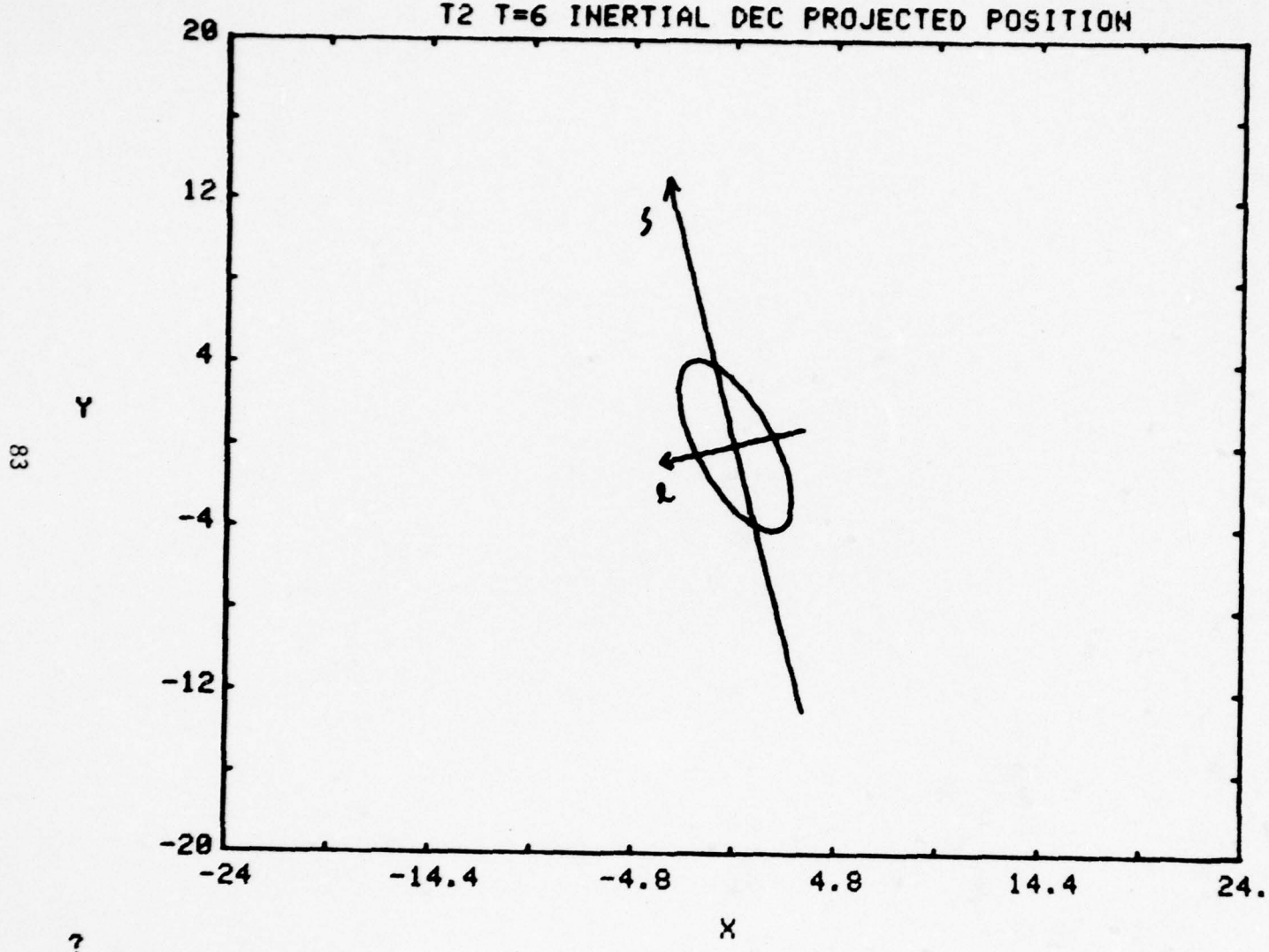
T2 T=6 INERTIAL DEC PROJECTED POSITION
20
12
4
-4
-12
-20
Y
-24
-14.4
-4.8
4.8
14.4
24.
X
S
L

FIGURE VI - 43

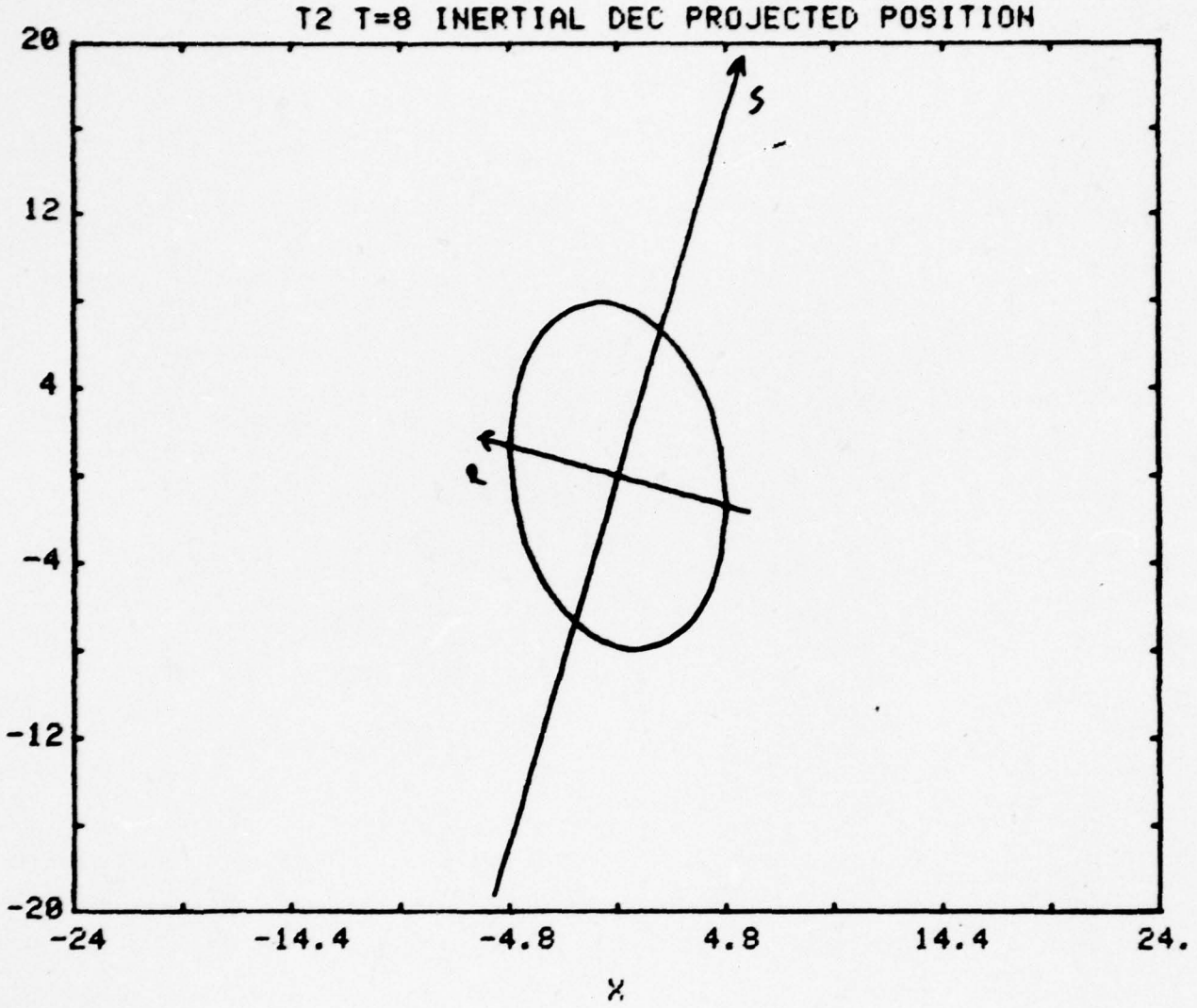
T2 T=8 INERTIAL DEC PROJECTED POSITION
20
12
4
-4
-12
-20
-24
-14.4
-4.8
4.8
14.4
24.
Y
X
S
R

FIGURE VI - 44

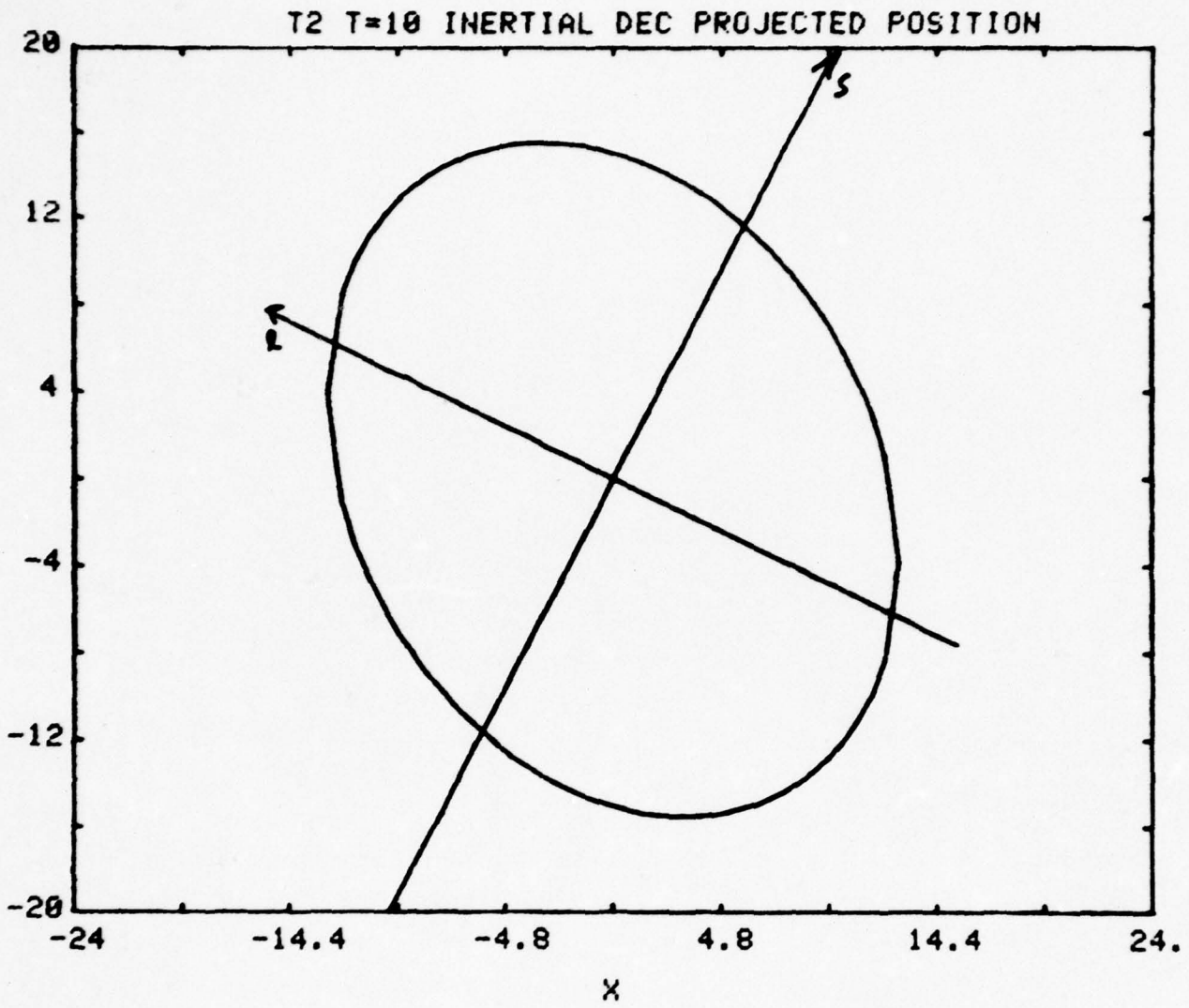
T2 T=10 INERTIAL DEC PROJECTED POSITION
20
12
4
-4
-12
-20
-24
-14.4
-4.8
4.8
14.4
24.
Y
X
S
L

FIGURE VI - 45

E. Results Not Obtained

As the result of careful computer program development with numerous consistency checks, it is believed that the results presented are accurate. However, the danger exists that general conclusions may be drawn from limited data. The further work that should be accomplished to generalize the conclusions is as follows:

F. Trajectories

A wider range of target trajectories is desirable, including straight lines at various ranges and velocities, and accelerating trajectories.

G. Computation Rates

Measurement incorporation rates of other than 8 Hz should be considered. Multiple propagation of variance stops in between measurements might aid in reducing the error due to approximate LOS propagation of variance. To this same end, a higher order approximation to Φ_L should be investigated.

H. Error Sources

The problem should be carefully reexamined to assure that all significant error sources have been adequately modeled.

I. A Fourth Formulation

This study has included rate gyro/LOS, IMU/LOS, and IMU/I. To round out the considerations, especially for new system design, rate gyro/I should be investigated.

J. Improvement on LOS Decoupling

The results obtained with respect to LOS decoupling suggest the possibility of the recovery of some of the lost decoupling accuracy with a relatively minor computational cost. This possibility should be pursued.

VII. References

1. Asher, R. B., Reeves, R. M., "Performance Evaluation of Suboptimal Filters", IEEE AES-11, No. 3, May 1975, pp 400-404.

2. Asher, R. B., "Analysis of Bias, Variance, and Mean Square Estimation Error in Reduced Order Filters", USAF Academy, Aug. 1974. AD-785197.

3. Burke, J. J., "Understanding Kalman Filtering and its Application to Realtime Tracking Systems", Mitre Corp./USAF Systems Command, July 1972. AD-751485.

4. Clark, B. L., "Development of an Adaptive Kalman Target Tracking Filter and Predictor for Five Control Applications", Dahlgren Naval Surface Weapons Center, March 1977. NSWC/DL JR-3445, AD A039907.

5. Crotteau, R. A., "Sub-Optimal Gain Schedules for the Discrete Kalman Filter", Naval Postgraduate School, June 1969. AD 703263.

6. Dziwak, W. J., Vitale, L., Mintz, M., "Investigation of Kalman Filter Designs for Air Defense Based on Arrack Aircraft Data", Frankford Arsenal, September 1976. AD A036440.

7. DeMoyer, R., "Target State Estimator Investigations", Final Report of Consulting Services to General Electric, 1978.

8. Farrell, J. L., Integrated Aircraft Navigation, Academic Press, 1976.

9. Frankford Arsenal, "The Frankford Arsenal Capabilities Test" (FACT), July 1974. FA-JR-74001.

10. Gaston, J. A., Rowland, J. R., "Real Time Digital Integration for Continuous Kalman Filtering in Nonlinear Systems", Computers and Electrical Eng., Vol. 2, 1975, pp 131-140. (G.B.)

11. Gelb, A., "Applied Optimal Estimation", MIJ Press, 1974.

12. Hampton, R. L. J., Cooke, J. R., "Unsupervised Tracking of Maneuvering Vehicles", IEEE AES-9, No. 2, March 1973, pp 197-207.

13. Johnson, F. V., Briggs, P., "Formulation of an Advanced Anti-Aircraft Gun Director through Kalman Estimation Techniques", GE/Frankford Arsenal, December 1973. AD 9160336.

14. Kolibaba, R. L., "Precision Radar Pointing and Tracking Using an Adaptive Extended Kalman Filter", Air Force Institute of Technology, June 1973. AD 768378.

15. Leondes, C. T., "Theory and Applications of Kalman Filtering", NATO AGARDograph No. 139, Feb. 1970. AD 704306.

16. Morgan, D. R., "A Target Trajectory Noise Model for Kalman Trackers", IEEE AES-12, No. 3, March 1973, pp 197-207.

17. NATO, "Practical Aspects of Kalman Filtering Implementation", AGARD-LS-82, 1976. AD A 024377.

18. Ramachandra, K. V., Srinivasar, V. S., "Steady State Results for the XYZ Tracking Filter", IEEE AES-13, July 1977, pp 419-423.

19. Singer, R. A., "Estimating Optimal Tracking Filter Performance for Manned Maneuvering Targets", IEEE AES-6, No. 4, July 1970, pp 473-483.

20. Singer, R. A., Behnke, K. W., "Real-time Tracking Filter Evaluation and Selection for Tactical Applications", IEEE AES-9, No. 1, Jan. 1971, pp 100-110.

21. Stubberud, A. R., Wismer, D. A."Suboptimal Kalman Filter Techniques", Chapter 5 of NATO AGARDograph 139.

22. Thornton, C. L., "Triangular Covariance Factorizations for Kalman Filtering", JPL, Oct. 1976, NASA Tech. Memo. 33-798.

23. Thorp, J. S. "Optimal Tracking of Maneuvering Targets", IEEE AES-9, No. 4, July 1973. pp 512-519.

24. Quigley, A. L. C., "Tracking Study: An Introduction to the Use of Kalman Filters", Admiralty Surface Weapons Establishment (G. B.), 1972. AD 747696.

25. Weideman, H. L., "Parametric Study: Advanced Forward Area Defense Weapon Systems (AFAADS) Final Report" (confidential), Hughes Aircraft, 1971. AD 514587.

AD-A063 704 NAVAL ACADEMY ANNAPOLIS MD DIV OF ENGINEERING AND WEAPONS F/G 19/5
A COMPARATIVE STUDY OF FIRE CONTROL TARGET STATE ESTIMATORS.(U)
NOV 78 R DEMOYER

UNCLASSIFIED USNA-EW-18-78 NL

2 OF 2
AD A063704

END
DATE FILMED
9-79
DDC

VIII. Appendix: Computer Programs

The two major programs which constitute the sub-optimal and truth model are, respectively, SMAIN and TMHIN. These programs call a sequence of subroutines, most of which are used by both. With a familiarity with the mathematical development in Chapter IV, along with the program comments, the programs should be easily followed.

```
100 * R. DEMOYER  1978
110 * SUB-OPTIMAL MAIN PROGRAM
120 COMMON/TIME/T,DT,TMX,NT,TF
130 COMMON/SUB/KSUB(20),KSO,KTRANS
140 * TEST PRINT FILE # 1
150 OPENFILE 1,"TP1"
160 REWIND 1
170 ENDFILE 1
180 * TEST PRINT FILE #2
190 OPENFILE 2,"TP2"
200 REWIND 2
210 ENDFILE 2
220 * TEST PRINT FILE #3
230 OPENFILE 3,"TP3"
240 REWIND 3
250 ENDFILE 3
260 * KALMAN GAIN FILE TO FORCE TRUTH MODEL
270 OPENFILE 4,"BTM","NUMERIC"
280 REWIND 4
290 ENDFILE 4
300 * PLOT FILE
310 OPENFILE 5,"BPLT","NUMERIC"
320 REWIND 5
330 ENDFILE 5
340 * OPTIMAL REFERENCE FILE
350 OPENFILE 6,"REFF","NUMERIC"
360 REWIND 6
370 LIBRARY "SICS"
380 LIBRARY "TTARG"
390 LIBRARY "TPTRAN"
400 LIBRARY "TSTM"
410 LIBRARY "TQ"
420 LIBRARY "TPROP"
430 LIBRARY "TRMAT"
440 LIBRARY "SKGAIN"
450 LIBRARY "TPOST"
460 LIBRARY "TPLOT"
470 LIBRARY "SPROJ"
480 LIBRARY "SUBOP"
490 * KFORM=1  RATE GYRO, LOS FRAME
500 * KFORM=2  DERIVED RATES, LOS FRAME
510 * KFORM=3  IMU, FIXED INERTIAL FRAME
520 * INITIAL CONDITONS
530 CALL SICS(KFORM)
540 * INITIAL WRITE TO PLOT FILE
550 CALL TPLOT
560 * NT FILTER STEPS
570 DO 1 N=1,NT
580 * COMPUTE STATE TRANSITION MATRIX
590 CALL TSTM(KFORM)
600 * COMPUTE STATE NOISE MATRIX
```

```
      CALL TQ(KFORM)
      T=N*DT
      * PROPAGATION OF VARIANCE
      CALL TPROP(KFORM)
      * A PRIORI VALUES TO PLOT FILE
      CALL TPLOT
      * COMPUTE MEASUREMENT NOISE MATRIX
      CALL TRMAT(KFORM)
      * COMPUTE KALMAN GAIN
      CALL SKGAIN(KFORM)
      * COMPUTE A POSTERIORI COVARIANCE
      CALL TPOST(KFORM)
      * PROJECT VARIANCE TO TIME OF IMPACT
      CALL SPROJ
      * A POSTERIORI VALUES TO PLOT FILE
      CALL TPLOT
    1 CONTINUE
      ENDFILE 1
      ENDFILE 2
      ENDFILE 3
      ENDFILE 4
      ENDFILE 5
      IF(KSUB(1).EQ.1) ENDFILE 6
      END
```

```
100 * R. DEMOYER  1978
110 * TRUTH MODEL
120 COMMON/TIME/T,DT,TMX,NT,TF
130 * TEST PRINT FILE #1
140 OPENFILE 1,"TP1"
150 REWIND 1
160 ENDFILE 1
170 * TEST PRINT FILE #2
180 OPENFILE 2,"TP2"
190 REWIND 2
200 ENDFILE 2
210 * TEST PRINT FILE #3
220 OPENFILE 3,"TP3"
230 REWIND 3
240 ENDFILE 3
250 * KALMAN GAIN FILE FROM SUB-OPTIMAL RUN
260 OPENFILE 4,"BTM","NUMERIC"
270 REWIND 4
280 * PLOT FILE
290 OPENFILE 5,"BPLT","NUMERIC"
300 REWIND 5
310 ENDFILE 5
320 * OPTIMAL REFERENCE FILE
330 OPENFILE 6,"REFF","NUMERIC"
340 REWIND 6
350 LIBRARY "TICS"
360 LIBRARY "TTARG"
370 LIBRARY "TPTRAN"
380 LIBRARY "TSTM"
390 LIBRARY "TQ"
400 LIBRARY "TPROP"
410 LIBRARY "TRMAT"
420 LIBRARY "TKGAIN"
430 LIBRARY "TPOST"
440 LIBRARY "TPLOT"
450 LIBRARY "TPROJ"
460 * KFORM = 1  RATE GYRO, LOS FRAME
470 * KFORM = 2  DERIVED RATES, LOS FRAME
480 * KFORM = 3  IMU,  FIXED INERTIAL FRAME
490 * INITILA CONDITIONS
500 CALL TICS(KFORM)
510 * INITIAL WRITE TO PLOT FILE
520 CALL TPLOT
530 * NT FILTER STEPS
540 DO 1 N=1,NT
550 * COMPUTE STATE TRANSITION MATRIX
560 CALL TSTM(KFORM)
570 * COMPUTE STATE NOISE MATRIX
580 CALL TQ(KFORM)
590 T=N*DT
600 * PROPAGATION OF VARIANCE
```

```
      CALL TPROP(KFORM)
      * A PRIORI VALUES TO PLOT FILE
      CALL TPLOT
      * COMPUTE MEAUREMENT NOISE MATRIX
      CALL TRMAT(KFORM)
      * COMPUTE KALMAN GAIN
      CALL TKGAIN(KFORM)
      * COMPUTE A POSTERIORI COVARIANCE
      CALL TPOST(KFORM)
      * PROJECT VARIANCE TO TIME OF IMPACT
      CALL TPROJ
      * A POSTERIORI VALUES TO PLOT FILE
      CALL TPLOT
      * COMPUTE SUM SQUARE ERROR
      CALL TEVAL(1)
    1 CONTINUE
      * PRINT SUM SQUARE ERROR, FIGURE OF MERIT
      CALL TEVAL(2)
      ENDFILE 5
      END
```

```
100 * R. DEMOYER  1978
110 * INITIAL CONDITIONS
120 SUBROUTINE SICS(KFORM)
130 COMMON/TST/XTI(6),XTL(6)
140 COMMON/TRAJ/XTRAJ(2,3)
150 COMMON/NPAR/NS,NM,ND
160 COMMON/TIME/T,DT,TMX,NT,TF
170 COMMON/COV/PTI(6,6),PTL(6,6)
180 COMMON/TRANS/A,AD,TM(2,2),TMF(6,6)
190 COMMON/RPAR/SIGR,SIGAZ,SIGANG,R(2,2)
200 COMMON/QPAR/SIGAC,TCAC,QBET(2)
210 COMMON/TEST/KT
220 COMMON/SUB/KSUB(20),KSO,KTRANS
230 DIMENSION KSB(20)
240 SAVE ALL
250 DATA KSUB/20*0/
260 * KFORM = FORMULATION #1,2, OR 3
270 * KT = TEST PRINT FILE NUMBER1,2,OR 3
280 * TMX = FINAL TIME
290 * NT = # FILTER STEPS
300 * TRAJ = KTR = TRAJECTORY # 1,2, OR 3
310 PRINT,"KFORM,KT,TMX,NT,TRAJ"
320 READ,KFORM,KT,TMX,NT,KTR
330 * SEE SUBROUTINE SUBOP FOR SUB-OPTIMAL CODES
340 PRINT,"#, SUB OPTS"
350 READ,NSUB,(KSB(I),I=1,NSUB)
360 * KSUB(1)=1 TO WRITE REFERENCE FILE
370 DO 30 I=1,NSUB
380 DO 30 J=1,20
390 30 IF(J.EQ.KSB(I)) KSUB(J)=1
400 KSO=0
410 * NOMINAL TIME BASE
420 T=0.
430 DT=TMX/NT
440 * TRAJECTORY
450 GO TO (110,120,130,140,150,160),KTR
460 * TRAJECTORY # 1
470 * X POSITION
480 110 CONTINUE
490 XTRAJ(1,1)=-1500.
500 * X VELOCITY
510 XTRAJ(1,2)=300.
520 * Y POSITION
530 XTRAJ(2,1)=500.
540 GO TO 300
550 * TRAJECTORY # 2
560 120 CONTINUE
570 S2=SQRT(2.)
580 XTRAJ(1,1)=-1000*S2
590 XTRAJ(1,2)=150*S2
600 XTRAJ(2,1)=-500*S2
```

```
610 XTRAJ(2,2)=150*S2
620 GO TO 300
630 130 GO TO 300
640 140 GO TO 300
650 150 GO TO 300
660 160 GO TO 300
670 300 CONTINUE
680 * 2 DIMENSIONAL MODEL
690 * ND = # DIMENSIONS
700 ND=2
710 * NM = # MEASUREMENTS (RANGE & CROSS RANGE)
720 NM=2
730 * NS = # STATES
740 NS=ND*3
750 * INITIAL TRAJECTORY
760 IF(KT.NE.0) WRITE(KT,200)
770 200 FORMAT(1X,"TICS")
780 CALL TTARG
790 * MEASUREMENT PARAMETERS
800 * RADAR RANGE S.D.
810 SIGR=5.
820 * RADAR CROSS RANGE ANGLE S.D.
830 SIGAZ=.001
840 * IMU ANGULAR RESOLUTION
850 SIGANG=.002
860 * RATE GYRO RATE S.D.
870 SIGBET=.005
880 QBET(1)=SIGBET**2
890 QBET(2)=0.
900 * SIGANG=0. FOR THUTH MODEL REFERENCE
910 IF(KSUB(1).EQ.1) SIGANG=0.
920 IF(KSUB(10).NE.1) GO TO 310
930 * PARAMETER MODIFICATION CAPABILITY
940 PRINT,"SIGR,SIGAZ,SIGANG,SIGBET"
950 READ,SIGR,SIGAZ,SIGANG,SIGBET
960 QBET(1)=SIGBET**2
970 310 CONTINUE
980 * INITIAL COVARIANCES
990 DO 1 IR=1,6
1000 DO 1 IC=1,6
1010 PTI(IR,IC)=0.
1020 1 PTL(IR,IC)=0.
1030 PTL(1,1)=5.**2
1040 PTL(2,2)=(XTL(1)*SIGAZ)**2
1050 PTL(3,3)=(300.)**2
1060 PTL(4,4)=(300.)**2
1070 PTL(5,5)=(20.)**2
1080 PTL(6,6)=(200.)**2
1090 * TRANSFORMED FROM LOS TO I
1100 CALL TPTRAN(2)
1110 * STATE NOISE PARAMETERS
```

```
1120 * SPECTRAL S.D.
1130 SIGAC=2.
1140 * MARKOV TIME CONSTANT
1150 TCAC=5
1160 * IC'S WRITTEN TO FILE BTM TO FORM TRUTH MODEL IC'S
1170 WRITE(4)XTI,XTL,XTRAJ,NS,NM,ND,T,DT,TMX,NT
1180 WRITE(4)PTI,PTL,A,AD,TM,TMF,SIGR,SIGAZ,SIGANG
1190 WRITE(4)R,SIGAC,TCAC,QBET,KFORM
1200 * DIAGNOSTIC PRINT
1210 IF(KT.NE.1) RETURN
1220 WRITE(KT,201)
1230 201 FORMAT(1X,"PTL")
1240 DO 101 IR=1,NS
1250 101 WRITE(KT,100)(PTL(IR,IC),IC=1,NS)
1260 100 FORMAT(1X,6(1PE11.3))
1270 WRITE(KT,202)
1280 202 FORMAT(1X,"PTI")
1290 DO 102 IR=1,NS
1300 102 WRITE(KT,100)(PTI(IR,IC),IC=1,NS)
1310 CALL TPTRAN(1)
1320 WRITE(KT,203)
1330 203 FORMAT(1X,"PTL RECOVERY CHECK")
1340 DO 103 IR=1,NS
1350 103 WRITE(KT,100)(PTL(IR,IC),IC=1,NS)
1360 RETURN
1370 END
```

```
100 * R. DEMOYER 1978
110 SUBROUTINE TICS(KFORM)
120 COMMON/TST/XTI(6),XTL(6)
130 COMMON/TRAJ/XTRAJ(2,3)
140 COMMON/NPAR/NS,NM,ND
150 COMMON/TIME/T,DT,TMX,NT,TF
160 COMMON/COV/PTI(6,6),PTL(6,6)
170 COMMON/TRANS/A,AD,TM(2,2),TMF(6,6)
180 COMMON/RPAR/SIGR,SIGAZ,SIGANG,R(2,2)
190 COMMON/QPAR/SIGAC,TCAC,QBET(2)
200 COMMON/TEST/KT
210 COMMON/SUB/KSUB(20),KSO,KTRANS
220 DATA KSUB/20*0/
230 * DIAGNOSTIC PRINT FILE NUMBER
240 PRINT,"KT"
250 READ,KT
260 * IC'S FROM SUB-OPTIMAL RUN
270 READ(4)XTI,XTL,XTRAJ,NS,NM,ND,T,DT,TMX,NT
280 READ(4)PTI,PTL,A,AD,TM,TMF,SIGR,SIGAZ,SIGANG
290 READ(4)R,SIGAC,TCAC,QBET,KFORM
300 * KSO=1 FOR TRUTH MODEL
310 KSO=1
320 KFORM=3
330 CALL TTARG
340 * SIGANG=0. FOR TRUTH MODEL
350 SIGANG=0.
360 RETURN
370 END
```

```
100 * R. DEMOYER  1978
110 * TARGET MODEL
120 SUBROUTINE TTARG
130 COMMON/TST/XTI(6),XTL(6)
140 COMMON/TRAJ/XTRAJ(2,3)
150 COMMON/NPAR/NS,NM,ND
160 COMMON/TIME/TI,DT,TMX,NT,TF
170 COMMON/TRANS/A,AD,TM(2,2),TMF(6,6)
180 COMMON/TEST/KT
190 COMMON/NTM/TNMF(6,6)
200 DO 10 IR=1,NS
210 DO 10 IC=1,NS
220 TMF(IR,IC)=0.
230 10 TNMF(IR,IC)=0.
240 * CONSTANT ACCELERATION TRUE TRAJECTORY
250 * ID = X, Y  DIRECTION
260 * N=1 : CURRENT TIME
270 * N=2 : NEXT TIME
280 DO 20 N=1,2
290 IF(N.EQ.1) T=TI+DT
300 IF(N.EQ.2) T=TI
310 * XTI : INERTIAL STATE VECTOR
320 DO 1 ID=1,ND
330 * POSITION
340 XTI(ID)=XTRAJ(ID,1)+XTRAJ(ID,2)*T+.5*XTRAJ(ID,3)*T**2
350 * VELOCITY
360 XTI(ND+ID)=XTRAJ(ID,2)+XTRAJ(ID,3)*T
370 * ACCELERATION
380 1 XTI(2*ND+ID)=XTRAJ(ID,3)
390 X=XTI(1)
400 XD=XTI(ND+1)
410 Y=XTI(2)
420 YD=XTI(ND+2)
430 * AZIMUTH
440 A=ATAN2(Y,X)
450 PI=3.1415926
460 IF(A.LT.0.) A=A+2*PI
470 * AZIMUTH RATE
480 AD=(X*YD-Y*XD)/(X**2+Y**2)
490 * INERTIAL TO LOS TRANSFORMATION
500 TM(1,1)=X/SQRT(X**2+Y**2)
510 TM(2,2)=TM(1,1)
520 TM(1,2)=Y/SQRT(X**2+Y**2)
530 TM(2,1)=-TM(1,2)
540 * FULL TRANSFORMATION  3 PARTITIONS
550 DO 2 IP=1,3
560 DO 2 IR=1,ND
570 DO 2 IC=1,ND
580 IRF=(IP-1)*ND+IR
590 ICF=(IP-1)*ND+IC
600 IF(N.EQ.1) TNMF(IRF,ICF)=TM(IR,IC)
```

```
      IF(N.EQ.2) TMF(IRF,ICF)=TM(IR,IC)
   20 CONTINUE
*  INERTIAL STATE TRANSFORMED TO LOS STATE
      DO 3 IR=1,NS
      XTL(IR)=0.
      DO 3 IRC=1,NS
    3 XTL(IR)=XTL(IR)+TMF(IR,IRC)*XTI(IRC)
*  DIAGNOSTIC PRINTS
      IF(KT.NE.1) RETURN
      WRITE(KT,200)
  200 FORMAT(1X,"TTARG")
      WRITE(KT,201)
  201 FORMAT(1X,"XTI")
      WRITE(KT,100)XTI
  100 FORMAT(1X,6(1PE11.3))
      WRITE(KT,202)
  202 FORMAT(1X,"XTL")
      WRITE(KT,100)XTL
      WRITE(KT,203)
  203 FORMAT(1X,"A,AD")
      WRITE(KT,100)A,AD
      WRITE(KT,204)
  204 FORMAT(1X,"TM")
      DO 101 IR=1,2
  101 WRITE(KT,100)(TM(IR,IC),IC=1,2)
      RETURN
      END
```

```
      * R. DEMOYER  1978
      * TRANSFORMATION OF COVARIANCE MATRIX
      SUBROUTINE TPTRAN(KF)
      * KF=1 :  INERTIAL TO LOS
      * KF=2 :  LOS TO INERTIAL
      COMMON/COV/PTI(6,6),PTL(6,6)
      COMMON/TRANS/A,AD,TM(2,2),TMF(6,6)
      COMMON/NPAR/NS,NM,ND
      DIMENSION TT(6,6)
      DOUBLE PRECISION S
      GO TO (100,200),KF
      * COVARINACE TRANSFORMATION  INERTIAL TO LOS
      * PTL = (TMF)(PTI)(TMF)T
  100 CONTINUE
      DO 1 IR=1,NS
      DO 1 IC=IR,NS
      S=0.
      DO 2 IRC1=1,NS
      DO 2 IRC2=1,NS
      IF(TMF(IR,IRC1).EQ.0.) GO TO 2
      IF(PTI(IRC1,IRC2).EQ.0.) GO TO 2
      IF(TMF(IC,IRC2).EQ.0.) GO TO 2
      S=S+TMF(IR,IRC1)*PTI(IRC1,IRC2)*TMF(IC,IRC2)
    2 CONTINUE
      PTL(IR,IC)=S
    1 PTL(IC,IR)=S
      RETURN
      * LOS TO INERTIAL
  200 CONTINUE
      DO 11 IR=1,NS
      DO 11 IC=IR,NS
      S=0.
      DO 12 IRC1=1,NS
      DO 12 IRC2=1,NS
      IF(TMF(IRC1,IR).EQ.0.) GO TO 12
      IF(PTL(IRC1,IRC2).EQ.0.) GO TO 12
      IF(TMF(IRC2,IC).EQ.0.) GO TO 12
      S=S+TMF(IRC1,IR)*PTL(IRC1,IRC2)*TMF(IRC2,IC)
   12 CONTINUE
      PTI(IR,IC)=S
   11 PTI(IC,IR)=S
      RETURN
      END
```

```
      * R. DEMOYER  1978
      * COMPUTATION OF STATE NOISE
      SUBROUTINE TQ(KFORM)
      COMMON/TST/XTI(6),XTL(6)
      COMMON/NPAR/NS,NM,ND
      COMMON/TIME/T,DT,TMX,NT,TF
      COMMON/TRANS/A,AD,TM(2,2),TMF(6,6)
      COMMON/QPAR/SIGAC,TCAC,QBET(2)
      COMMON/TEST/KT
      COMMON/QNOISE/Q(6,6)
      COMMON/SUB/KSUB(20),KSO,KTRANS
      DIMENSION G(6)
      DO 1 IR=1,NS
      DO 1 IC=1,NS
    1 Q(IR,IC)=0.
      * QU = ALONG AXIS SPECTRAL JERQUE TERM FROM
      * MARKOV ACCELERATION PARAMETERS
      QU=2.*SIGAC**2/TCAC
      * QV = CROSS AXIS TERM
      QV=4.*QU
      * EQUAL SPECTRAL SUB OP
      IF(KSUB(7).EQ.1) QU=.5*(QU+QV)
      IF(KSUB(7).EQ.1) QV=QU
      GO TO (100,200,300,400),KFORM
      * TRANSFORM VX,VY TO VS,VL
  200 VS=TM(1,1)*XTI(3)+TM(1,2)*XTI(4)
      VL=TM(2,1)*XTI(3)+TM(2,2)*XTI(4)
      GO TO 150
      * VS,VL FROM STATE VECTOR
  100 VS=XTL(3)
      VL=XTL(4)
  150 V1=VS
      V2=VL
      GO TO 600
      * VX,VT FROM STATE VECTOR
  400 CONTINUE
  300 VX=XTI(3)
      VY=XTI(4)
      V1=VX
      V2=VY
      * TRANSFORMATION OF TARGET FIXED SPECTRAL TERMS
      * TO COMPUTATIONAL FRAME
  600 VSQ=V1**2+V2**2
      Q(5,5)=DT*(V1**2*QU+V2**2*QV)/VSQ
      Q(6,6)=DT*(V2**2*QU+V1**2*QV)/VSQ
      Q(5,6)=DT*(V1*V2*QU-V1*V2*QV)/VSQ
      Q(6,5)=Q(5,6)
      IF(KFORM.EQ.3) GO TO 500
      IF(KSUB(2).NE.1) GO TO 500
      * G MATRIX TERMS FOR LOS FRAME
      G(1)=XTL(2)
```

```
      610 G(2)=-XTL(1)
      620 G(3)=XTL(4)
      630 G(4)=-XTL(3)
      640 G(5)=XTL(6)
      650 G(6)=-XTL(5)
      660 DT2=DT**2
      670 DO 160 IR=1,NS
      680 DO 160 IC=IR,NS
      690 Q(IR,IC)=Q(IR,IC)+G(IR)*G(IC)*QBET(KFORM)*DT2
      700 160 Q(IC,IR)=Q(IR,IC)
      710 500 IF(KT.NE.1) RETURN
      720 * DIAGMOSTIC PRINTS
      730 WRITE(KT,501)
      740 501 FORMAT(1X,"TQ")
      750 WRITE(KT,502)
      760 502 FORMAT(1X,"QU,QV,VS,VL,VX,VY,V1,V2")
      770 WRITE(KT,503)QU,QV,VS,VL,VX,VY,V1,V2
      780 503 FORMAT(1X,6(1PE11.3))
      790 IF(KFORM.EQ.1) WRITE(KT,504)
      800 504 FORMAT(1X,"G")
      810 IF(KFORM.EQ.1) WRITE(KT,503)G
      820 WRITE(KT,505)
      830 505 FORMAT(1X,"Q")
      840 DO 506 IR=1,NS
      850 506 WRITE(KT,503)(Q(IR,IC),IC=1,NS)
      860 RETURN
      870 END
```

```
      * R. DEMOYER  1978
      * STATE TRANSITION MATRIX COMPUTATION
      SUBROUTINE TSTM(KFORM)
      COMMON/TIME/T,DT,TMX,NT,TF
      COMMON/STM/PHI(6,6)
      COMMON/TEST/KT
      COMMON/TRANS/A,AD,TM(2,2),TMF(6,6)
      COMMON/NPAR/NS,NM,ND
      COMMON/QPAR/SIGAC,TCAC,QBET(2)
      DIMENSION PH(6,6)
      COMMON/NTM/TNMF(6,6)
      COMMON/SUB/KSUB(20),KSO,KTRANS
      DOUBLE PRECISION S
      SAVE PH,PHI
      IF(T.GT.0.) GO TO 50
      B=1./TCAC
      EBT=EXP(-B*DT)
      DO 10 IR=1,NS
      DO 10 IC=1,NS
   10 PH(IR,IC)=0.
      BT=B*DT
      * EXACT INERTIAL STATE TRANSITION MATRIX
      PH(1,1)=PH(2,2)=PH(3,3)=PH(4,4)=1.
      PH(1,3)=PH(2,4)=DT
      PH(1,5)=PH(2,6)=(EBT+BT-1.)/B**2
      PH(3,5)=PH(4,6)=(1.-EBT)/B
      PH(5,5)=PH(6,6)=EBT
   50 GO TO (100,100,300),KFORM
      * LOS STM
      * PHL=(TMF)*(PH)*(TMF)T
  100 CONTINUE
      ** DIAGNOSTIC PRINT ELIMINATED **
      IF(KT.NE.99) GO TO 150
      WRITE(2,111)KFORM
  111 FORMAT(1X,"STM, KFORM = ",I3)
      WRITE(2,112)
  112 FORMAT(1X,"TMF")
      DO 113 IR=1,NS
  113 WRITE(2,114)(TMF(IR,IC),IC=1,NS)
  114 FORMAT(X,6(1PE11.3))
      WRITE(2,115)
  115 FORMAT(1X,"TNMF")
      DO 116 IR=1,NS
  116 WRITE(2,114)(TNMF(IR,IC),IC=1,NS)
      WRITE(2,117)
  117 FORMAT(1X,"PH")
      DO 118 IR=1,NS
  118 WRITE(2,114)(PH(IR,IC),IC=1,NS)
  150 CONTINUE
      * APPROXIMATE PHI L SUB OPS
      IF(KSUB(3).EQ.1) GO TO 160
```

```
610 * LOS STM TRANSFORMED FROM INERTIAL STM
620 * BY ROTATION MATRICES AT T=N AND N+1
630 DO 101 IR=1,NS
640 DO 101 IC=1,NS
650 S=0.
660 DO 103 IRC1=1,NS
670 DO 103 IRC2=1,NS
680 103 S=S+TNMF(IR,IRC1)*PH(IRC1,IRC2)*TMF(IC,IRC2)
690 101 PHI(IR,IC)=S
700 GO TO 500
710 * SEE SUBROUTINE SUBOP FOR SUB-OPTIMIZATIONS
720 160 IF(KSUB(4).EQ.1) CALL SUBOP(4)
730 IF(KSUB(3).EQ.1) CALL SUBOP(3)
740 GO TO 500
750 * INERTIAL STM
760 300 IF(T.GT.0.) GO TO 500
770 DO 301 IR=1,NS
780 DO 301 IC=1,NS
790 301 PHI(IR,IC)=PH(IR,IC)
800 500 IF(KT.NE.2) RETURN
810 WRITE(KT,501)KFORM
820 501 FORMAT(1X,"STM, FORM = ",I2)
830 DO 502 IR=1,NS
840 502 WRITE(KT,503)(PHI(IR,IC),IC=1,NS)
850 503 FORMAT(1X,6(1PE11.3))
860 WRITE(KT,505)
870 505 FORMAT(1X,"TMF")
880 DO 504 IR=1,NS
890 504 WRITE(KT,503)(TMF(IR,IC),IC=1,NS)
900 RETURN
910 END
```

```
      * R. DEMOYER  1978
      * PROPAGATION OF VARIANCE
      SUBROUTINE TPROP(KFORM)
      COMMON/TIME/T,DT,TMX,NT,TF
      COMMON/COV/PTI(6,6),PTL(6,6)
      COMMON/STM/PHI(6,6)
      COMMON/QNOISE/Q(6,6)
      COMMON/NPAR/NS,NM,ND
      COMMON/TEST/KT
      COMMON/SUB/KSUB(20),KSO,KTRANS
      DIMENSION T1(6,6),T2(6,6)
      DOUBLE PRECISION S
      * T1 = TEMPORARY ARRAY
      DO 1 IR=1,NS
      DO 1 IC=1,NS
      IF(KFORM.LT.3) T1(IR,IC)=PTL(IR,IC)
    1 IF(KFORM.GE.3) T1(IR,IC)=PTI(IR,IC)
      * (PHI)*(P)*(PHI)T
      DO 10 IR=1,NS
      DO 10 IC=IR,NS
      S=0.
      DO 11 IRC1=1,NS
      DO 11 IRC2=1,NS
      IF(PHI(IR,IRC1).EQ.0.) GO TO 11
      IF(T1(IRC1,IRC2).EQ.0.) GO TO 11
      IF(PHI(IC,IRC2).EQ.0.) GO TO 11
      S=S+PHI(IR,IRC1)*T1(IRC1,IRC2)*PHI(IC,IRC2)
   11 CONTINUE
      T2(IC,IR)=S
   10 T2(IR,IC)=S
      CALL TTARG
      * STATE NOISE ADDED
      DO 20 IR=1,NS
      DO 20 IC=1,NS
      IF(KFORM.LT.3) PTL(IR,IC)=T2(IR,IC)+Q(IR,IC)
   20 IF(KFORM.GE.3) PTI(IR,IC)=T2(IR,IC)+Q(IR,IC)
      * SUB-OPTIMAL OPTIONS
      IF(KSUB(5).EQ.1) CALL SUBOP(5)
      IF(KSUB(6).EQ.1) CALL SUBOP(6)
      * COVARIANCE TRANSFORMATION
      IF(KFORM.LT.3) CALL TPTRAN(2)
      IF(KFORM.GE.3) CALL TPTRAN(1)
      IF(KT.NE.2) RETURN
      * DIAGNOSTIC PRINTS
      WRITE(KT,100)KFORM,DT
  100 FORMAT(1X,"TPROP,  ,FORM=",I3," DT=",F8.4)
      WRITE(KT,101)
  101 FORMAT(1X,"T1",
      DO 102 IR=1,NS
  102 WRITE(KT,10 ),(T1(IR,IC),IC=1,NS)
  103 FORMAT(1X,  (1PE11.3))
```

```
610 WRITE(KT,104)
620 104 FORMAT(1X,"T2")
630 DO 105 IR=1,NS
640 105 WRITE(KT,103)(T2(IR,IC),IC=1,NS)
650 WRITE(KT,106)
660 106 FORMAT(1X,"PTL")
670 DO 107 IR=1,NS
680 107 WRITE(KT,103)(PTL(IR,IC),IC=1,NS)
690 WRITE(KT,108)
700 108 FORMAT(1X,"PTI")
710 DO 109 IR=1,NS
720 109 WRITE(KT,103)(PTI(IR,IC),IC=1,NS)
730 RETURN
740 END
```

```
100 * R. DEMOYER  1978
110 * COMPUTATION OF MEASUREMENT VARIANCE TERMS
120 SUBROUTINE TRMAT(KFORM)
130 COMMON/TST/XTI(6),XTL(6)
140 COMMON/NPAR/NS,NM,ND
150 COMMON/TRANS/A,AD,TM(2,2),TMF(6,6)
160 COMMON/RPAR/SIGR,SIGAZ,SIGANG,R(2,2)
170 COMMON/TEST/KT
180 COMMON/SUB/KSUB(20),KSO,KTRANS
190 DATA R/4*0./
200 DS=XTL(1)
210 DL=XTL(2)
220 * RANGE
230 R11=SIGR**2
240 * CROSS RANGE
250 R22=(SIGR*DL/DS)**2+(SIGAZ*DS)**2
260 IF(KFORM.GE.2) R22=R22+(SIGANG*DS)**2
270 R(1,1)=R11
280 R(2,2)=R22
290 IF(KFORM.LT.3) GO TO 100
300 * TRANSFORMATION FROM LOS TO I
310 CA=COS(A)
320 SA=SIN(A)
330 R(1,1)=R11*CA**2+R22*SA**2
340 R(2,2)=R22*CA**2+R11*SA**2
350 R(1,2)=R(2,1)=CA*SA*(R11-R22)
360 IF(KSUB(6).EQ.1) R(1,2)=R(2,1)=0.
370 * DIAGNOSTIC PRINTS
380 100 IF(KT.NE.3) RETURN
390 WRITE(KT,101)KFORM
400 101 FORMAT(1X,"TRMAT,  KFORM=",I3)
410 WRITE(KT,102)
420 102 FORMAT(1X,"R11,R22")
430 WRITE(KT,103)R11,R22
440 103 FORMAT(1X,2(1PE11.3))
450 WRITE(KT,104)
460 104 FORMAT(1X,"R")
470 DO 105 IR=1,NM
480 105 WRITE(KT,103)(R(IR,IC),IC=1,NM)
490 RETURN
500 END
```

```
      * R. DEMOYER  1978
      * SUB-OPTIMAL KALMAN GAIN COMPUTATION
      SUBROUTINE SKGAIN(KFORM)
      COMMON/TRANS/A,AD,TM(2,2),TMF(6,6)
      COMMON/NPAR/NS,NM,ND
      COMMON/COV/PTI(6,6),PTL(6,6)
      COMMON/RPAR/SIGR,SIGAZ,SIGANG,R(2,2)
      COMMON/GAIN/KG(6,2)
      COMMON/TEST/KT
      COMMON/SUB/KSUB(20),KSO,KTRANS
      DIMENSION PP(6,6),RM(2,2),RMI(2,2),CG(6,2)
      REAL KG
      DOUBLE PRECISION S
      * PP = TIMPORARY COVARIANCE ARRAY
      DO 1 IR=1,NS
      DO 1 IC=1,NS
      IF(KFORM.LT.3) PP(IR,IC)=PTL(IR,IC)
    1 IF(KFORM.GE.3) PP(IR,IC)=PTI(IR,IC)
      * MEASUREMENT COVARIANCE
      DO 2 IR=1,NM
      DO 2 IC=1,NM
    2 RM(IR,IC)=PP(IR,IC)+R(IR,IC)
      * INVERSE
      DET=RM(1,1)*RM(2,2)-RM(1,2)*RM(2,1)
      RMI(1,1)=RM(2,2)/DET
      RMI(1,2)=-RM(1,2)/DET
      RMI(2,1)=-RM(2,1)/DET
      RMI(2,2)=RM(1,1)/DET
      * KALMAN GAIN IN APPROPRIATE FRAME
      DO 3 IR=1,NS
      DO 3 IC=1,NM
      S=0.
      DO 4 IRC=1,NM
    4 S=S+PP(IR,IRC)*RMI(IRC,IC)
    3 KG(IR,IC)=S
      IF(KFORM.LT.3) GO TO 200
      * KL=(TMF)*(KT)*(TM)T
      DO 110 IR=1,NS
      DO 110 IC=1,NM
      S=0.
      DO 111 IRC1=1,NS
      DO 111 IRC2=1,NM
  111 S=S+TMF(IR,IRC1)*KG(IRC1,IRC2)*TM(IC,IRC2)
  110 CG(IR,IC)=S
      * INERTIAL GAIN WRITTEN TO FILE BTM DIRECTLY FOR KFORM=3
      WRITE(4)KG
      GO TO 300
  200 CONTINUE
      * KI=(TMF)T*(KL)*(TM)
      * GAIN TRANSFORMED FROM LOS TO INERTIAL BEFORE WRITING
      * TO FILE FOR KFORM =1 OR 2.
```

```
      DO 210 IR=1,NS
      DO 210 IC=1,NM
      S=0.
      DO 211 IRC1=1,NS
      DO 211 IRC2=1,NM
  211 S=S+TMF(IRC1,IR)*KG(IRC1,IRC2)*TM(IRC2,IC)
  210 CG(IR,IC)=S
      WRITE(4)CG
  300 CONTINUE
      IF(KT.NE.3)RETURN
      WRITE(KT,100)
  100 FORMAT(1X,"COMPUTED GAIN")
      DO 101 IR=1,NS
  101 WRITE(KT,102)(KG(IR,IC),IC=1,NM)
  102 FORMAT(1X,6(1PE11.3))
      WRITE(KT,301)
  301 FORMAT(1X,"TRANSFORMED GAIN")
      DO 302 IR=1,NS
  302 WRITE(KT,102)(CG(IR,IC),IC=1,NM)
      RETURN
      END
```

```
100 * R. DEMOYER  1978
110 * KALMAN GAIN READ FROM FILE BTM FOR TRUTH MODEL
120 SUBROUTINE TKGAIN(KFORM)
130 COMMON/TRANS/A,AD,TM(2,2),TMF(6,6)
140 COMMON/NPAR/NS,NM,ND
150 COMMON/COV/PTI(6,6),PTL(6,6)
160 COMMON/RPAR/SIGR,SIGAZ,SIGANG,R(2,2)
170 COMMON/GAIN/KG(6,2)
180 COMMON/TEST/KT
190 COMMON/SUB/KSUB(20),KSO,KTRANS
200 REAL KG
210 * GAIN READ IN INERTIAL FRAME
220 READ(4)KG
230 RETURN
240 END
```

```
100 * R. DEMOYER  1978
110 * A POSTERIORI COVARIANCE
120 SUBROUTINE TPOST(KFORM)
130 COMMON/COV/PTI(6,6),PTL(6,6)
140 COMMON/NPAR/NS,NM,ND
150 COMMON/RPAR/SIGR,SIGAZ,SIGANG,R(2,2)
160 COMMON/GAIN/KG(6,2)
170 COMMON/TEST/KT
180 COMMON/SUB/KSUB(20),KSO,KTRANS
190 DIMENSION P(6,6),IKH(6,6),PJ(6,6)
200 DOUBLE PRECISION S
210 REAL KG,IKH
220 * P = TIMPORARY COVARIANCE ARRAY
230 DO 1 IR=1,NS
240 DO 1 IC=1,NS
250 IF(KFORM.LT.3) P(IR,IC)=PTL(IR,IC)
260 1 IF(KFORM.GE.3) P(IR,IC)=PTI(IR,IC)
270 * (I-KG*H)
280 DO 2 IR=1,NS
290 DO 2 IC=1,NS
300 IKH(IR,IC)=0.
310 IF(IR.EQ.IC) IKH(IR,IC)=1.
320 2 IF(IC.LE.NM) IKH(IR,IC)=IKH(IR,IC)-KG(IR,IC)
330 IF(KSO.EQ.1) GO TO 400
340 * SHORT FORM A POSTERIORI
350 * SUB-OPTIMAL FORM
360 * P=(I-KG*H)*P
370 DO 10 IR=1,NS
380 DO 10 IC=IR,NS
390 S=0.
400 DO 11 IRC=1,NS
410 11 S=S+IKH(IR,IRC)*P(IRC,IC)
420 IF(KFORM.NE.3) PTL(IC,IR)=S
430 IF(KFORM.NE.3) PTL(IR,IC)=S
440 IF(KFORM.EQ.3) PTI(IC,IR)=S
450 10 IF(KFORM.EQ.3) PTI(IR,IC)=S
460 GO TO 200
470 * TRUTH MODEL JOSEPH FORM
480 400 CONTINUE
490 DO 20 IR=1,NS
500 DO 20 IC=IR,NS
510 S=0.
520 DO 21 IRC1=1,NS
530 DO 21 IRC2=1,NS
540 21 S=S+IKH(IR,IRC1)*P(IRC1,IRC2)*IKH(IC,IRC2)
550 DO 22 IRC1=1,NM
560 DO 22 IRC2=1,NM
570 22 S=S+KG(IR,IRC1)*R(IRC1,IRC2)*KG(IC,IRC2)
580 PJ(IR,IC)=S
590 IF(KFORM.NE.3) PTL(IC,IR)=S
600 IF(KFORM.NE.3) PTL(IR,IC)=S
```

```
610 IF(KFORM.EQ.3) PTI(IC,IR)=S
620 IF(KFORM.EQ.3) PTI(IR,IC)=S
630 20 PJ(IC,IR)=S
640 200 CONTINUE
650 * SEE SUBROUTINE SUBOP FOR SUV-OPTIMAL CODES
660 IF(KSUB(5).EQ.1) CALL SUBOP(5)
670 IF(KSUB(6).EQ.1) CALL SUBOP(6)
680 IF(KFORM.LT.3) CALL TPTRAN(2)
690 IF(KFORM.GE.3) CALL TPTRAN(1)
700 IF(KT.NE.3) RETURN
710 * DIAGNOSTIC PRINTS
720 WRITE(KT,100)
730 100 FORMAT(1X,"A PRIORI COVARIANCE")
740 DO 101 IR=1,NS
750 101 WRITE(KT,102)(P(IR,IC),IC=1,NS)
760 102 FORMAT(1X,6(1PE11.3))
770 WRITE(KT,103)
780 103 FORMAT(1X,"A POSTERIORI COVARIANCE")
790 DO 104 IR=1,NS
800 IF(KFORM.LT.3) WRITE(KT,102)(PTL(IR,IC),IC=1,NS)
810 104 IF(KFORM.GE.3) WRITE(KT,102)(PTI(IR,IC),IC=1,NS)
820 WRITE(KT,110)
830 110 FORMAT(1X,"TRANSFORM CHECK")
840 DO 111 IR=1,NS
850 IF(KFORM.LT.3) WRITE(KT,102)(PTI(IR,IC),IC=1,NS)
860 111 IF(KFORM.GE.3) WRITE(KT,102)(PTL(IR,IC),IC=1,NS)
870 WRITE(KT,105)
880 105 FORMAT(1X,"JOSEPH FORM")
890 DO 106 IR=1,NS
900 106 WRITE(KT,102)(PJ(IR,IC),IC=1,NS)
910 RETURN
920 END
```

```
100 * R. DEMOYER  1978
110 * PROPAGATION OF VARIANCE TO TIME IF IMPACT
120 SUBROUTINE SPROJ
130 COMMON/NPAR/NS,NM,ND
140 COMMON/TST/XTI(6),XTL(6)
150 COMMON/COV/PTI(6,6),PTL(6,6)
160 COMMON/QPAR/SIGAC,TCAC,QBET(2)
170 COMMON/PCV/PSP(2,2),PTP(2,2)
180 COMMON/TEST/KT
190 COMMON/SUB/KSUB(20),KSO,KTRANS
200 COMMON/TIME/T,DT,TMX,NT,TF
210 DIMENSION PH(6,6),P(6,6)
220 DOUBLE PRECISION S
230 DATA BV,CP/1200.,.007/
240 B=1./TCAC
250 TF=.01
260 CBV=.5*CP*SQRT(BV)
270 * TIME OF FLIGHT ITERATION
280 1 BT=B*TF
290 EBT=EXP(-BT)
300 TFP=TF
310 XP=XTI(1)+XTI(3)*TF+XTI(5)*(EBT+BT-1.)/B**2
320 YP=XTI(2)+XTI(4)*TF+XTI(6)*(EBT+BT-1.)/B**2
330 RP=SQRT(XP**2+YP**2)
340 TF=RP/(BV-RP*CBV)
350 IF(ABS(TF-TFP).GT..01) GO TO 1
360 * SPECTRAL TERMS
370 QU=2.*SIGAC**2/TCAC
380 QV=4.*QU
390 VX=XTI(3)
400 VY=XTI(4)
410 VSQ=VX**2+VY**2
420 Q55=(VX**2*QU+VY**2*QV)/VSQ
430 Q66=(VY**2*QU+VX**2*QV)/VSQ
440 Q56=(VX*VY*QU-VX*VY*QV)/VSQ
450 NI=1+2*TF
460 DTF=TF/NI
470 BT=B*DTF
480 EBT=EXP(-BT)
490 * PROPAGATION OF COVARIANCE IN INERTIAL CLOSED FORM
500 DO 21 IR=1,NS
510 DO 21 IC=1,NS
520 P(IR,IC)=PTI(IR,IC)
530 21 PH(IR,IC)=0.
540 PH(1,1)=PH(2,2)=PH(3,3)=PH(4,4)=1.
550 PH(1,3)=PH(2,4)=DTF
560 PH(1,5)=PH(2,6)=(EBT+BT-1.)/B**2
570 PH(3,5)=PH(4,6)=(1.-EBT)/B
580 PH(5,5)=PH(6,6)=EBT
590 DO 40 I=1,NI
600 DO 10 IR=1,NS
```

```
      DO 10 IC=IR,NS
      S=0.
      DO 11 IRC1=1,NS
      DO 11 IRC2=1,NS
   11 S=S+PH(IR,IRC1)*P(IRC1,IRC2)*PH(IC,IRC2)
      IF(IR.EQ.5.AND.IC.EQ.5) S=S+Q55*DTF
      IF(IR.EQ.5.AND.IC.EQ.6) S=S+Q56*DTF
      IF(IR.EQ.6.AND.IC.EQ.6) S=S+Q66*DTF
      P(IR,IC)=S
   10 P(IC,IR)=S
   40 CONTINUE
      * PROJECTED POSITION COVARIANCE OF OPTMAL FILTER
      * WRITTEN TO FILE REFF
      DO 41 IR=1,2
      DO 41 IC=IR,2
   41 PSP(IR,IC)=P(IR,IC)
      IF(KSUB(1).EQ.1) WRITE(6)PSP
      IF(KT.NE.2) RETURN
      WRITE(2,100)
  100 FORMAT(1X,"SPROJ")
      WRITE(2,101)TF
  101 FORMAT(1X,"TF=",1PE11.3)
      WRITE(2,102)
  102 FORMAT(1X,"PSP")
      DO 103 IR=1,ND
  103 WRITE(2,104)(PSP(IR,IC),IC=1,ND)
  104 FORMAT(1X,6(1PE11.3))
      RETURN
      END
```

```
100 * R. DEMOYER  1978
110 * PROPAGATION OF COVARIANCT TO TIME OF IMPACT
120 SUBROUTINE TPROJ
130 COMMON/NPAR/NS,NM,ND
140 COMMON/TST/XTI(6),XTL(6)
150 COMMON/COV/PTI(6,6),PTL(6,6)
160 COMMON/QPAR/SIGAC,TCAC,QBET(2)
170 COMMON/PCV/PSP(2,2),PTP(2,2)
180 COMMON/TEST/KT
190 COMMON/TIME/T,DT,TMX,NT,TF
200 DIMENSION PH(6,6),P(6,6)
210 DOUBLE PRECISION S
220 DATA BV,CP/1200.,.007/
230 B=1./TCAC
240 TF=.01
250 CBV=.5*CP*SQRT(BV)
260 * TIME OF FLIGHT ITERATION
270 1 BT=B*TF
280 EBT=EXP(-BT)
290 TFP=TF
300 XP=XTI(1)+XTI(3)*TF+XTI(5)*(EBT+BT-1.)/B**2
310 YP=XTI(2)+XTI(4)*TF+XTI(6)*(EBT+BT-1.)/B**2
320 RP=SQRT(XP**2+YP**2)
330 TF=RP/(BV-RP*CBV)
340 IF(ABS(TF-TFP).GT..01) GO TO 1
350 * SPECTRAL TERMS
360 QU=2.*SIGAC**2/TCAC
370 QV=4.*QU
380 VX=XTI(3)
390 VY=XTI(4)
400 VSQ=VX**2+VY**2
410 Q55=(VX**2*QU+VY**2*QV)/VSQ
420 Q66=(VY**2*QU+VX**2*QV)/VSQ
430 Q56=(VX*VY*QU-VX*VY*QV)/VSQ
440 NI=1+2*TF
450 DTF=TF/NI
460 BT=B*DTF
470 EBT=EXP(-BT)
480 * PROPAGATION OF COVARIANCE IN INERTIAL CLOSED FORM
490 DO 21 IR=1,NS
500 DO 21 IC=1,NS
510 P(IR,IC)=PTI(IR,IC)
520 21 PH(IR,IC)=0.
530 PH(1,1)=PH(2,2)=PH(3,3)=PH(4,4)=1.
540 PH(1,3)=PH(2,4)=DTF
550 PH(1,5)=PH(2,6)=(EBT+BT-1.)/B**2
560 PH(3,5)=PH(4,6)=(1.-EBT)/B
570 PH(5,5)=PH(6,6)=EBT
580 DO 40 I=1,NI
590 DO 10 IR=1,NS
600 DO 10 IC=IR,NS
```

```
      S=0.
      DO 11 IRC1=1,NS
      DO 11 IRC2=1,NS
   11 S=S+PH(IR,IRC1)*P(IRC1,IRC2)*PH(IC,IRC2)
      IF(IR.EQ.5.AND.IC.EQ.5) S=S+Q55*DTF
      IF(IR.EQ.5.AND.IC.EQ.6) S=S+Q56*DTF
      IF(IR.EQ.6.AND.IC.EQ.6) S=S+Q66*DTF
      P(IR,IC)=S
   10 P(IC,IR)=S
   40 CONTINUE
      DO 41 IR=1,2
      DO 41 IC=IR,2
   41 PTP(IR,IC)=P(IR,IC)
      * PROJECTED OPTIMAL POSITION COVARIANCE READ FROM FILE REF
      READ(6)PSP
      IF(KT.NE.2) RETURN
      WRITE(2,100)
  100 FORMAT(1X,"TPROJ")
      WRITE(2,101)TF
  101 FORMAT(1X,"TF=",1PE11.3)
      WRITE(2,102)
  102 FORMAT(1X,"PTP")
      DO 103 IR=1,ND
  103 WRITE(2,104)(PTP(IR,IC),IC=1,ND)
  104 FORMAT(1X,6(1PE11.3))
      RETURN
      END
      * EVALUATION SUBROUTINE
      SUBROUTINE TEVAL(KF)
      COMMON/PCV/PSP(2,2),PTP(2,2)
      COMMON/TIME/T,DT,TMX,NT,TF
      SAVE
      IF(T.GE.2.) GO TO 50
      SSS=SST=TN=0.
      N=0
      IF(T.LT.2.) RETURN
   50 GO TO (100,200),KF
  100 RSPS=SQRT(PSP(1,1)+PSP(2,2))
      RSPT=SQRT(PTP(1,1)+PTP(2,2))
      * SSS = OPTIMAL SUM SQUARE POSITION ERROR
      SSS=SSS+PSP(1,1)+PSP(2,2)
      * SST = TRUTH MODEL SUM SQUARE POSITION ERROR
      SST=SST+PTP(1,1)+PTP(2,2)
      N=N+1
      TH=TH+RSPS/RSPT
      RETURN
  200 TH=TH/N
      RMSS=SQRT(SSS/N)
      RMST=SQRT(SST/N)
      PRINT 201,TH
  201 FORMAT(1X,"PC = ",F10.6)
```

```
1120 PRINT 202, SSS, SST
1130 202 FORMAT(1X, "SSS=", 1PE12.4, " SST=", 1PE12.4)
1140 PRINT 203, RMSS, RMST
1150 203 FORMAT(1X, "RMSS=", 1PE12.4, " RMST=", 1PE12.4)
1160 RETURN
1170 END
```

```
100 * R. DEMOYER  1978
110 * PLOT SUBROUTINE -- DATA WRITTEN TO FILE BPLT
120 * FOR SUBSEQUENT CRT PLOTTING
130 SUBROUTINE TPLOT
140 COMMON/TIME/T,DT,TMX,NT,TF
150 COMMON/TST/XTI(6),XTL(6)
160 COMMON/TRANS/A,AD,TM(2,2),TMF(6,6)
170 COMMON/RPAR/SIGR,SIGAZ,SIGANG,R(2,2)
180 COMMON/QNOISE/Q(6,6)
190 COMMON/GAIN/KG(6,2)
200 COMMON/COV/PTI(6,6),PTL(6,6)
210 COMMON/PCV/PSP(2,2),PTP(2,2)
220 REAL KG
230 DIMENSION V(105)
240 N=0
250 DO 1 I=1,6
260 N=N+1
270 1 V(N)=XTL(I)
280 DO 2 I=1,6
290 N=N+1
300 2 V(N)=XTI(I)
310 V(13)=A
320 V(14)=AD
330 V(15)=R(1,1)
340 V(16)=R(1,2)
350 V(17)=R(2,2)
360 N=17
370 DO 3 IR=1,6
380 DO 3 IC=IR,6
390 N=N+1
400 3 V(N)=Q(IR,IC)
410 DO 4 IR=1,6
420 DO 4 IC=1,2
430 N=N+1
440 4 V(N)=KG(IR,IC)
450 DO 5 IR=1,6
460 DO 5 IC=IR,6
470 N=N+1
480 5 V(N)=PTL(IR,IC)
490 DO 6 IR=1,6
500 DO 6 IC=IR,6
510 N=N+1
520 6 V(N)=PTI(IR,IC)
530 V(93)=PSP(1,1)
540 V(94)=PSP(1,2)
550 V(95)=PSP(2,2)
560 V(96)=PTP(1,1)
570 V(97)=PTP(1,2)
580 V(98)=PTP(2,2)
590 V(99)=TF
600 V(105)=T
```

```
610 WRITE(*,*)
620 * VAR = VARIABLE NUMBER KEY
630 * XTL = LOS STATE VECTOR
640 * V(1)-V(6)
650 * XTI = INERTIAL STATE VECTOR
660 * V(7)-V(12)
670 * A = AZIMUTH   AD = AZIMUTH RATE
680 * V(13),V(14)
690 * R = MEASUREMENT COVARINACE TERMS
700 * 14 16
710 *    17
720 * Q = STATE NOISE TERMS
730 * 18 19 20 21 22 23
740 *    24 25 26 27 28
750 *       29 30 31 32
760 *          33 34 35
770 *             36 37
780 *                38
790 * KT = KALMAN GAIN TERMS
800 * 39 40
810 * 41 42
820 * 43 44
830 * 45 46
840 * 47 48
850 * 49 50
860 * PTL = LOS COVARIANCE
870 * 51 52 53 54 55 56
880 *    57 58 59 60 61
890 *       62 63 64 65
900 *          66 67 68
910 *             69 70
920 *                71
930 * PTI = INERTIAL COVARIANCE
940 * 72 73 74 75 76 77
950 *    78 79 80 81 82
960 *       83 84 85 86
970 *          87 88 89
980 *             90 91
990 *                92
1000 * OPTIMAL PROJECTED POSITION TERMS
1010 * PSP=V(93,94,95)
1020 * TRUTH MODEL PROJECTED POSTIION TERMS
1030 * PTP=V(96,97,98)
1040 * TF = V(99),TIME OF FLIGHT
1050 * TIME = V(105)
1060 RETURN
1070 END
```

```
SUBOP                09/27/78            15:10:32            PAGE    1


100 * R. DEMOYER  1978
110 * SUBOPTIMIAZTION OPTIONS
120 SUBROUTINE SUBOP(KS)
130 * KS=1  REFERENCE FILE WRITTEN
140 * KS=2  QBET(1) ADDED
150 * KS=3  PHI L = I + FL*DT
160 * KS=4  AD COMPUTED BY NUMERICAL DIFFERENCE
170 * KS=5  DECOUPLING IN LOS
180 * KS=6  DECOUPLING IN INERTIAL
190 * KS=7  EQUAL SPECTRAL TERMS
200 * KS=10  USED AS FLAG TO READ ERROR PARAMETERS IN SICS
210 COMMON/TIME/T,DT,TMX,NT,TF
220 COMMON/STM/PHI(6,6)
230 COMMON/TRANS/A,AD,TM(2,2),TMF(6,6)
240 COMMON/NPAR/NS,NM,ND
250 COMMON/QPAR/SIGAC,TCAC,QBET(2)
260 COMMON/RPAR/SIGR,SIGAZ,SIGANG,R(2,2)
270 COMMON/COV/PTI(6,6),PTL(6,6)
280 COMMON/SUB/KSUB(20),KSO,KTRANS
290 SAVE AP
300 GO TO (50,100,150,200,250,250,300),KS
310 * KS = 1    REFERENCE FILE WRITTEN ELSESHERE
320 50 RETURN
330 * KS = 2    QBET(1) ADDED IN TQ
340 100 RETURN
350 * PHI L = I + FL*DT
360 150 B=1./TCAC
370 DO 101 IR=1,NS
380 DO 101 IC=1,NS
390 PHI(IR,IC)=0.
400 101 IF(IR.EQ.IC) PHI(IR,IC)=1.
410 PHI(1,3)=PHI(2,4)=PHI(3,5)=PHI(4,6)=DT
420 PHI(1,2)=PHI(3,4)=PHI(5,6)=AD*DT
430 PHI(2,1)=PHI(4,3)=PHI(6,5)=-AD*DT
440 PHI(5,5)=PHI(6,6)=1.-B*DT
450 RETURN
460 * AD COMPUTED BY NUMERICAL DIFFERENCE
470 200 IF(T.GT.0.) GO TO 201
480 AP=A
490 RETURN
500 * GAUSSIAN RANDOM NUMBER
510 201 S=0
520 DO 202 I=1,12
530 202 S=S+(RRAND(1.)-.5)
540 S=S/12.
550 AE=A+SIGANG*S
560 AD=(AE-AP)/DT
570 AP=AE
580 RETURN
590 * DECOUPLING OF COVARIANCE
600 250 DO 251 IR=1,NS
```

```
      DO 251 IC=IR,NS
      DO 252 I=1,5,2
      IRP=IR+I
      IF(IR.EQ.1.AND.IC.EQ.2.AND.KSUB(9).EQ.1) GO TO 252
      IF(IC.EQ.IRP.AND.KS.EQ.5) PTL(IR,IC)=0.
      IF(KSUB(8).EQ.1) PTL(1,2)=.5
      IF(IC.EQ.IRP.AND.KS.EQ.6) PTI(IR,IC)=0.
  252 CONTINUE
      PTL(IC,IR)=PTL(IR,IC)
  251 PTI(IC,IR)=PTI(IR,IC)
C     FOR KS=6, R(1,2)=R(2,1)=0.  IN TRMAT
      RETURN
C     EQUAL SPECTRAL TERMS IN TQ
  300 RETURN
      END
```

```
100 * R. DEMOYER  1978
110 * CONSTRUCTION OF ERROR ELLIPSES FROM COVARIANCE MATRICES
120 DIMENSION XE(82),YE(82),V(105)
130 OPENFILE 6,"PF"
140 REWIND 6
150 ENDFILE 6
160 OPENFILE 5,"BPLT","NUMERIC"
170 2 REWIND 5
180 PRINT,"TIME, FUNCTION"
190 READ,T,KF
200 1 READ(5,END=2)V
210 IF(T.NE.V(105)) GO TO 1
220 * A PRIORI POS, VEL, ACC ELLIPSES FOR KF=1,2,3
230 * IMPACT ELLIPSE FOR KF=4
240 IF(KF.EQ.4) READ(5)
250 C=1.180
260 XT=V(7)
270 IF(XT.EQ.0.) XT=.00001
280 YT=V(8)
290 SL=YT/XT
300 GO TO (50,60,70,75,80),KF
310 50 P11=V(72)
320 P12=V(73)
330 P22=V(78)
340 PRINT,"A PRIORI POSITION ELLIPSE"
350 GO TO 85
360 60 P11=V(83)
370 P12=V(84)
380 P22=V(87)
390 PRINT,"A PRIORI VELOCITY ELLIPSE"
400 GO TO 85
410 70 P11=V(90)
420 P12=V(91)
430 P22=V(92)
440 PRINT,"A PRIORI ACCELERATION ELLIPSE"
450 GO TO 85
460 75 P11=V(96)
470 P12=V(97)
480 P22=V(98)
490 PRINT,"PROJECTED TRUTH POSITION ELLIPSE"
500 GO TO 85
510 80 P11=V(93)
520 P12=V(94)
530 P22=V(95)
540 PRINT,"PROJECTED SUBOPTIMAL POSITION ELLIPSE"
550 85 CONTINUE
560 * COVARIANCE INVERSE
570 DET=P11*P22-P12**2
580 C11=P22/DET
590 C12=C21=-P12/DET
600 C22=P11/DET
```

```
      XLM=SQRT(C22*C**2/(C11*C22-C12**2))
      DX=XLM/40.
      N=0
      DO 20 K=1,2
      DO 20 J=1,41
      IF(K.EQ.1) X=-XLM+(J-1)*DX*2
      IF(K.EQ.2) X=XLM-(J-1)*DX*2
      N=N+1
      XE(N)=X
      DIS=ABS(X**2*(C12**2-C11*C22)+C22*C**2)
      IF(K.EQ.1) YE(N)=(-X*C12-SQRT(DIS))/C22
   20 IF(K.EQ.2) YE(N)=(-X*C12+SQRT(DIS))/C22
      TERM=1.E37
      DO 30 J=1,82
   30 WRITE(6,33)XE(J),YE(J)
   33 FORMAT(1X,2(1PE11.3))
      WRITE(6,33)TERM,TERM
      DO 40 K=1,2
      DO 41 J=1,41
      X=-XLM+(J-1)*DX*2
      XL=1.2*X
      IF(K.EQ.1) YL=XL*SL
      IF(K.EQ.2) YL=-XL/SL
   41 WRITE(6,33)XL,YL
   40 WRITE(6,33)TERM,TERM
      END
```

```
100 * R  DEMOYER  1978
110 * GENERATION OF STANDARD PLOTTING FORMAT FILE FOR L. IG***: TEKGRAF
120 DIMENSION A(10,200),V(105),NVN(10),T(200)
130 OPENFILE 5,"BPLT","NUMERIC"
140 REWIND 5
150 OPENFILE 6,"PF"
160 REWIND 6
170 ENDFILE 6
180 PRINT,"# AND VARIABLES"
190 READ,NV,(NVN(I),I=1,NV)
200 TERM=1.E37
210 NT=0
220 1 READ(5,END=100)V
230 NT=NT+1
240 DO 2 I=1,NV
250 NN=NVN(I)
260 2 A(I,NT)=V(NN)
270 T(NT)=V(105)
280 GO TO 1
290 100 DO 101 I=1,NV
300 DO 102 N=1,NT
310 102 WRITE(6,103)T(N),A(I,N)
320 101 WRITE(6,103)TERM,TERM
330 103 FORMAT(1X,2(1PE11.3))
340 ENDFILE 6
350 END
```

SECURITY CLASSIFICATION OF THIS PAGE (When Data Entered)

REPORT DOCUMENTATION PAGE

READ INSTRUCTIONS BEFORE COMPLETING FORM

1. REPORT NUMBER: EW-18-78	2. GOVT ACCESSION NO.
3. RECIPIENT'S CATALOG NUMBER	
4. TITLE (and Subtitle): A Comparative Study of Fire Control Target State Estimators	5. TYPE OF REPORT & PERIOD COVERED: Final Report 7/78 - 8/78
	6. PERFORMING ORG. REPORT NUMBER
7. AUTHOR(s): Robert DeMoyer, Jr.	8. CONTRACT OR GRANT NUMBER(s)
9. PERFORMING ORGANIZATION NAME AND ADDRESS: U. S. Naval Academy Annapolis, MD 21402	10. PROGRAM ELEMENT, PROJECT, TASK AREA & WORK UNIT NUMBERS
11. CONTROLLING OFFICE NAME AND ADDRESS	12. REPORT DATE: November 1978
	13. NUMBER OF PAGES: 125
14. MONITORING AGENCY NAME & ADDRESS (if different from Controlling Office): Naval Surface Weapons Center Dahlgren, VA	15. SECURITY CLASS. (of this report): Unclassified
	15a. DECLASSIFICATION DOWNGRADING SCHEDULE

16. DISTRIBUTION STATEMENT (of this Report)

Approved for public release; distribution unlimited

17. DISTRIBUTION STATEMENT (of the abstract entered in Block 20, if different from Report)

Approved for public release; distribution unlimited

18. SUPPLEMENTARY NOTES

19. KEY WORDS (Continue on reverse side if necessary and identify by block number)

Target State Extimation
Kalman Filtering
Sub-Optimization
Rotating Coordinate Frame

20. ABSTRACT (Continue on reverse side if necessary and identify by block number)

Application of the Kalman Filter to the fire control problem is considered. While the theory and practice in this field are well developed, conflicting claims have been made regarding the relative advantages of statistical decoupling in fixed inertial coordinates as compared to rotating non-inertial coordinates. An error analysis model, consisting of a sub-optimal filter and truth model, shows the error added, in each of three formulations, due to several sub-optimal approximations. Plots, including error ellipses, help to provide an intuitive feel for the results of decoupling.

DD FORM 1 JAN 73 1473 EDITION OF 1 NOV 65 IS OBSOLETE
S/N 0102-014-6601

SECURITY CLASSIFICATION OF THIS PAGE (When Data Entered)

INITIAL DISTRIBUTION LIST

		NO. OF COPIES
1.	Defense Documentation Center Cameron Station Alexandria, VA 22314	5
2.	Library U. S. Naval Academy Annapolis, MD 21402	4
3.	Director of Research U.S. Naval Academy Annapolis, MD 21402	1
4.	Commander Naval Surface Weapons Center Dahlgren, VA 22498 ATTN: Mr. E. Price (Code N55)	10
5.	Captain J. R. Eshman, USN Director, Division of Engineering & Weapons U. S. Naval Academy Annapolis, MD 21402	1
6.	Professor C. F. Olsen Chairman, Weapons & Systems Engineering Department U. S. Naval Academy Annapolis, MD 21402	1
7.	Assistant Professor R. DeMoyer, Jr. U. S. Naval Academy Annapolis, MD 21402	5